SAPIENZA
UNIVERSITÀ DI ROMA

DOTTORATO DI RICERCA IN BIOCHIMICA

CICLO XXIX (A.A. 2013-2016)

Crosstalk between oxidative stress and inflammation in Alzheimer-like dementia

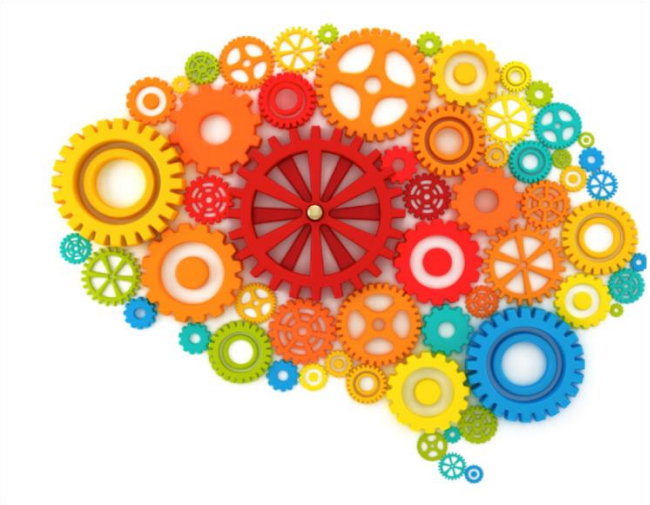

Docente guida

Prof. Chiara Cini

Coordinatore

Prof. Francesco Malatesta

Dottorando

Andrea Arena

INDEX

LIST OF ABBREVIATIONS

3'UTR	3' untranslated region
3-NT	3-nitrotyrosine
8-OHG	8-hydroxyguanine
AD	Alzheimer's disease
AGEs	Advanced glycation end products
AGO	Argonaute protein
ALDH	Aldehyde dehydrogenases
ALS	Autophagy-lysosome pathway
AP-1	Activator protein 1
APP	Amyloid precursor protein
ARE	Antioxidant responsive element
Atg	Autophagy related proteins
Aβ	Amyloid beta-peptide
BACE-1	β-secretase β-site amyloid precursor protein–cleaving enzyme 1
BACE-2	β-amyloid cleavage enzyme 2
Bach1	BTB domain and CNC homolog 1
BBB	Blood brain barrier
BIR	Brain Insulin resistance
BVR-A	Biliverdin reductase A
CAT	Catalase
CBS	Cystathionine-beta-synthase
CFH	Complement factor H
Chr 21	Chromosome 21
CMA	Chaperone-mediated autophagy
CO	Carbon monoxide
CX3CL1	Ligand fractalkine
CX3CR1	Fractalkine receptor
DG	Dentate gyrus
DS	Down syndrome
DSCR	Down syndrome critical region
ERK1/2	Signal-regulated kinases 1/2
ETS-2	ETS proto-oncogene 2 transcription factor
GCL	Glutamate-cysteine ligase
GPX	Glutathione peroxidase
GST	Glutathione S-transferase

GW	Gestational week
H_2O_2	Hydrogen peroxide
HNE	4-hydroxy-2-nonenal
HO•	Hydroxyl radical
HO-1	Heme oxygenase 1
IFNγ	Interferon γ
IGF-1R	Insulin-like growth factor receptors
IL-1β	Interleukin 1β
IL-6	Interleukin 6
iNOS	Inducible nitric oxide synthase
IR	Insulin receptor
IRAK1	Interleukin-1 receptor-associated kinase-like 1
IRAK2	Interleukin-1 receptor-associated kinase-like 2
IRS-1	Insulin receptor substrate-1
LC3	Microtubule-associated protein 1A/1B-light chain 3
LC3-I	Cytosolic form of LC3
LC3-II	LC3-phosphatidylethanolamine conjugate
LTP	Long-term potentiation
MAPK	Mitogen-activated protein kinases
MDA	Malondialdehyde
MeSOX	Methionine sulfoxide
miRNA	microRNA
MRC1	Mannose receptor C1
mTOR	Mammalian target of rapamycin
NFTs	Neurofibrillary tangles
NF-κB	Nuclear factor-kappa B
NLRP3	NOD-like receptor protein 3
NOS	Nitric oxide synthase
NOX4	NADPH oxidase 4
NQO1	Quinone oxidoreductase-1
Nrf2	Erythroid-devived 2-like 2
O_2	Molecular oxygen
O2−•	Superoxide anion
OS	Oxidative stress
PC	Protein carbonyls
PI3K	Fosfoinositide 3-chinasi
pri-miRNA	Primary miRNA
PTMs	Post-translational modifications

PUFAs	Polynsatured fatty acid
RISC	RNA-induced silencing complex
RNS	Reactive nitrogen species
ROS	Reactive oxygen species
S100B	S100 calcium binding protein B
sAD	Sporadic AD
SHIP1	Src homology 2 domain-containing inositol-5 -phosphatase 1
siRNA	Small-interfering RNA
SOD1	Superoxide dismutase
SVZ	Subventicular zone
TIR	Toll-like and interleukin-1 receptor
TNFα	Tumor necrosis factor α
TRAF6	TNF receptor associated factor 6 ligase
UCH-L1	Ubiquitincarboxy-hydroxyl lyase 1
UPS	Ubiquitin-proteasome system
VZ	Ventricular zone

1 INTRODUCTION

1.1 Down syndrome and Alzheimer's disease

Aneuploidy is a genetic alteration due to an abnormal number of copies of a genomic region. The trisomy, complete or partial, is the most common aneuploidy of the chromosome 21 (Chr 21) and is the unique autosomal trisomy to produce a viable and functional human. John Langdon Down described this condition in 1862 but only after 1932, it became clear that it was a consequence of a chromosomal abnormality. Trisomy of Chr 21, commonly known as Down syndrome (DS), is the most prevailing genetic cause of intellectual disability with an incidence of 1:700 births. In the last decade, DS neuropathology has become an attractive field of research for several reasons: i) it can be regarded as a human model of accelerated aging; ii) it allows correlation between genetic defects and pathological phenotypes; iii) it allows correlation among neurogenesis defects, brain development abnormalities and cognitive decline.

Complete triplication of the entire Chr 21 is not necessary to produce the clinical phenotype of DS individuals, indeed the triplication of just a portion of the distal long arm, described as DS critical region (DSCR), has been identified as sufficient [1]. The 95% of DS cases are caused by nondisjunction of chromosome in meiosis I, during the formation of gametes, that results in the presence of 24 chromosomes instead of the usual 23. The zygote obtained after fertilization of the gamete with extra Chr 21 and a gamete with a normal chromosomal set will have 47 chromosomes instead of 46 [2]. While the 3.2% and 1.8% of residual DS cases are caused respectively by translocation and mosaicism [3]. Translocation refers to a partially or fully, additional copy of the Chr 21 attached to another chromosome and is present in every cell of the individual [2]. Instead in mosaic not all cells of the body carry an extra copy of Chr 21 and two different mechanisms have been

proposed to explain this phenomenon: i) the zygote has three copies of Chr 21 in every cell but during cell division, at least one cell line loses the extra copy of Chr 21; ii) the zygote has two copies of Chr 21 but during the cell division one of the cells has a duplication of the Chr 21 obtaining so the copy extra [4].

The effects of the trisomy 21 vary widely from one individual to the other and not every DS subjects show all the phenotypic features caused by trisomy. Therefore it is conceivable to separate DS features in two types: i) those seen in all patients, as the cognitive decline or facial dysmorphology; and ii) those that have variable penetrance, such as the congenital heart defect that is observed in the 40% of the cases [5]. Furthermore, for the same phenotypic feature different grades of severity are also observed. In addition to the chromosomal abnormality on Chr 21 it is believed that additional environmental factors can play an important role in determining different phenotypes. Mainly, two hypotheses have been proposed to explain the phenotypic variability observed in trisomy 21 subjects: the "gene dosage hypothesis" and the "amplified developmental instability hypothesis". The first hypothesis proposes that the overexpression of trisomic genes and their encoded proteins is directly responsible for the different phenotypical alterations in DS [6, 7]. The second hypothesis postulates that the presence of multiple phenotypes is caused by the effects of the overexpression of trisomic genes on dysomic genes leading to an imbalance in their expression [8]. So far, results obtained by the analysis of DS cases and the development of DS mouse models support both hypotheses. Therefore, the combination of these two hypothesis indicates a complex scenario where the consistently over or down-expression of a subset of dosage-sensitive genes lead to different phenotypic features. The pathology of DS is commonly accompanied by the alteration of nervous, respiratory, cardiovascular, gastrointestinal, hematologic, immune, endocrine, musculoskeletal, renal and genitourinary systems. Clinical features documented in DS subjects are microcephaly, craniofacial abnormalities, neuromotor

dysfunction, accelerated aging, cognitive and language defects, impaired mitochondrial function, increased oxidative damage and accumulation of damaged/misfolded protein aggregates. Some of the most consistent and striking alterations in DS involve the brain, which demonstrates reduced neuronal content, reduced frontal lobe volume and narrowed superior temporal gyrus. DS individuals, after the age of 40, develop a type of dementia that closely resembles that of Alzheimer's disease (AD), the most common cause of dementia in older people, with deposition of senile plaques containing amyloid beta-peptide (Aβ) and neurofibrillary tangles (NFTs) composed of hyperphoshorylated tau and also cholinergic and serotonergic reduction [6]. Because AD is virtually inevitable in DS subjects the DS neuropathology can be considered a "natural model" of early AD and could contribute to understanding the overlapping mechanisms that lead to the neuropathophysiological progression of AD. The deposition of Aβ plaques is the most prominent and detrimental neuropathological change in AD brain and occur in cortical regions that are important in acquiring, storing and retrieving information. These regions include temporal lobe structures, such as the hippocampus, as well as frontal and parietal regions. Patients with AD are characterized by deterioration in control, thought, memory, language skills and personality changes associated with inappropriate or psychotic behaviors causing the decline in the ability to carry out daily activities [9]. Characteristic features in AD brain are weakening of synaptic networks, neuronal loss and increase of brain atrophy [10]. Aβ and tau lesions affect several brain regions in DS, including prefrontal cortex, hippocampus, basal ganglia, thalamus, hypothalamus and midbrain and are believed to underlie the development of cognitive decline and dementia. However, although the depositions of Aβ plaques have been observed in fetus and young DS individuals [11, 12], signs of dementia are clearly manifested many years later.

Inflammation and oxidative stress (OS) are known to occur in the brains of both AD and DS patients in response to the presence of Aβ plaques and NFTs [6, 13] and several studies demonstrated the involvement of OS and inflammation in accelerated senescence. In addition to OS and inflammation, also brain insulin resistance (BIR), described as an inadequate response to insulin, is considered one of the major events for the progression of AD-like pathology. Interestingly the evaluation of insulin signaling in DS brain has revealed the presence of insulin resistance similar to AD patients [14]. It is hypothesized a link between OS and BIR where increased OS leads to the reduction of both insulin secretion and sensitivity [15], in turn defective insulin signaling makes neurons more vulnerable to oxidative damage [16, 17]. Therefore, it is believed that these defects (OS, inflammation and BIR) could contribute to the severity of AD and act as potential accelerators in the progression of AD in DS subjects (Fig. 1). The identification and characterization of the genes and proteins Chr 21-encoded is crucial to understand the mechanisms through which the chromosomal abnormality could contribute to the development of AD in DS people and could provide insights into the mechanisms that cause dementia in the general population. The entire sequence of human Chr 21 has been resolved in 233 coding genes, 299 long non-coding genes (Ensembl release 78) and 29 microRNAs (miRBase release 21) [18]. After investigation with Swiss-Prot and analysis with Gene Ontology Annotation the 207 proteins Chr21-encoded: i) take part in 87 different biological processes and 11 proteins are involved in signal transduction; ii) have 81 different molecular functions among which DNA binding and transcription factor activity are the most prevalent with 15 proteins; iii) are localized in 26 different cellular components, nucleus and the plasma membrane with 19 and 15 proteins respectively are the most predominant cellular localizations [5]. Interestingly, several genes mapped in the Chr 21, such as CuZn superoxide dismutase (*Sod1*), amyloid precursor protein (*App*), ETS proto-oncogene 2 transcription factor (*Ets-2*), S100 calcium binding

protein B (*S100b*), cystathionine-beta-synthase (*Cbs*), β-amyloid cleavage enzyme 2 (*Bace2*) and BTB domain and CNC homolog 1 (*Bach1*), are known to be involved in processes associated with inflammation, OS and insulin signaling (Fig. 1). Accordingly, the overexpression of these genes and their effect on disomic genes (as postulated by gene dosage hypothesis and by the amplified developmental instability hypothesis) can lead to impaired of specific processes underlying the onset of neuropathological hallmarks in DS individuals.

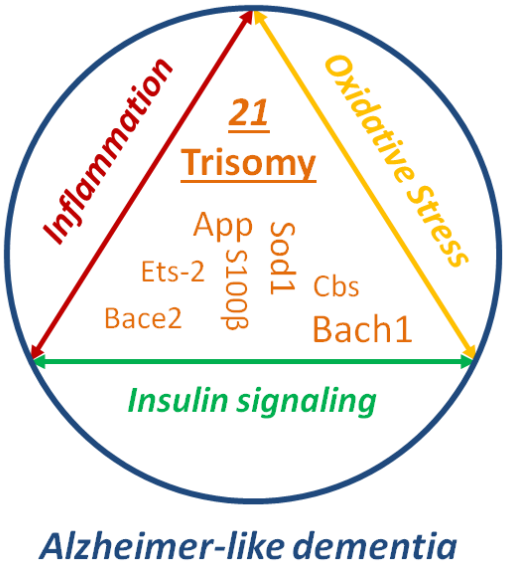

Fig. 1. Link between inflammation, OS and insulin signaling in DS and AD pathology. Several genes Chr 21-encoded involve in these processes.

1.2 Oxidative stress

Increased OS has been implicated into the development and progression of neurodegenerative diseases [19] and increasing number of studies have recently shown that it occurs in the brains of both AD and DS subjects. OS is caused by an imbalance in the redox state of the cell, either by overproduction of reactive oxygen and nitrogen species (ROS/RNS), or by decreased antioxidant response. The high lipid content of nervous tissue, together with the high aerobic metabolic activity, leaves the brain particularly susceptible to oxidative damage [20]. Accordingly, it has been reported a strong correlation between augmented OS and several cellular toxic processes during neurodegenerative diseases: increased levels of ROS make neurons more susceptible to apoptosis and may alter APP processing promoting intracellular accumulation of Aβ. ROS such as superoxide anion ($O_2^{-}\bullet$), hydrogen peroxide (H_2O_2) and hydroxyl radical ($HO\bullet$), are either radical or non-radical oxygen species generated as by-products of aerobic respiration and various other catabolic and anabolic processes [21]. The major source of free radicals is the mitochondrial oxidative phosphorylation pathway, in which electron leakage from the electron transport chain causes the formation of $O_2^{-}\bullet$ that, in turn, is converted by mitochondrial-resident SOD into H_2O_2 and O_2 [22]. Once released, H_2O_2 is relatively stable and can diffuse through membrane. In the cytosol, H_2O_2 can be efficiently removed by antioxidant systems such as catalase (CAT), glutathione peroxidase (GPX) and thioredoxin peroxidase (Fig. 2). Other than mitochondria, a number of cytosolic enzymes are able to generate ROS [23] in response to different environmental stimuli such as growth factors, inflammatory cytokines, ionizing radiation, chemotherapeutics, toxins and transition metals [24]. It is important to highlight that the ROS are not always harmful and their effects depend on their amount: i) at low concentration, ROS acts as signaling molecules and can activate many protective cellular apparatus

including cell growth, cell proliferation and cellular signal transduction [25]; ii) at high concentration, ROS acts as damaging by-products causing irreversible damage to the intracellular macromolecules (Fig. 2). Watson postulated also that several diseases including diabetes, dementias and cancer can be accelerated or even caused by failure to generate sufficient ROS [26].

In fact, recent studies showed that insufficient levels of ROS could promote survival of malignant cells, due to failure to induce apoptosis, contributing to the tumor growth [27, 28]. Thus ROS, at least in some situations, can produce beneficial effects. Similarly, the antioxidants can be both harmful and healthy depending on the situation. For example, in premalignant stage, the antioxidants inhibiting ROS-induced DNA damage block the malignant transformation [29, 30] while in transformed cells inhibiting ROS-induced apoptosis lead to increased cell survival, proliferation and carcinogenesis [27, 28]. At physiological conditions, intracellular ROS are kept at low but measurable levels that result from the rate of production and the rate of scavenging by various antioxidants [31]. Considering that aging is the most important risk factor for neurodegenerative disorders, the progressive and irreversible accumulation of oxidative damage during aging can be a causative or at least a collateral factor in the development of neuropathologies. In parallel, the premature changes in the redox-responsive signaling cascades observed in DS subjects may have a similar or even greater impact than the accumulation of oxidative damage due to age on development of neurodegenerative disorders like AD pathology [25]. Proteomics studies, on AD and DS samples, identified several proteins, members of antioxidant systems, proteostasis networks, energy metabolism and maintenance of cell structure, to be specific targets of oxidative modifications. The main targets of ROS are proteins, lipids and nucleic acid so both loss of scavenging mechanisms and an increase in the cellular oxidants result in damage that takes the form of oxidation of these molecules.

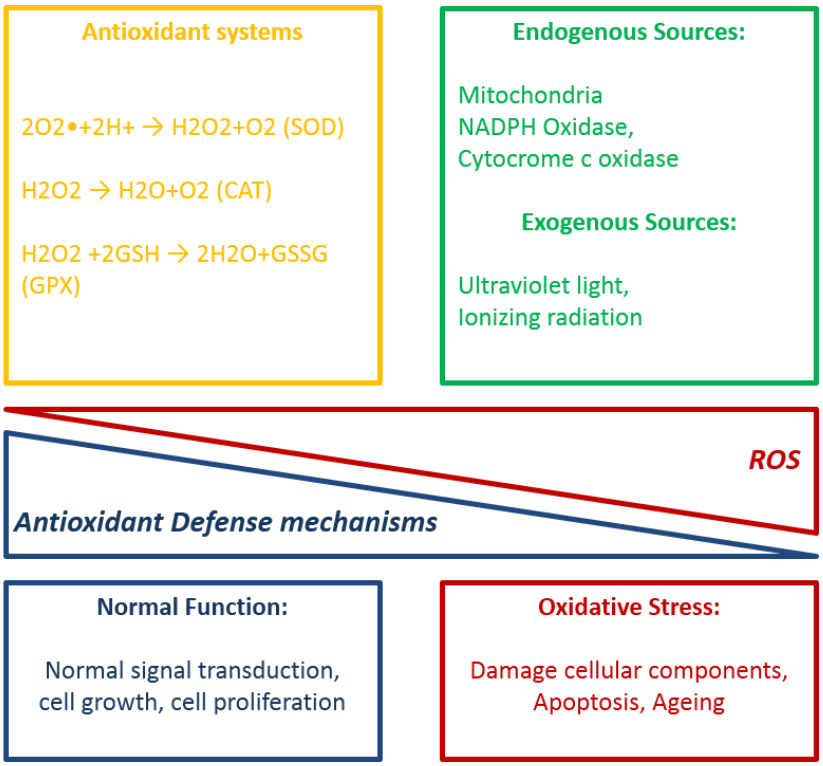

Fig. 2. ROS can be produced endo- or exogenously. The level of ROS is regulated by antioxidants defense mechanisms. Low levels of ROS production are required to maintain physiological functions, including: proliferation, signal transduction and cell growth. Under normal conditions, antioxidant defense mechanisms decrease excess ROS and maintain cellular homeostasis. However, overproduction of ROS generates OS, leading to senescence, damage to cellular components, modulation of signal transduction pathways and apoptosis.

Protein oxidative modification. The proteins can be oxidized by direct ROS attack, by secondary oxidation products, such as the reactive aldehyde formed as final by-products of lipid peroxidation, or by glycoxidation reactions. The carbonylation is one of the most common oxidative post-translational modifications (PTMs) and often forms reactive aldehydes or ketones. Oxidation is, in the majority of cases, a non-reversible phenomenon that could alter the three-dimensional conformation of peptides resulting in a loss or, in a few cases, a gain of function. In addition, protein oxidation could affect different processes including protein turnover, cell signaling, increased susceptibility to proteolysis and fragmentation enhancing the formation of protein aggregates often toxic to cells if allowed to accumulate [32-35]. The OS-associated irreversible damage to proteins seems to be involved in physiological aging and neurological degeneration [34]. Protein carbonyl groups are generated by direct oxidation of several aminoacid side chain, backbone fragmentation, α-carbon hydrogen extraction and Michael addition reactions of His, Lys and Cys residues with products of lipid peroxidation. Protein carbonyls also are produced by glycation/glycoxidation of Lys amino groups, forming advanced glycation end products (AGEs). All aminoacid residues can be attacked by ROS, but Met and Cys residues are particularly sensitive. In the case of Met, low levels of ROS lead to formation of Met sulfoxide (MeSOX) that in turn can be reduced by MeSOX reductases. In addition, the oxidation of sulfhydryl groups, often resulting in the formation of intra- or intermolecular disulphides, is reduced by disulfide reductases/isomerases. Since these two oxidative modifications can be enzymatically restored, in mammalian cells, it is likely they play a key regulatory role and sense the cells to changes in the redox environment. Indeed, a number of signaling pathways, such as JNK, p38 mitogen-activated protein kinases (MAPK), are strongly responsive to redox regulation. However, the interplay between individual redox-sensitive signaling proteins to redox-regulated processes in vivo

is quite complex. Lipid peroxidation is another source of free radicals, which directly damages membranes and generates a number of secondary products responsible for extensive cellular damage. The free radical attack to polynsatured fatty acid (PUFAs) leads to the formation of highly reactive electrophilic aldehydes, including malondialdehyde (MDA), 4-hydroxy-2-nonenal (HNE), the most abundant products and 2-propenal (Acrolein) the most reactive. The peroxidation of membrane lipids can result in increased membrane rigidity, decreased activity of membrane-bound enzymes (e.g. sodium pump), impairment of membrane receptors and altered permeability [21]. In addition, radicals also can directly attack membrane proteins and induce lipid–protein and protein–protein crosslinking, altering membrane integrity. Although the modulation of the proteins by HNE is mainly based their oxidative modification, there are also example of regulation of gene expression by targeting transcription factors such as NF-κB (nuclear factor-kappa B) and AP-1 (activator protein 1). HNE is also involved in the activation of the transcription factor Nrf2 (erythroid-devived 2-like 2), which transactivates the antioxidant responsive element (ARE). In this way, HNE stimulates the cellular antioxidant defenses through the upregulation of the expression of various genes such as heme oxygenase 1 (HO-1), aldehyde dehydrogenases (ALDH), glutathione S-transferase (GST). By its multiple impacts on protein regulation through transcriptional and post-translational modifications, HNE takes part in the maintenance of cellular homeostasis. However, higher levels of OS can lead to HNE accumulation, which could interfere with normal cellular signaling through the membrane damage and lead to the development of pathological conditions as it occurs in several neurodegenerative diseases [36]. Indeed, high levels of HNE deplete the cell of nucleophilic compounds that serve as antioxidants (glutathione, lipoic acid and thioredoxin) by covalently modifying proteins via Michael addition in a secondary protein carbonylation reaction [37].

Protein bound and free reactive aldehydes are being investigated as potential markers of OS and disease progression in conditions ranging from neurodegeneration to brain infarction [38, 39].

Protein degrading systems can sustain cellular homeostasis by repairing or removing the oxidized products [40]. However, reduced activity of these mechanisms may render the cell incapable of efficiently removing oxidized biomolecules, resulting in their toxic accumulation. Two major pathways are responsible for the proteolysis of intracellular proteins, either for damage and self-renewal: the ubiquitin-proteasome system (UPS) [41] and the autophagy-lysosome pathway (ALS) [42]. The UPS is located in the cytosol and the nucleus, it is responsible for the degradation of more than 70–80% of intracellular proteins and it is characterized by a high degree of specificity. In proteosomal degradation the protein substrates in order to be recognized undergo a covalent modification, known as ubiquitination, that requires the attachment of ubiquitin to the ε-amino group of an Lys residue of the protein substrate [43, 44]. In contrast, the degradation into the ALS seems to be non-specific [45] and includes: macroautophagy (indicated as autophagy), microautophagy and chaperone-mediated autophagy (CMA). All three mechanisms share a common destiny of lysosomal degradation, but are mechanistically different one from another [46-48]. Experimental evidence suggests that failure of the UPS or ALS may contribute to neurodegeneration and that the up-regulation of these systems occurs in response to OS to remove oxidized proteins. However, in presence of high levels of free radicals, the degradation of oxidized proteins may be inefficient [49]. Indeed, oxidative modifications induce crosslinking/misfolding that may block the entrance of protein substrates in the proteolytic cavity of the proteasome [32]. In addition, oxidatively modified proteins may directly damage components of the degradation systems and ROS can damage lysosomal membranes [40].

Therefore, the accumulation of oxidatively modified proteins become a potential new source of free radicals. Taken together these considerations, it is clear that in addition to protein oxidation with accumulation of dysfunctional/damaged protein aggregates, the neurodegenerative processes also include the dysfunction of intracellular degradative systems such as UPS and ALS (Fig. 3).

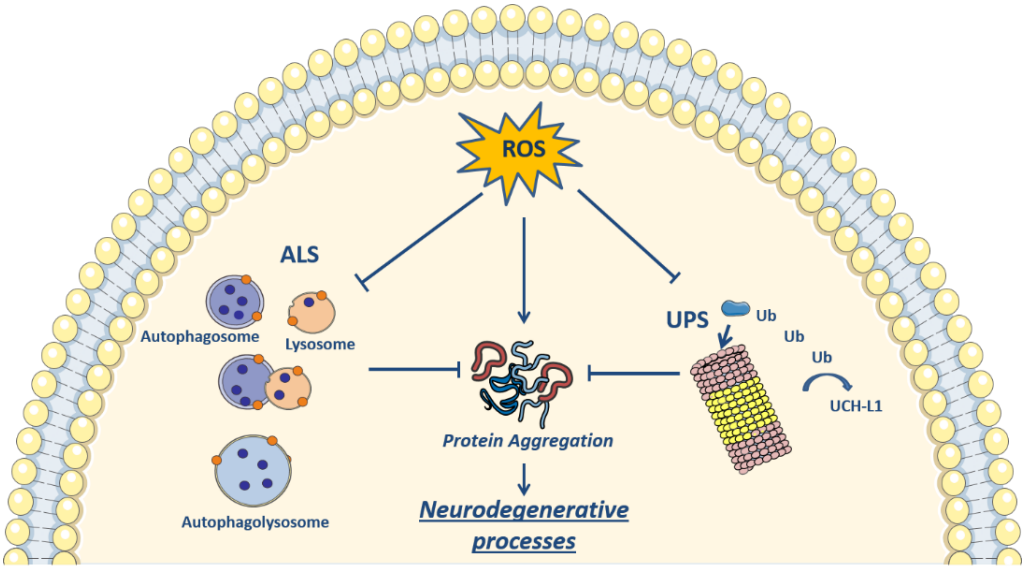

Fig. 3. Interplay between OS and protein degrading systems.

Recently our group demonstrated that ubiquitincarboxy-hydroxyl lyase 1 (UCH-L1), an enzyme with ubiquitin ligase/hydrolase activity, is a target of oxidative damage in DS brains, with a reduction of its enzymatic activity [50]. In this study, redox proteomics approach was used to analyze the frontal cortex from DS subjects under the age of 40 compared with age-matched controls and proteins found to be increasingly carbonylated were identified. Thus we observed an increased carbonylation levels of UCH-L1 with 2.12-fold associated to the reduction, about 30%, of UCH-L1 enzyme activity in DS subjects compared with controls. Therefore, we suggested that the oxidative modifications causing irreversible alteration in the conformation and/or enzymatic activity of UCH-L1 result in

deleterious effects by impaired proteasome proteolytic system with accumulation of damaged proteins and formation of protein aggregates. Interestingly, a defective protein ubiquitination could result in reduced intracellular protein degradation, also in the presence of adequate proteasome activity. Therefore, the aberrant ubiquitin hydrolase and/or ligase activity, as result of UCH-L1 oxidative modifications, might lead to dysfunction of the neuronal ubiquitination/deubiquitination machinery, causing synaptic deterioration and neuronal degeneration in DS as well as demonstrated in AD brains [51-53]. Thus, we hypnotize that these mechanisms may play a crucial role in the development of Alzheimer-like dementia in DS population. The impairment of autophagy has been largely implicated in AD neurodegeneration [54] and several studies suggested that it is likely to be caused by the hyperactivation of the mammalian target of rapamycin (mTOR) [55-57]. mTOR is a serine/threonine protein kinase that acts as regulator of autophagy because directly involved in the initiation step of this process by regulating the formation of the phagophore [48]. Indeed, autophagy involves several autophagy related proteins (Atg) that coordinate vesicle formation in three different steps: initiation, elongation and maturation. The initiation step is triggered in response to starvation by inhibition of mTOR that leads to the activation of the ULK1 kinase complex which comprises ULK1/Atg1-Atg13-FIP200/Atg17-Atg101 and causes the activation of another complex that comprises (among other proteins) PI3K, Vps34 and the protein Beclin-1 (Fig. 4). The later steps of autophagy the elongation and the closure of the autophagosome are dependent on the activity of the LC3-conjugation system. Consequently, the autophagosome matures by fusing with an endosome and/or lysosome, thus forming an autophago-lysosome. Therefore in physiological conditions mTOR, by inhibiting ULK1 complex, suppresses the phagophore formation that is essential for autophagy induction [58]. In addition, several studies suggested a link between mTOR signaling and Aβ and tau neuropathology [59-

62]. Therefore it has been hypothesized that a sustained activation of mTOR can impact directly the AD pathology because it regulates the processing and clearance of Aβ and tau aggregates.

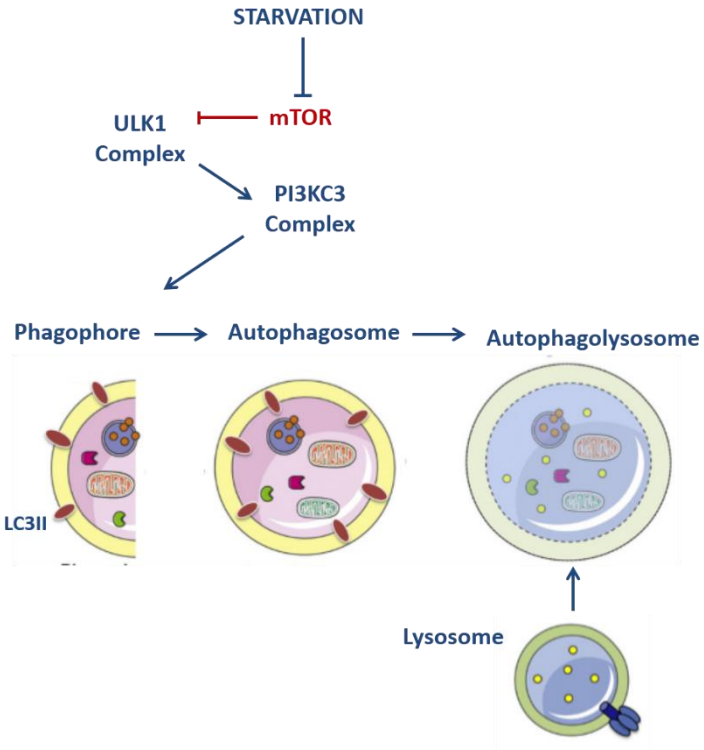

Fig. 4. mTOR and autophagy.

DNA damage and mitochondrial dysfunction. The ROS are able to cause structural alterations in DNA: OH• generates a multiplicity of products from all four DNA bases while O_2 selectively attacks the guanine. The most commonly product of oxidative DNA damage is 8-hydroxyguanine (8-OHG). If damage is not properly repaired, it generates a mutation caused by the incorrect pairing during replication. The mitochondrial dysfunction is a crucial event for neurodegeneration because of the central role of mitochondria in many cell functions such as ATP generation, intracellular Ca^{2+} homeostasis, ROS formation and apoptosis. The neurons, accordingly with their high-energy demand, are sensitive to mitochondrial dysfunction and the role of mitochondrial dysfunction in AD is well established [63, 64]. Altered mitochondrial activity has been reported also in DS fibroblasts [65] and both DS neurons and DS astrocytes display an abnormal pattern of protein processing consistent with chronic energy deficits [66]. A link between OS and mitochondrial dysfunction is observed. Both DS and AD neurons are vulnerable to increased ROS levels and decreased mitochondrial function indicating that these events may participate in a self-sustaining vicious cycle leaving neurons highly susceptible to death.

1.2.1 Oxidative stress and trisomy 21

Several studies have recently associated the increased OS that occur in DS pathogenesis at the deregulation of triplicated genes that, directly or indirectly, participate to create an imbalance between production and clearance of ROS. Among these, the most relevant OS-inducers are *Sod1*, *App*, *Bace2*, *Ets-2*, *S100b* and *Bach1*. One interesting aspect of this complex process is that ROS can be generated during the early phases of protein self-aggregation [67] and considering that ROS-damage induces protein aggregation, these events may participate in a self-sustaining vicious cycle. Therefore, we suggest that an increased OS can be due not only to the overproduction of ROS and/or by decreased antioxidant defense system but also from the accumulation of protein oxidative damage in the presence of reduced degradative protein system.

SOD1 is an antioxidant enzyme that catalyzes the dismutation of $O_2^{-}\bullet$, a by-product of oxidative metabolism, to produce H_2O_2 and O_2. Therefore, SOD1 protects the cells against ROS and consequently it is thought as a neuroprotective agent but, as demonstrated by Shin et al, transgenic mice overexpressing wild-type human SOD1 (Tg-SOD1) displayed mitochondrial alterations and learning and memory deficits [68]. In addition to the anti-oxidation effects, SOD1 generates H_2O_2, that is a potential source of oxidative damage, which turn is neutralized with O_2 by CAT and by GPX in H_2O [69]. DS subjects present in erythrocytes, B and T lymphocytes, and in fibroblasts, levels of SOD1 approximately 50% higher than normal subjects, while both CAT and GPX are generally expressed at lower levels in DS subjects compared with normal subjects [20]. The increase of SOD1 expression and low levels of CAT and GPX produces an imbalance between SOD1 activity and GPX/CAT activity which can results in the accumulation of H_2O_2 (Fig. 5). In turn, the accumulation of H_2O_2, in the presence of Fe(II) or Cu(I), leads to hydroxyl radical formation, which damages membrane lipids, proteins and nucleic

acids. However, as also shown by a proteomics study from Gulesserian et al. [70] increased OS in fetal DS brain is not only a consequence of SOD1 overexpression, which alone cannot explain the generalized increase of oxidative damage.

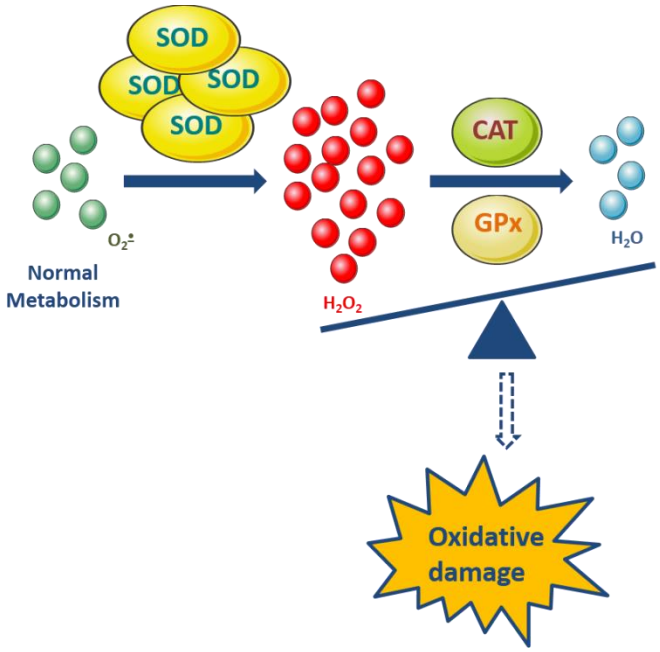

Fig. 5. Imbalance activity between SOD1 and GPX/CAT can result in H_2O_2 accumulation resulting in oxidative damage.

APP is the precursor protein of Aβ, the major component of plaques, found in the brain of AD patients and in middle-aged individuals DS. APP is a transmembrane protein and is differentially cleaved by enzymes called secretases. Three secretases are responsible for the cleavage of APP. Aβ is generated by the sequential proteolytic processing of APP throughout the β-secretase β-site amyloid precursor protein–cleaving enzyme 1 (BACE-1) and γ-secretase a protein complex with Presenilin. The γ-secretase can generate several isoforms of Aβ with different length: Aβ40 and Aβ42 are the most common isoforms. Instead the cleavage of APP by primarily α-secretase and subsequently γ-secretase results in the formation of a peptide called p3. Aβ soluble peptides spontaneously aggregate to form oligomers and fibrils that are subsequently deposited within the brain to form both diffuse and dense core amyloid plaques (Fig. 6). Accordingly with the gene-dosage effect, DS individuals show the overexpression of APP, which might lead to the increased production of Aβ [15-17]. APP has been considered as a probable OS-inducer, indeed, as supposed by "AD amyloid hypothesis" and then demonstrated by experimental evidence, Aβ is toxic to cells because it induces the production of H_2O_2 and mitochondrial dysfunction [67, 71-74]. Indeed Aβ inserts into the bilayer acts as a catalytic producer of ROS, initiating the lipid peroxidation [73, 75] where a carbon centered radical is produced on a PUFA by the abstraction of an allylic hydrogen from sulfuranyl free radical on Met-35 of Aβ(1-42). Molecular oxygen, which lacks a dipole moment, diffuses into the lipid bilayer where it may react with the carbon centered radical to form a lipid peroxyl-radical [76, 77]. The lipid peroxyl-radical may then abstract an allylic hydrogen from an adjacent poly-unsaturated lipid which propagates the chain reaction and forms a lipid hydroperoxide that may then undergo cleavage forming an array of possible reactive aldehydes such as F2-isoprostane, HNE and Acrolein. An imbalance between production, clearance and aggregation of peptides causes Aβ accumulation and this excess may be the initiating factor in AD. However, the

additional copy of App in DS does not typically cause substantial Aβ accumulation until the second or third decade of life, but the subtler Aβ changes occur in younger patients with the activation of endocytic uptake and recycling of Aβ. This lack of early Aβ accumulation may be due to App not becoming dosage sensitive until adulthood [78-80]. However, increased levels of soluble Aβ42 are found in ~50% of DS fetal brains [12], suggesting that App may be dosage sensitive during fetal development but that this change may not be sufficient to cause extensive Aβ deposition in the developing. It is important to highlight that App is not necessary for the development of DS phenotype, but its triplication can be necessary for the development of AD pathology in DS patients. This idea has been confirmed by the exceptional case DS of 78 year old with partial trisomy 21 that did not include the App gene, although of extremely advanced age without clinical or pathological evidence of AD [81].

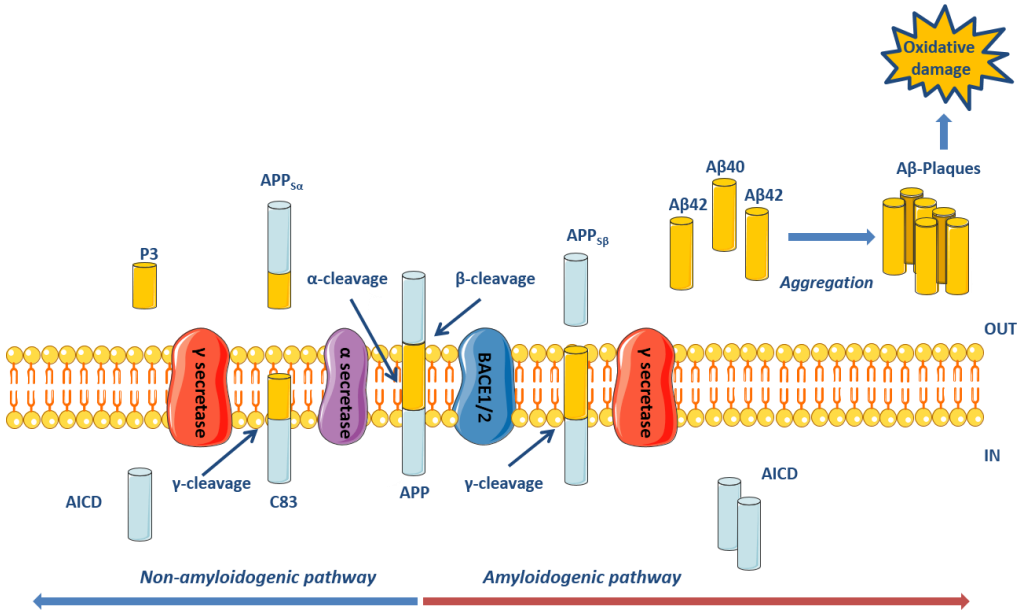

Fig. 6. APP processing and Aβ generation.

APP-cleaving 2 enzyme (BACE2) and the transcription factor ETS-2 have been suggested to modulate APP processing and Aβ generation. BACE2, homologous to BACE1, is a cleavage enzyme essential for processing of APP in Aβ 40 and Aβ42 (Fig. 6) [78, 82]. While ETS-2 is thought to trans-activate the APP promoter, leading to its overexpression. The presence of App, Est2 and Bace2 on Chr 21 and the resulting co-overexpression of these genes could reinforce the link between trisomy 21, OS and the development and progression of AD in DS [83].

S100B is an astroglial-derived Ca^{2+}-binding protein that acts as neurotrophic factor on neurons and glial cells by modulating cell proliferation, differentiation and interaction with many immunological functions of the brain. In addition, it is involved in the regulation of energy metabolism by stimulating the enzymatic activity of fructose-1,6-bisphosphate aldolase and phosphoglucomutase [84]. The effects of S100B depend on its concentration: at nanomolar concentrations the neuroprotective effects prevail, while at micromolar concentrations neurodegenerative or apoptosis-inducing effects are observed [84, 85]. The neurotoxic actions of S100B could be due to the increased expression of nitric oxide synthase (NOS) with release of nitric oxide [86] and mobilization of calcium stored in neurons by stimulation of phosphoinositide hydrolysis by phospholipase C [87]. S100B is overexpressed in the brains of DS fetuses [88], and this overexpression continues throughout life [85].

BACH 1 is a transcription repressor that plays an important role in the regulation of the expression of genes involved in the cell stress response. BACH1, under physiologic conditions, forms heterodimers with small Maf proteins (i.e., MafK, MafF and MafG), which bind the ARE of DNA thus inhibiting the expression of specific proteins. By contrast, increased OS levels suppress the function of BACH1 [89-91] by promoting BACH1 nuclear export and enhancing the

expression its genes target. When the intracellular heme levels increase, as under pro-oxidant condition, nuclear BACH1 binds heme and dissociates from the AREs thus allowing the expression of genes [92] such as: Quinone oxidoreductase-1 (NQO1), glutathione S-transferase (GST), glutamate-cysteine ligase (GCL) and HO-1 (Fig. 7) [93]. HO-1 catalyzes the first and rate-limiting enzymatic step of heme degradation, producing equimolar amounts of carbon monoxide (CO), Fe(II) and biliverdin [94-96]. The biliverdin is latter converted into the powerful antioxidant bilirubin by biliverdin reductase A (BVR-A). BVR-A is also a Ser/Thr/Tyr kinase that interacts with members of the MAPK family, in particular the extracellular signal-regulated kinases 1/2 (ERK1/2) that once translocated into the nucleus regulates the expression of oxidative-stress responsive genes such as HO-1 or inducible nitric oxide synthase (iNOS) [97, 98]. The HO-1/BVR-A axis represents one of the main systems through which cells counteract/prevent OS-induced intracellular damage [92, 99-102] and any imbalance of activity its elements would result in increased oxidative stress levels. The upregulation of *Bach1*, due to trisomy 21, can promote the lack of induction of antioxidant controlled by AREs, therefore promoting OS increase in the cell (Fig. 7).

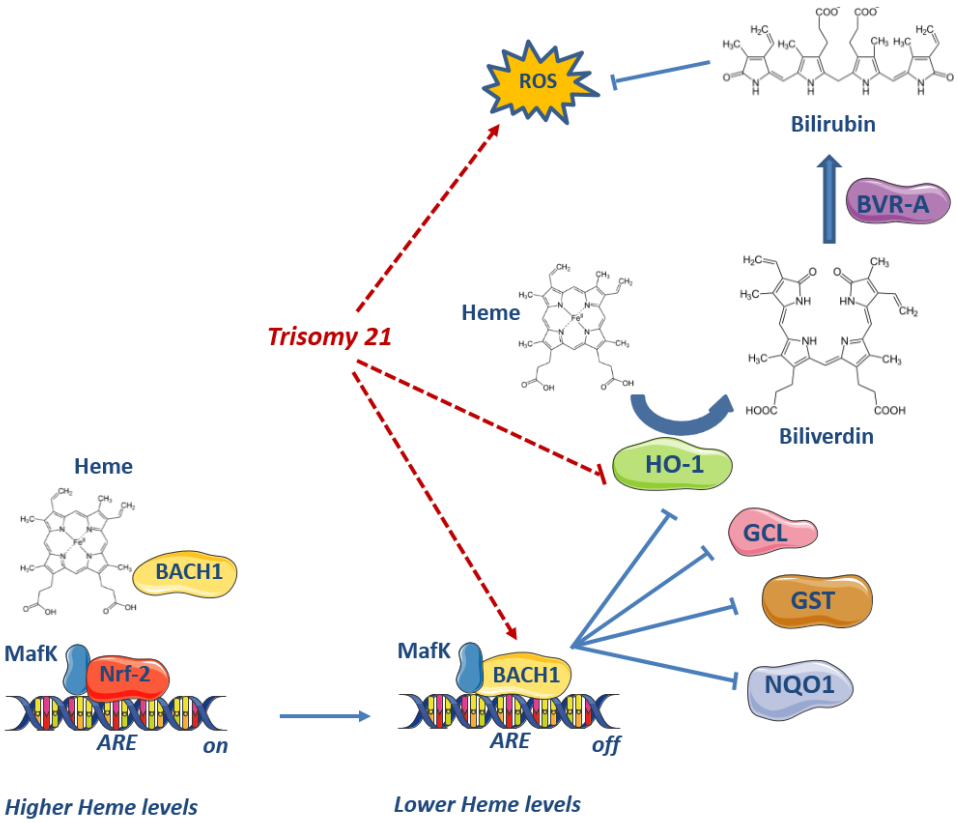

Fig. 7. Regulation of OH-1 by Bach1 and heme. BACH1 occupies ARE enhancers to repress transcription under normal conditions. An increase in heme levels, as under pro-oxidant condition, alleviates BACH1-mediated repression through inhibition of its DNA-binding activity and subsequent nuclear export, making ARE available for activating Maf complexes including Nrf2. HO-1 catalyzes the first and rate-limiting enzymatic step of heme degradation, producing biliverdin which is then converted into the powerful antioxidant bilirubin by BVR-A. The upregulation of Bach1 due to trisomy 21 related could promote the lack of induction of antioxidant controlled by AREs, therefore promoting OS increase.

1.3 Inflammation

Inflammation is known to occur in the brains of both AD and DS patients due to the presence of Aβ plaques and NFTs. Inflammation is a protective response to exogenous and endogenous stimuli, however exaggerated or prolonged inflammatory process can induce tissue damage. Although the role of the inflammation in the progression AD is well-established, it is poorly understood how inflammation may affect the pathology of DS and how genetic alteration in DS may alter the inflammatory response. The brain, once considered "immunologically privileged", is now recognized to exhibit an almost complete spectrum of inflammatory responses. The primary immune effector cells of the brain are the microglial cells an ameboid-like cell that can be labeled immunocytochemically using macrophage cell surface markers [103, 104]. Microglial cells play a fundamental role in maintaining brain homeostasis by taking up cellular debris and protecting the brain from invading pathogens. Astrocytes and neurons also can contribute to the inflammatory response, although their contribution is considered lower than that of the microglia [105]. Microglial cells, like other tissue macrophages, respond to their local environment and so that cells located in different brain area can show distinct phenotypes [106]. In AD, activated microglia is highly localized to the area immediately surrounding an Aβ plaque or NFTs [107] and their number/size directly increases in proportion to plaque dimension [108-110]. Additionally, microglial cells at the periphery of Aβ deposits can also proliferate, allowing for the accumulation of these cells [111, 112]. However, the role of the microglia during neurodegeneration is controversial because its activation could have both a beneficial effect, playing a neuroprotective role removing the abnormal protein deposits from AD brain, and a detrimental effect contributing to the neurotoxicity observed in AD. Most likely, both the effects occur in AD brain but at different pathology degree. Receptor complexes

located on the microglial cell surface allow to recognize fibrillar forms of Aβ and their activation initiates an intracellular signaling cascade that results in microglia activation through NF-κB mediated gene transcription [113-115]. In AD, many inflammatory cytokines and chemokines have been found to be increased, including interferon γ (IFNγ), Tumor necrosis factor α (TNFα), Interleukin 1β (IL-1β) and Interleukin 6 (IL-6) [116-120]. IFNγ or TNFα stimulation in neurons increase the production of Aβ from APP while in microglial cells impair the ability to degrade Aβ [118]. The microglia exposure to fibrillary forms of Aβ has been demonstrated *in vitro* to provoke the synthesis and secretion of pro-inflammatory cytokines (including IL-1β, IL-6, TNFα), chemokines, ROS and RNS [116, 121-125]. These studies support the idea that the inflammation might impact negatively the ability of microglial cells to take up Aβ deposits and suggest that the inhibition of inflammatory signaling can enhance Aβ clearance. Although the inflammation plays beneficial roles in pathogen removal, it can also be detrimental if the response is not downregulated. Thus, the CNS can suppress microglial activation through interactions between microglial and neurons or other glial cell types. For example, the interaction between the fractalkine receptor (CX3CR1) expressed on microglial cell surface and its ligand fractalkine (CX3CL1) expressed on neurons and astrocytes prevents microglia activation. It is thought that, due to loss of neurons, this ligand-receptor interaction is lost and can contributes to the activation of microglial cells during neurodegeneration [126]. Similarly, at CX3CR1 and CX3CL1, the interaction between CD200 receptor located on neurons and CD200 ligand expressed on microglial cells also inhibits microglia-mediated inflammation and *in vitro* can attenuate Aβ-induced glial activation [127]. Interestingly both are reduced in the hippocampus and cortex of AD patients [128]. Also CD45, a microglia transmembrane protein-tyrosine phosphatase, plays a similar role and the interaction with its ligand, CD22, inhibits the production of pro-inflammatory cytokines by microglia in response to lipopolysaccharide [129]. CD22 is normally

secreted by neurons. In contrast, the interaction between CD40 receptor and its ligand promotes an inflammatory response leading to the production of TNFα and IL-1β [130]. In human AD brain the expression of CD40 and its ligand is increased around Aβ plaque [131, 132] while in AD mouse model deficient for CD40 ligand a marked reduction in Aβ load and microglial activation has been revealed [133]. These observations suggest that many mechanisms that act to ensure tight control of microglial activation are compromised in the AD brain which can promote the inflammatory responses observed in AD.

1.3.1 Inflammation and trisomy 21

Given that Chr 21 contains critical genes involved in pro-inflammatory and anti-inflammatory processes it is imaginable that the triplication of these inflammatory-associated genes in DS causes a unique inflammatory environment that could promote and influence the development of clinical and neuropathological manifestations of AD. Therefore, the study of inflammation in DS could be useful to understand the role of these inflammatory pathways in neurodegenerative disorders. Among the inflammatory associated genes found on Chr 21 the most relevant in cytokines are:

Cxadr that encodes for a protein called coxsackie virus and adenovirus receptor. In the heart, it induces stress-activated MAPK pathways that result in increased production of IFNγ, IL-12, IL- 1β, TNFα and IL-6 [134]. Therefore it is imaginable that in DS brain the overexpression of Cxadr could contribute both to increase the IL-1β levels and tangle formation by hyperphosphorylation of tau MAPK-p38-dependent [135, 136].

Ifnra1, Ifnar2 and Ifngr2 that encode for interferon receptors IFNα1, IFNα2 and IFN-γ [137, 138]. Upon ligand binding they activate the signaling pathway leading to induction of IL-1β, TNFα, and IL-6 expression [139]. Their overexpression could make DS individuals hyper-responsive to IFN and therefore to contribute to the elevated inflammatory response both in the brain and systemically.

Ripk4 that encode for a protein kinase involved in the signaling pathway for the activation of NF-κB [116, 117] and in the signaling cascade of the TNFα receptor TNFR1 [140].

Cbs that encodes for the cystathionine beta synthase [141] a cytosolic enzyme that catalyzes the desulfhydration of Cys for production of hydrogen sulfide an atypical cellular messenger [142, 143]. The effects of CBS depend on its concentration: at low levels appear to be anti-inflammatory, while high levels appear to intensify neuroinflammatory processes [144, 145].

Prmt2 that encodes for an enzyme that catalyzes the methylation of Arg. It has been shown that Arg methylation is necessary for regulation of the JAK/STAT signaling pathway which is key for the expression of IFNγ, IFNα IL-6 [146] and promotes the apoptosis by inhibition of NF-κB [147].

According to the systemic immune macrophage profiles it is possible to discern four distinct inflammatory states in response to a stimulus in microglial/macrophage cells: M1, M2a, M2b and M2c [148, 149].
M1state is induced by IFNγ and TNFα and is characterized by release of IL-1β, IL-6 and IL-12. ***M2a*** response is initiated by IL-4 and IL-13 and it is characterized by tissue remodeling factors FIZZ and YM1 as well as AG1 and mannose receptor C1(MRC1). ***M2b*** response has components of both M1 and M2a states. It is characterized by elevations of: M1 markers particularly IL-1β, TNF-a and IL-6 and M2 marker including CD86. ***M2c*** response is stimulated by IL-10 and it is characterized by a series of markers that antagonize M1 signaling pathways.
Since most of the Chr 21 genes are primarily associated with the M1 inflammatory response, it could hypnotize that M1 is the main glial activation state in the DS brain. Indeed the triplication of interferon receptors Ifnra1, Ifnar2 and Ifngr2 could enhance interferon signaling in DS and therefore increase the production of M1 markers such as IL-1β, TNFα and IL-6 (Fig. 8). Wilcock et al. [150], examining the expression of the macrophage phenotypes markers in DS brain, observed a strong M2b response. This unexpected result would suggest that there might be

over-riding factors beyond the genetics of DS responsible of this phenotype (Fig. 8). The analysis of such markers in AD brain demonstrated a broad heterogeneity in the neuroinflammatory state, indeed early AD stages show half of the cases with M1 phenotype and the other half with M2a response, while late AD stages show a more homogeneous neuroinflammatory state, with markers of M1, M2a, and M2c being elevated (Fig. 8). Interestingly, the M2b phenotype was never seen in the AD samples therefore this findings highlight distinct differences between the DS brain and AD brain and suggest that, neuroinflammation has unique features in the DS aging brain that could directly modulate responses to interventions that include immunotherapy or anti-inflammatories.

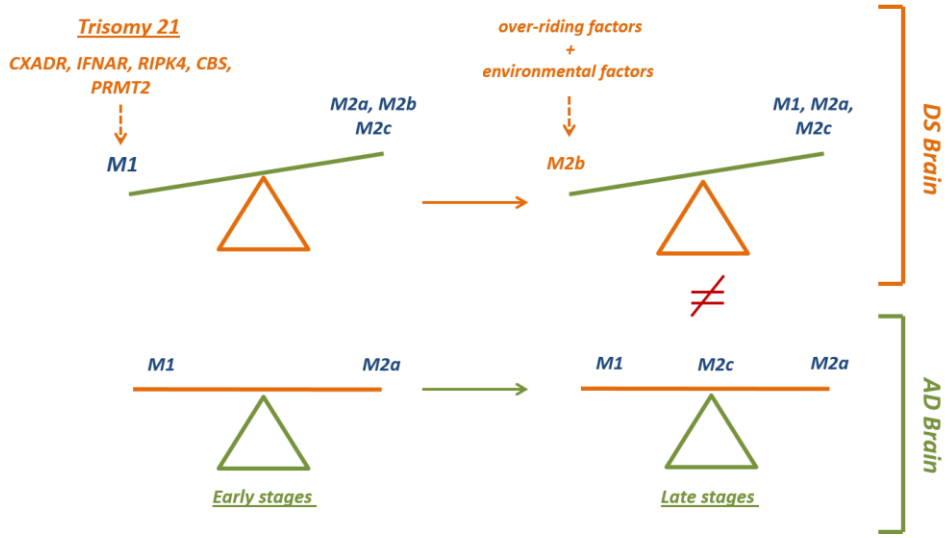

Fig. 8. Inflammatory states in DS and AD brains. Although Chr 21 genes are primarily associated with the M1 inflammatory response in DS brain is observed a strong M2b response suggesting that there might be over-riding factors beyond the genetics of DS responsible of this phenotype. Interestingly, the M2b phenotype was never seen in the AD samples. These findings highlight that DS aging brain shows a unique inflammatory environment distinct from AD brain.

1.3.2 Inflammation as accelerator of AD in DS: the cytokine cycle

The discovery that in AD brain both microglia and astrocytes express excessive amounts of IL-1β and S100B opened the possibility that events in AD pathogenesis could be driven by cytokines. Interestingly in DS brains of fetuses, neonates and children prominent glial activation with excessive expression of both IL-1β and S100B has been observed compared with non-DS individuals of similar ages [88]. It is important to highlight that such changes occur years before the appearance of the senile plaques [151-153] indeed the substantial Aβ accumulation is not typically observed until the second or third decade of life. Thus, premature changes in these cytokines could render the DS brain more susceptible to AD pathogenesis promoting later the development of Aβ plaques and NFTs in DS. Several studies support the importance of these changes for the development of AD neuropathological anomalies in DS brain showing (Fig. 9): i) the capacity of both IL-1β and S100B to induce the synthesis of APP [154, 155]; ii) the capacity of IL-1β to induce the synthesis of S100B [156]; iii) the induction of tau phosphorylation through IL-1β-induced activation of MAPKp-38 [157]; iv) the capacity of both APP and S100B to induce the overexpression of IL-1β [158, 159].

In this complex scenario the upregulation of trisomy 21-related genes such as App and S100b could be sufficient to promote IL-1β overexpression and favor the start and self-sustaining of this vicious cycle (Fig. 9) and explain why the levels of APP and S100B protein are greater than the expected from the 1.5-fold gene load. The lifelong overexpression of IL-1β, in DS brain, could promote neurodegenerative process not only by Aβ plaques and NFTs deposition but also promoting : i) the synthesis and the activity of acetylcholinesterase, favoring the breakdown of acetylcholine[160], an important neurotransmitter in learning and memory [161], which is known to be decreased in AD [162, 163]; ii) the decreases in the expression of synaptophysin [135], which is a hallmark of the synaptic loss in AD [164, 165]; iii) the direct toxic effect on cortical neurons [166], that may also

contribute to neurotoxicity plaque-associated in the promotion of microglial activation [167]. Taken together these reports suggest the existence of a positive feed-forward loop potentially chronic where IL-1β and S100B both induce microglial and astrocytic activation with overexpression of themselves, as well as of neuronal expression of APP [151, 155].

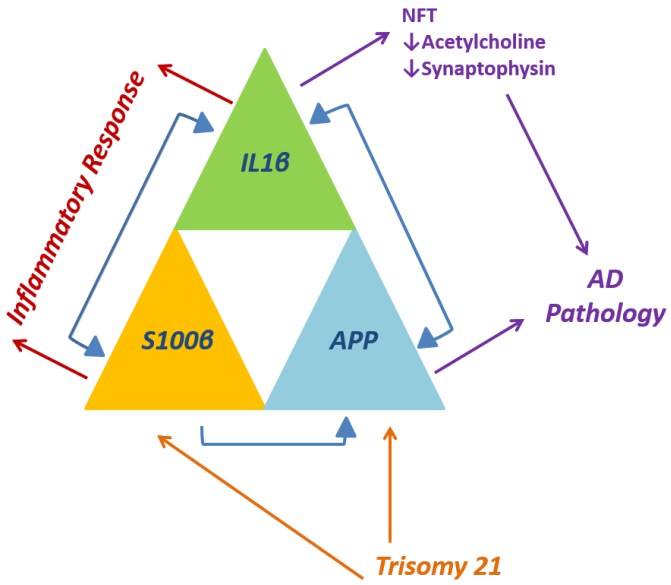

Fig. 9. Interplay between AD, Trisomy 21 and Inflammatory cytokine.

1.3.3 Crosstalk between Oxidative Stress and Inflammation

OS and inflammation are closely related processes and often are simultaneously found in many pathological conditions. It is important to note that OS can be induced by inflammation and vice-versa (Fig.10).

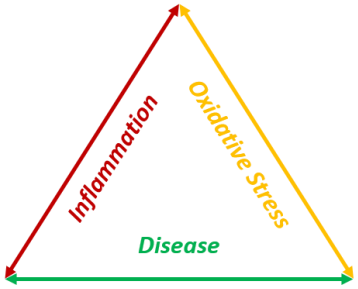

Fig 10. Inflammation and OS work together creating a vicious cycle.

In fact, inflammatory cells can release ROS/RNS promoting exaggerated OS [168], on the other hand, the ROS/RNS can initiate intracellular signaling cascade that enhances pro-inflammatory gene expression [169, 170]. Numerous studies support an interdependent relationship between inflammation and OS, as reviewed by *Brasier and Castellani* [171, 172]. Under pathological inflammatory conditions an increased generation of reactive species takes place as result of direct production by professional phagocytic cells or in response to proinflammatory cytokines by non-phagocytic cells [173, 174]. Recent finding suggests that the costimulation of TLRs produces OS with unbalance of pro-inflammatory and anti-inflammatory cytokine production [175] (Fig 11): i) IFNγ has been found to increase ROS production enhancing the expression of Duox2, a NADPH oxidase, through the TLR4-NF-*k*B pathway [173]; ii) IL-6 has been found to produce ROS increasing the expression of NADPH oxidase 4 (NOX4) as well as the NOX4 overexpression has been found to enhance IL-6 production [174].

Through, the increased OS can induce inflammation (Fig 11): i) H_2O_2 can activate NF-*k*B inducing the inflammatory responses [169, 170]; ii) The ROS released from damaged mitochondria has been shown to activate NOD-like receptor protein 3 (NLRP3) inflammasome an oligomeric molecular complex involved in the maturation of proinflammatory cytokines like IL-1β and IL-18 [176-178].Based on these observations it is possible to hypothesize the presence of a vicious cycle between mediators of inflammation and OS [179]. Thus, if OS appears as the early defect, inflammation will lastly evolve and will further exaggerate OS. Conversely, if inflammation is the primary abnormality, OS will develop its consequence and will further accentuate inflammation [179]. Therefore, identification of primary abnormality could be of great clinical importance, as the treatment of the primary cause is likely to ensure a sustained relief from the problem.

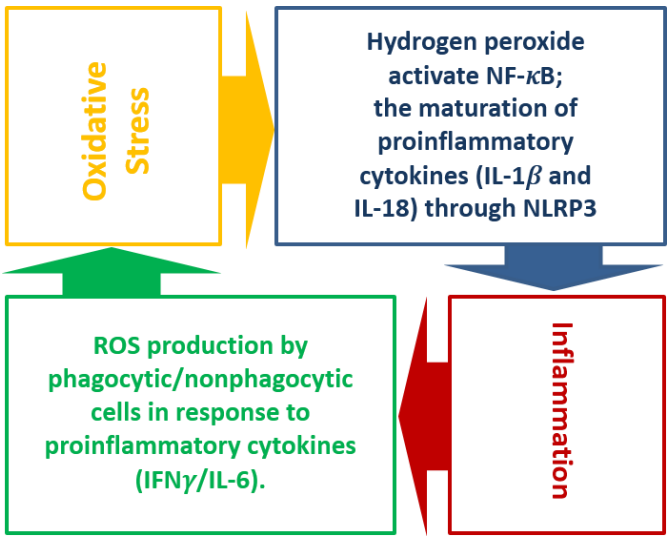

Fig 11. Interdependent relationship between inflammation and OS.

1.3.4 MicroRNA and Inflammation

MicroRNA (miRNA) are a class of highly conserved small non-coding RNA molecules, approximately 22 nucleotides in length, involved in the regulation of gene expression by binding the 3' untranslated region (3'-UTR) of target messenger RNAs (mRNAs). miRNAs act at post-transcriptional level promoting gene silencing through two distinct mechanisms sequence-dependent: i) cleavage of mRNAs with subsequent degradation or ii) translation inhibition of corresponding protein. Typically, a miRNA can bind to many targets and each target may be regulated by multiple miRNAs. Thus the miRNAs take part into many biological processes including differentiation, growth, homeostasis, stress responses and apoptosis. Increasing evidence supports also their involvement in brain development. Interestingly, compared with other organs, the brain has a particularly high percentage of tissue-specific and tissue-enriched miRNAs [180-183]. Although it has been suggested that the altered expression or function of miRNAs could critically contribute to brain injury including neurodegenerative diseases the full scope of miRNA-mediated regulation of brain functions is largely unknown. Mature miRNAs are transcribed from longer RNA molecules, with a stem loop structure, called primary miRNA (pri-miRNA) by RNA polymerase II or RNA polymerase III. Within the nucleus the pri-miRNA is cleaved by the Drosha-DGCR8 complex into a smaller RNA molecule termed pre-miRNA, which is then actively transported to the cytoplasm by Exportin 5 in complex with Ran-GTP. In the cytoplasm, the pre-miRNA is cleaved into mature miRNA with 3' overhangs by the Dicer-TRBP complex and finally loaded onto the Argonaute protein (AGO) to form the RNA-induced silencing complex (RISC). The miRNA in the RISC complex functions as a guide binding the 3'-UTR of target mRNAs in sequence-dependent manner and the degree of the complementarity between the miRNA and mRNA determine the gene silencing mechanism: slicer-dependent mRNA degradation or slicer-independent translation inhibition [184]. The

miRNAs, controlling the expression of different genes, in convergent or divergent manner, may affect diverse cellular and metabolic pathways and therefore profoundly influence the cellular behavior. Altered expression of miRNAs has been shown to be responsible for inducing different disease phenotypes including cancer, metabolic disorders, immune disorders and neurological abnormalities. In addition, several miRNAs have been shown to play a critical role in the microglia-mediated inflammatory response, such as miR-146a and miR-155. Both miR146a and miR155 are involved in the TLR-signaling, expressed in NF-*k*B-dependent manner and associated with IL-1β pathways [185]. Emerging evidence [186] shows that the IL-1β signaling is differentially modulated by overexpression of miR146a and miR155, which resulted in anti- or pro-inflammatory effects respectively (Fig. 12). miR-146a can modulate the TLR-signaling pathway by direct targeting of Interleukin-1 Receptor Associated Kinase-1 (IRAK1) and TNF receptor associated factor 6 ligase (TRAF6) [187-191], important components for activation of the TLRs signaling. miR146a blocks the TLR-signalling by suppressing NF-*k*B transcriptional activity and sequentially suppresses the production of type I IFNs, TNF, IL-1β, and IL-6 [188-190]. In contrast miR-155 inhibits Src homology 2 domain-containing inositol-5 -phosphatase 1 (SHIP1), a negative regulator of TLR-signaling to enhance the inflammatory responses [192-195]. SHIP1 negatively regulates TLR-signaling by inhibiting PI3K activation and suppressing ERK1/2, JNK and NF-*k*B pathways [196-198]. Both miR-146a and miR-155 seem to play a fundamental role in the microglial inflammatory profile. While miR-146a acts as a negative regulator of inflammation by suppressing NF-*k*B transcriptional activity, miR-155 acts to potentiate the microglial-mediated pro-inflammatory responses and may act as a negative feedback regulator of miR-146a and vice-versa.

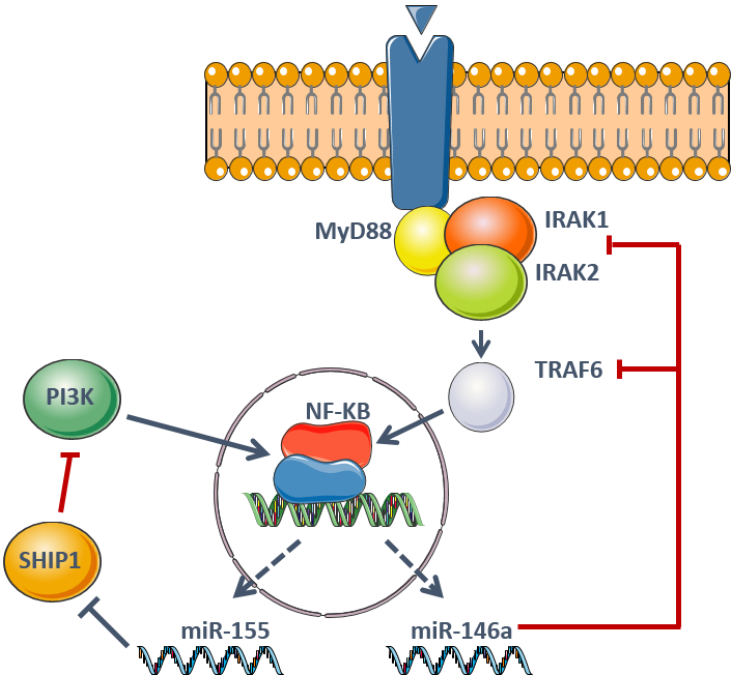

Fig. 12. Positive and negative regulation of inflammation mediated by miRNA. miR-155 and miR146 are induced by proinflammatory stimuli such as TLR ligands, LPS and cytokines such as IL-1β and through the activation of proinflammatory transcription factors NF-*k*B. miR-146 is thought to negatively regulate TLR signaling through control of expression of key signaling intermediates IRAK-1 and TRAF-6. In contrast miR-155 inhibits SHIP1 a negative regulator of TLR-signaling to enhance the inflammatory responses.

1.4 Insulin resistance in AD

Epidemiological studies have shown that glucose intolerance and impairment of insulin secretion are associated with a higher risk to develop dementia [199-202]. Insulin is a peptide released from pancreatic β-cells under hyperglycemic conditions and is transported into the CNS across the blood brain barrier (BBB) by a saturable receptor-mediated process [203, 204]. A portion of the insulin is locally produced in the CNS as proved by the detection of c-peptide (which is an integral part of the pro-insulin molecule) and insulin mRNA in the brain [205].

In the brain the activation of insulin signaling cascade does not induce a significant glucose uptake [206, 207] as it does in peripheral tissues, but, rather it modulates energy homeostasis, neuronal survival, longevity, learning and memory [208, 209] (Fig. 13). The binding of insulin to insulin receptor (IR) induces the autophosphorylation of specific Tyr residues on the β-subunit of the receptor with the consequent recruitment of the insulin receptor substrate-1 (IRS-1) [20, 210]. This latter, in turn, activates two main signaling pathways (Fig. 13): i) PI3K pathway, which is involved in the maintenance of synaptic plasticity and memory consolidation [211, 212]; ii) MAPK cascade that is responsible for the induction of the genes required for neuronal and synapse growth, maintenance and repair processes, as well as serving like a modulator of hippocampal synaptic plasticity that underlies learning and memory [213]. The alteration of all these processes are potentially implicated in the development of neurodegenerative defects. AD brain is characterized by defective insulin signaling and postmortem AD brain shows reduced sensitivity of IR, reduced expression of IR and Insulin-Like Growth Factor receptors (IGF-1R) and hypophosphorylation of IR and IRS-1 (Fig. 13). These abnormalities in AD brain are convincingly linked with a dysregulation of the insulin machinery and consistent with an inadequate response to insulin known as BIR. Although BIR is now widely accepted to be one of the major risk factors for

driving the progression of AD pathology, the mechanisms that underlie this process are not fully elucidated.

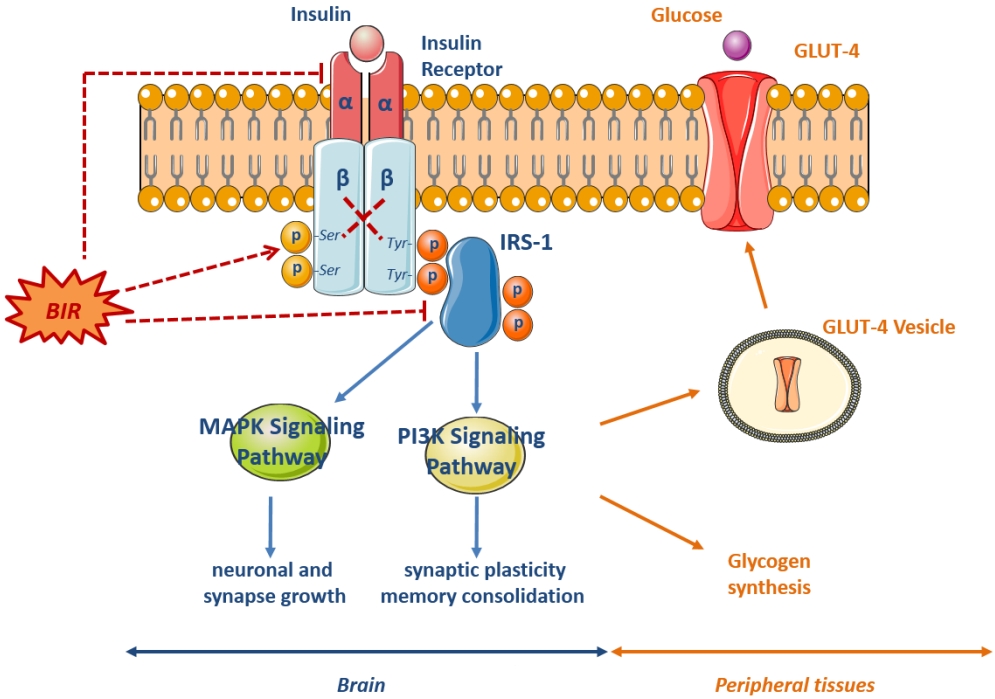

Fig. 13. Mechanism(s) underlying insulin resistance. Under normal conditions binding of insulin to IR promotes IR activation through IR dimerization and autophosphorylation of specific Tyr residues. Stimulation of IR kinase activity is then followed by Tyr phosphorylation of a variety of endogenous substrates, including IRS-1. These events lead to the activation of multiple signaling pathways required for insulin's pleiotropic action, including: (i) PI3K) pathway and (ii) MAPK pathway. In the brain the activation of insulin signaling cascade does not induce a significant glucose uptake but, rather it modulates energy homeostasis, neuronal survival, longevity, learning and memory. AD brain is characterized by defective insulin signaling with reduced sensitivity of IR, reduced expression of IR and hypophosphorylation of IR and IRS-1.

As mentioned before, BVR-A is characterized by the ability to carry out a Ser/ Thr/Tyr kinase activity through which BVR-A regulates cell signaling and gene expressions (reviewed in [97]). BVR-A kinase activity requires the phosphorylation of Tyr198/228/291 promoted by IR [214]. Therefore BVR-A is a direct target of IR kinase activity and once IR-phosphorylated is able to phosphorylates IRS1 on Ser inhibitory domains, thus representing an upstream regulator in the insulin signaling cascade [214] (Fig. 14). In addition, BVR-A contains specific motifs in its sequence through which modulates IR kinase activity both negatively and positively [215] (Fig. 14). Based on the involvement of BVR-A in the insulin signaling we hypothesize that an impairment of the kinase activity of BVR-A could be associated with the onset of BIR in AD.

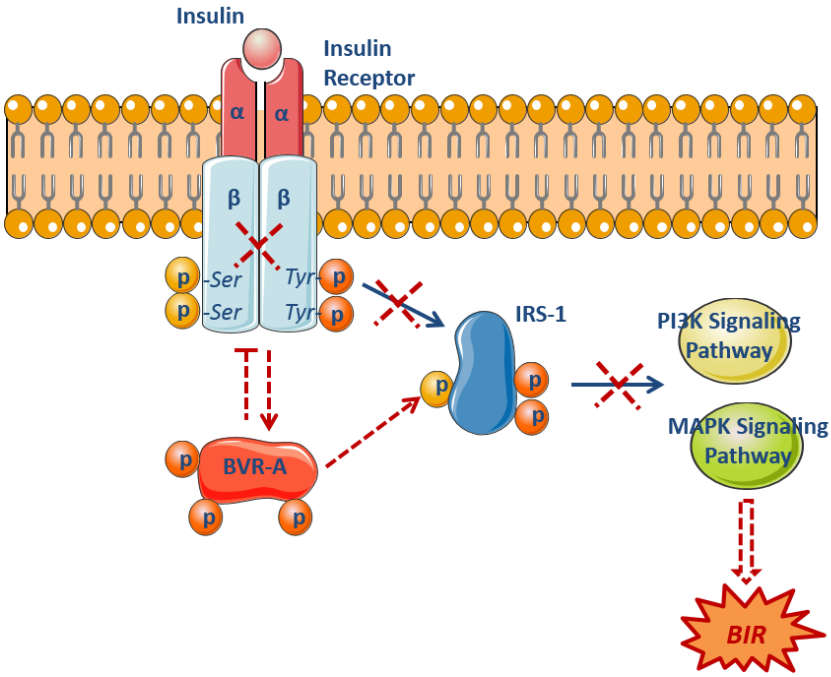

Fig. 14. Proposed mechanism leading to BIR in AD. BVR-A once IR-phosphorylated is able to phosphorylates IRS1 on Ser inhibitory domains. In addition, BVR-A modulates IR kinase activity both negatively and positively.

2 AIMS OF THIS WORK

Within this scenario, we focused our attention on the impairment of molecular pathways, including autophagy, insulin signaling and inflammation, that might be involved in neurodegenerative process responsible to the development of Alzheimer-like dementia in DS subjects. We propose that the alteration of these processes is joined by a "leitmotif" -OS- as cause and/or consequence of increased free radical burden. One of the main goals of this research is to clarify the intricate relationship between increased OS and alteration of mTOR/autophagy signaling. To this aim, we analyzed the mTOR axis in DS mouse model (Ts65Dn) at different ages and evaluated the effects of autophagy inhibition (by rapamycin) on protein oxidative damage in neuroblastoma cell line (SH-SY5Y) (*Project 1*).

Increasing evidence supports the involvement of inflammation-related miRNAs in neural development and neural function under pathological conditions [229-231]. We hypothesize that an inflammation-mediated dysregulation of both miR146a and miR155 could contribute to development of neurobehavioral abnormalities as well as contribute to age-related inflammatory neurodegenerative disorders including AD (*project 2*). To this purpose, we investigated the expression and cell-specific distribution of both miR146a and miR155 in the developing hippocampus from controls, DS subjects with and without AD pathology. In addition, we evaluated the levels of these miRNAs, their putative targets as well as the levels of IL-1β in human hippocampus from sporadic AD (sAD) at different stages of the disease and in experimental models of DS (Ts65Dn) and AD (APP/PS1mice). Based on the discovery that AD brain is characterized by BIR and because we previously demonstrated that OS induced impairment of BVR-A, an upstream inhibitory regulator in the insulin signaling, we hypothesize the involvement of OS-induced BVR-A dysregulation in the onset of BIR in AD (*Project 3*). To this

purpose, we evaluated the age dependent changes of (i) BVR-A levels and activation, (ii) total amount of OS markers (PC, HNE, 3-NT) as well as (iii) IR/IRS1 levels and activation in AD mouse model (3xTg-AD). Furthermore, *ad hoc* in-vitro experiments have been performed to clarify the contribution of ROS/RNS on insulin resistance and considering that mTOR is able to phosphorylate IRS1 we investigated whether the insulin resistance is associated with mTOR hyperactivation.

3 MATERIALS AND METHODS

3.1 Cell Culture and Treatment

The SH-SY5Y neuroblastoma cells were grown in Dulbecco's modified Eagle's medium (DMEM) supplemented with 10% fetal bovine serum (FBS), 2 mM L-glutamine, penicillin (20 U/ml) and streptomycin (20 mg/ml; GIBCO, Gaithersburg, Md., USA). Cells were maintained at 37°C in a saturated humidity atmosphere containing 95% air and 5% CO_2.

Rapamycin Treatment SH-SY5Y were seeded at a $40 \times 10^3/ cm^2$ density in 6-well culture dishes. After 24 h incubation, the medium was replaced with DMEM with 1% FBS for the starved group (St) and DMEM with 1% FBS and rapamycin (Pfizer Italia, Latina, Italy) 1μM for the rapamycin-treated (Rp) group. Rapamycin treatment was repeated daily to maintain the inhibition of mTOR, and cells were harvested at 24, 48 and 72h after the first treatment. Experimental analyses were performed on SH-SY5Y cells prior to rapamycin treatment to assess the subchronic increase in OS cells cultured with 1% FBS, as also reported by literature data [216, 217] and to assess the therapeutic concentration of rapamycin (data not shown).

Insulin Treatment SH-SY5Y were seeded at a $40 \times 10^3/ cm^2$ density in 6-well culture dishes. To test the responsiveness of our cellular model to insulin signaling the cells were pre-treated with insulin (Humulin, Ely-Lilly, Inadianapolis, IN, USA) 0.1 μM or vehicle (PBS) for 24 h. Insulin concentration has been selected based on previous reports [218, 219]. Then, medium was discarded, cells were washed twice with PBS, and rechallenged with DMEM with 1% FBS containing insulin (0.1–0.5–1–5 μM) or vehicle (PBS) for an additional hour to mimic insulin over-exposure.

Peroxynitrite/Hydrogen peroxide Treatment SH-SY5Y were seeded at a 40×10^3/ cm^2 density in 6-well culture dishes. After 24 h incubation, the medium was replaced with DMEM with 1% FBS and the cells were treated with peroxynitrite (ONOO, 50–500 µM) or hydrogen peroxide (H_2O_2, 1–50 µM) (Sigma-Aldrich, St Louis, MO, USA, #16911) or vehicle (PBS) for 24 h.

BVR-A Silencing To test the effects of BVR-A silencing on the insulin signaling, SH-SY5Y were seeded at a 40×10^3/ cm^2 density in 6-well culture dishes. After 24 h incubation, medium was replaced with DMEM with 1% FBS without antibiotics and the cells were treated in parallel with insulin (0.1 µM), transfected with 25pmol of BVR-A small-interfering RNA (siRNA) (Ambion, Life Technologies, LuBioScience GmbH, Lucerne, Switzerland, #4392420) using Lipofectamine RNAiMAX reagent (Invitrogen, Life Technologies, LuBioScience GmbH, Lucerne, Switzerland, #13778-030) according to the manufacturer's protocol, or co-treated with insulin (0.1 µM) and BVR-A siRNA for 24 h. At the end of each treatment, cells were washed twice with ice could PBS, collected by mechanical scraping and the proteins were extracted as described below.

3.2 Animals

Mice were housed in clear Plexiglas cages (20 × 22 × 20 cm) under standard laboratory conditions at a temperature of 22 ± 2°C, 70% humidity, 12 h light/dark cycle and free access to food and water. All the experiments were performed in strict compliance with animal welfare National Laws (DL 116/92) and European Communities Council Directives (86/609/EEC). All efforts were made to minimize the number of animals used in the study and their suffering. Animals were sacrificed at the selected age and brain area sectioned and store at -80°C until use.

Ts65Dn mice were generated by repeatedly backcrossing Ts65Dn trisomic females with (C57BL/6JxC3H/HeJ) F1 hybrid males; the parental generations were purchased from The Jackson Laboratories Inc. These breeding pairs produce litters containing both trisomic (Ts65Dn) and disomic (2N) offspring. The animals employed in this study were produced by two generations of backcrossing. Pups were genotyped to determine the trisomy using standard PCR, as described by Reinholdt et al. [220]. In addition, in all animals the recessive retinal degeneration 1 mutation (Pdebrd1), which results in blindness in homozygotes, was detected by using a standard PCR [221]. Mice were sacrificed at 4-5 weeks and at 6, 12 and 18 months of age, hippocampus and frontal cortex ware extracted (Ts65Dn mice, n= 23; 5M/18F), flash-frozen and stored at -80°C until further use.

3xTg-AD mice represent a mouse model of Alzheimer's disease that express 3 mutant human genes (APPSwe, PS1M146V, and tauP301L) and have been genetically engineered by *La Ferla and colleagues* at the Department of Neurobiology and Behavior, University of California, Irvine [222]. Colonies of homozygous 3xTg-AD and WT mice were established at the vivarium of the Experimental Zooprophylactic Institute of Puglia and Basilicata (Foggia, Italy).
The 3xTg-AD mice background strain is C57BL6/129SvJ hybrid and genotypes were confirmed by PCR on tail biopsies [222]. 3, 6, 12 and 18 months-old 3xTg-AD male mice (n=6 per group) and their wild-type (WT) male littermates (n=6 per group) were sacrificed and the hippocampus was extracted, flash-frozen, and stored at -80°C until further use.

APP/PS1 mice are a double transgenic mouse model of AD, which express a chimeric mouse/human amyloid precursor protein (APP, Mo/HuAPP695swe: APP Swedish mutation) and a mutant human Presenilin 1 (PS1-dE9), leading to an increased in the amount and an accelerated deposition rate of Aβ throughout the brain and memory impairment earlier than single APP transgenic littermates. Hippocampi from wild type (WT) and APP-PS1 male mice were collected at 3, 11-13 and 19-21 months of age (n=5). Brain tissue was fresh-frozen in liquid nitrogen and stored at -80°C until used for RNA isolation.

3.3 Human material

The subjects included in this study were selected from the databases of the Departments of Neuropathology of the Academic Medical Center, University of Amsterdam, The Netherlands, from the Institute of Neurology, Medical University of Vienna, Austria (in the frame of a project approved by the Ethical Committee of the Medical University of Vienna, entitled "Molecular neuropathologic examinations of neurodegeneration-related proteins in Down-syndrome, Ek Nr. 1316/2012), from the Netherlands Brain Bank (NBB) and from the Institut de Neuropatologia, Servicio Anatomia Patologica, Hospital Bellvitge, Barcelona, Spain. Informed consent was obtained for the use of brain tissue and for access to medical records for research purposes. Tissue was obtained and used in a manner compliant with the Declaration of Helsinki and the Academic Medical Center (AMC) Research Code provided by the Medical Ethics Committee of the AMC (Amsterdam, The Netherlands). The local ethical committees of the participating centers gave permission to undertake the study. We included brains of fetuses at different gestational weeks (9-41 GW), neonates and children from control and DS patients (Table 1). Fetal brains were preserved after spontaneous or induced abortions with appropriate maternal written consent for brain autopsy. We performed a careful histological and immunohistochemical analysis and evaluation of clinical data (including genetic data, when available). We only included, as control cases, specimens displaying a normal hippocampal and cortical structure for the corresponding age and without any significant brain pathology. Furthermore (Table 1), we obtained adult brain tissue at autopsy from adult controls (without evidence of degenerative changes, and lacking a clinical history of cognitive impairment), DS patients with AD and sAD cases at different stages of the disease; pathology was staged according to criteria recommended for neurofibrillary degeneration [223]. We acknowledge that in studies using

postmortem fetal tissue the availability of brain tissue represent a major limitation, because the number of cases with permission for brain autopsy at early developmental stages is limited and frozen representative material (i.e. hippocampus) is often not available.

Table 1. Cases included in this study (hippocampus)

Group	***Age range***	***n***	***Sex (m/f)***
Controls	13-23 gw	10	5/5
	24-32 gw	12	7/5
	33-41 gw	8	4/4
	1-15 d	6	3/3
	2 -8 m	8	4/4
	1-15 yrs	5	2/3
	25-86 yrs	30	15/15
Down Syndrome	14-23 gw	10	5/5
	24-32 gw	5	2/3
	33-41 gw	5	2/3
	1-15 d	5	3/2
	2 -8 m	5	3/2
	1-15 yrs	5	2/3
	50-64 yrs	6; 3, stage V; 3, VI;	4/2
Alzheimer's disease	61-99 yrs	26: 9 stage II; 8 stage III; 9 stage IV	15/11

gw: weeks of gestation; d/wk/yrs: postnatal days/weeks years; m = male; f = female; neurofibrillary tangle, NFT stage: II-VI.

3.4 Sample Preparation and Western blot analysis

Total protein extracts were prepared in RIPA buffer (pH 7.4) containing Tris-HCl (50 mM, pH 7.4), NaCl (150 mM), 1% NP-40, 0.25% sodium deoxycholate, EDTA (1 mM), 0.1% sodium dodecyl sulfate (SDS), supplemented with proteases inhibitors [phenylmethylsulfonyl fluoride (PMSF, 1 mM), sodium fluoride (NaF, 1 mM) and sodium orthovanadate (Na3VO4, 1 mM)]. Hippocampus, frontal cortex and the cellular pellets of different treatment were homogenized by 20 passes with a Wheaton tissue homogenizer and centrifuged for 1h at 16,000 g, 4°C to remove cellular debris. The supernatant was then extracted to determine the total protein concentration by the bicinchoninic acid assay (Pierce, Rockford, IL., USA). For Western blots, 30μg of were resolved on 12% and 7.5% SDS–PAGE using Criterion Gel TGX and blotted onto a nitrocellulose membrane (Bio-Rad, Hercules, Calif., USA). Before the transfer process, the image of the total protein load was acquired to perform normalization of blot data analysis. The membranes were blocked with 3% bovine serum albumin in 0.5% Tween-20/Trisbuffered saline (TTBS) and incubated overnight at 4°C with primary antibodies: anti-BVR-A (1:5000, abcam, Cambridge, United Kingdom, #ab90491), anti-BVR-A (1:1000, Sigma-Aldrich, St Louis, MO, USA, #B8437), anti-IRβ (1:1000, Cell Signaling, Bioconcept, Allschwill, Switzerland, #3020), anti-phospho(Tyr1162/ 1163)-IRβ (1:500, Santa Cruz, Santa Cruz, CA, USA, #sc-25103), anti-IRS1 (1:1000, Cell Signaling, Bioconcept, Allschwill, Switzerland, #3407), anti-phospho(Ser307)-IRS1 (1:500, Cell Signalling, Bioconcept, Allschwill, Switzerland, #2381), anti-phospho (Tyr632)-IRS1 (1:500, Santa Cruz, Santa Cruz, CA, USA, #sc-17196), anti-mTOR (1:1000, Cell Signaling, Bioconcept, Allschwill, Switzerland, #2983), anti-phospho(Ser2448)-mTOR (1:500, Cell Signaling, Bioconcept, Allschwill, Switzerland, #5536), anti-HO1 (1:1000, Enzo Life Sciences, Farmingdale, NY, USA, #ADI-SPA-895), anti-TNF-α (1:1000, EMD Millipore, Billerica, MA, USA,

#AB1837P), anti-phospho-Tyrosine (1:2000, Cell Signaling, Bioconcept, Allschwill, Switzerland, #9416), anti-3NT (1:500, Santa Cruz, Santa Cruz, CA, USA, #sc-32757) and anti-LC3 (Novus Biologicals, Littleton, Colo., USA). After 3 washes with TTBS the membranes were incubated for 60 min at room temperature with anti-rabbit/mouse/goat IgG secondary antibody conjugated with horseradish peroxidase (1:5000; Sigma-Aldrich, St Louis, MO, USA). Membranes were developed with the Super Signal West Pico chemiluminescent substrate (Thermo Scientific, Waltham, MA, USA), acquired with Chemi-Doc MP (Bio-Rad, Hercules, CA, USA) and analyzed using Image Lab software (Bio-Rad, Hercules, CA, USA) that permits the normalization of a specific protein signal with the β-actin signal in the same lane or total proteins load.

3.5 Slot Blot

For total Protein Carbonyls (PC) levels: total protein extract samples (5µl), 12% SDS, and 20 mM 2,4- dinitrophenylhydrazine (DNPH) were incubated at room temperature for 20 min, followed by neutralization with neutralization solution (2 M Tris in 30% glycerol) and then loaded onto nitrocellulose membrane as described below.

For total (i) protein-bound 4-hydroxy-2-nonenals (HNE) and (ii) 3-nitrotyrosine (3-NT) levels: total protein extract samples (10µl), 10µl of Laemmli buffer containing 0.125 M Tris base, pH 6.8, 4% (v/v) SDS and 20% (v/v) glycerol were incubated for 20 min at room temperature and then loaded onto nitrocellulose membrane as described below.

The resulting samples (250 ng) were loaded in each well onto a nitrocellulose membrane with a slot blot apparatus under vacuum pressure. The membrane was blocked for 2h with a solution of 3% (w/v) bovine serum albumin in TBS containing 0.2% (v/v) Tween 20 and incubated with anti-2,4-dinitrophenylhydrazone (DNP) adducts polyclonal antibody (1:100, EMD

Millipore, Billerica, MA, USA, #MAB2223) or HNE polyclonal antibody (1:2000, Novus Biologicals, Abingdon, United Kingdom, #NB100-63093) or anti-3-NT polyclonal antibody (1:1000, Santa Cruz, Santa Cruz, CA, USA, #sc-32757), respectively, for 2 h at room temperature. Membranes were washed and incubated with anti-rabbit IgG alkaline phosphatase secondary antibody (1:5000, Sigma-Aldrich) for 1 h at room temperature. After 3 washes the membrane was developed with Sigma fast tablets (5-bromo-4-chloro-3-indolyl phosphate/nitroblue tetrazolium substrate [BCIP/NBT substrate]). Blots were dried, acquired with Chemi-Doc MP (Bio-Rad, Hercules, CA, USA) and analyzed using Image Lab software (Bio-Rad, Hercules, CA, USA). No non-specific binding of antibody to the membrane was observed.

3.6 Immunoprecipitation

The immunoprecipitation procedure was performed as previously described [224], with minor modifications. Briefly, 150 µg of proteins were dissolved in 500 µl of RIPA buffer (10 mM Tris, pH 7.6; 140 mM NaCl; 0.5% NP-40) supplemented with proteases inhibitors and incubated with 1 µg anti-BVR-A polyclonal antibody at 4°C overnight. Immunocomplexes were collected using protein A/G suspension for 2h at 4°C and washed 5 times with immunoprecipitation buffer. Immunoprecipitated BVR-A was recovered by re-suspending the pellets in reducing SDS buffers and electrophoresing them on 12% gels, followed by western blot analysis. Total BVR-A was used as a loading control as previously described [215, 219, 225, 226].

3.7 2′,7′-Dichlorofluorescein Assay

ROS levels were detected by the 2′,7′-dichlorofluorescein method [227] with minor modifications. Briefly, cells were challenged with 10 mM 2′,7′-dichlorofluorescein diacetate for 30 min in the incubator, then washed twice with PBS and finally gently scraped into 1 ml of PBS. The cellular suspension was then transferred into a fluorescence cuvette where the ROS-driven conversion to the highly fluorescent 2′,7′-dichlorofluorescein was monitored by fluorescence intensity measured by an FP 6300 Jasco spectrofluorometer with excitation wavelength at 502 nm (bandwidth 5 nm) and emission wavelength at 520 nm (bandwidth 5 nm).

3.8 BVR-A reductase activity

We determined BVR-A activity in hippocampal tissues extracted from both 3xTg-AD and WT mice using a BVR assay kit (Sigma-Aldrich, St Louis, MO, USA #CS1100) as per manufacturer's instructions with minor modification. Briefly, 150 µg of proteins were prepared for the assay and loaded in the 96 well plates. BVR positive control solution (2.5, 5, 10, 15 and 20 µL) was included in the assay for generation of a standard curve. 50 µL assay buffer and 150 µL working solution (containing NAPDH, substrate solution and assay buffer) were added to each standard and sample on the plate. The plate was placed on the UV–vis plate reader at 37°C and read every minute for 10 min. The reading at 5 min had a linear reaction rate, and was chosen for BVR activity calculations. Values are expressed as Unit (U)/ml [Unit definition as per manufacturer's instruction: 1 unit of BVR will transform 1 nanomole of biliverdin to bilirubin in an NADPH dependent reaction at pH 8.5 at 37°C].

3.9 Tissue preparation and *In situ* hybridization

Paraffin-embedded tissue was sectioned at 5 μm, mounted on pre-coated glass slides (Star Frost, Waldemar Knittel GmbH, Brunschweig, Germany), and used for in situ hybridizations and immunocytochemistry. Sections of all specimens were processed for hematoxylin and eosin (HE), as well as for immunocytochemical stainings for a number of neuronal and glial markers.

In situ hybridization (ISH) for miR146a and miR155 were performed on 5 μm thick FFPE tissue using 5′ - fluorescein (FAM) or 5′-3′ double digoxygenin (DIG)-labeled Superior probes as described previously [228]. The probe sequences used were: miR146a-5p: 5’ FAM-AacCcaTggAauTcaGuuCucA; miR155-5p: 5’ DIG-AccCcuAucAcgAuuAgcAuuaA -DIG (capital = LNA modification, small = 2-o-methyl modification) all from Ribotask ApS (Odense, Denmark). Briefly, after the sections were deparaffinized and heat treated to undo protein crosslinks (10 min at 120°C in a pressure cooker), the probes were hybridized at 56°C for 1h. The hybridization was detected with an alkaline phosphatase (AP)-labeled anti-DIG or anti-FAM antibody (Roche Applied Science, Basel, Switzerland). NBT/BCIP was used as chromogenic substrate for AP. Negative controls sections were with a scrambled probe or without any probe in the hybridization step and without primary antibody. Aβ (Mouse clone 6F/3D; DAKO; 1:200), was used in the routine immunocytochemical analysis of DS-AD and sAD cases. Single-label immunocytochemistry was developed using the Powervision kit (Immunologic, Duiven, The Netherlands). 3,3-Diaminobenzidine (Sigma, St. Louis, USA) was used as the chromogen. Sections were counterstained with hematoxylin. For the double-staining, combining immunohistochemistry with ISH, the sections were first processed for ISH and then processed for immunohistochemistry with glial fibrillary acidic protein (GFAP; monoclonal mouse, Sigma, St. Louis, Mo, USA; 1:4000), GFAPδ. polyclonal rabbit, Kindly provided by Dr. E.M. Hol [39]; 1:500),

Vimentin (mouse clone V9 DAKO, Glostrup, Denmark 1:1000) and HLA-DP/DQ/DR (HLA-DR, mouse clone CR3/43; Dako; 1:100) antibodies. Signal was detected using the chromogen 3-amino-9 ethylcarbazole (Sigma-Aldrich, St. Louis, MO, USA).

3.10 Evaluation of *In situ* hybridization

The intensity of labeling was evaluated, as previously described [229, 230], using a semi-quantitative scale ranging from 0 to 3 (0: negative; 1: weak; 2: moderate; 3: strong staining). The score represents the predominant cell staining intensity found for each case. The frequency of positive glial cells was also evaluated using a semi-quantitative scale ranging from 1 to 3, including score 1 (rare labeling observed in <10% of cells), 2 (sparse, labeling observed in 11 to 50% of cells), and 3 (high, labeling observed in >50% of cells) to assess the relative number of positive glial cells within the hippocampus. As proposed before [229-231], the product of these two values (intensity and frequency scores) was taken to give the overall score (total labeling score).

3.11 RNA isolation

For RNA isolation, frozen tissue material was homogenized in Qiazol Lysis Reagent (Qiagen Benelux, Venlo, The Netherlands). The total RNA including the miRNA fraction was isolated using the miRNeasy Mini kit (Qiagen Benelux, Venlo, the Netherlands) according to manufacturer's instructions. The concentration and purity of RNA were determined at 260/280 nm using a Nanodrop 2000 spectrophotometer (Thermo Scientific, Wilmington, DE, USA).

3.12 Real-time quantitative analysis (qPCR)

miRNA (miR146a, miR155 and the reference small nuclear RNAs, Rnu6B and Rnu44) expression was analyzed using Taqman microRNA assays (Applied Biosystems, Foster City, CA). cDNA was generated using Taqman MicroRNA reverse transcription kit (Applied Biosystems, Foster City, CA) according to manufacturer's instructions and the PCRs were run on a Roche Lightcycler 480 thermocycler (Roche Applied Science, Basel, Switzerland). Quantification of data was performed using the computer program LinRegPCR in which linear regression on the Log (fluorescence) per cycle number data is applied to determine the amplification efficiency per sample [232, 233]. The starting concentration of each specific product was divided by the starting concentration of reference genes (geometric mean of Rnu6B and Rnu44 values) and this ratio was compared between groups. To evaluate IL-1β and the miRNA targets (IRAK1, IRAK2, CFH, TRAF6, SHIP1), 2.5μg of total RNA was reverse-transcribed into cDNA using oligo dT primers. PCR primers (Eurogentec, Belgium) were designed using the Universal ProbeLibrary of Roche (https://www.roche-applied-science.com) on the basis of the reported cDNA sequences. We used the following primers: IL-1β (mouse, forward: tgaagttgacggaccccaaa; reverse: tgatgtgctgctgcgagatt; human, forward: gcatccagctacgaatctcc; reverse: gaaccagcatcttcctcagc), IRAK1 (mouse, forward: ggatcagctccaccttcaga; reverse: cccagaagaatgtccagtcg; human, forward: gcccgaggagtacatcaaga; reverse: ctctgaccagccaaggtctc), IRAK2 (mouse, forward: tctgccggaacacttcatca; reverse: ggtaaggacctcggccaata; human, forward: cctcctctgaggcctgtgt; reverse: tgatctcaatttgccacgaa), TRAF6 (mouse, forward: ttgcacattcagtgtttttgg; reverse: tgcaagtgtcgtgccaag; human, forward: tggcattacgagaagcagtg; reverse: tggacatttgtgacctgcat), CFH (mouse, forward: gaaaaaccaaagtgccgaga; reverse: ggaggtgatgtctccattgtc; human, forward:

cctgacctcccaatatgtaaaga; reverse: ttccttaacattcccattgagg), EF1A (human, forward: atccacctttgggtcgcttt; reverse: ccgcaactgtctgtctcatatcac), Small Nuclear Ribonucleoprotein D3 polypeptide 18kDa (SNRPD3, human, forward: atacagagatggccgagtgg; reverse: taacatgggtgcgttcttca), TATA box-binding protein (Tbp, mouse; foward: ggagaatcatggaccagaaca; reverse: gatgggaattccaggagtca) and hypoxanthine phosphoribosyl transferase (Hprt; mouse, forward: tcctcctcagaccgctttt; reverse: cctggttcatcatcgctaatc). For each PCR, a mastermix was prepared on ice, containing per sample: 1 µl cDNA, 2.5 µl of 2x SensiFAST^{TM} SYBR Green Reaction Mix (Bioline Inc, Taunton, MA, USA), 0.4 µM of both reverse and forward primers and the PCRs were run on a Roche Lightcycler 480 thermocycler (Roche Applied Science, Basel, Switzerland). Quantification of data was performed as described for the Taqman PCR and the starting concentration of each specific product was divided by the geometric mean of the starting concentration of reference genes (Tbp and Hprt for mouse; EF1A and SNRPD3 for human) and this ratio was compared between patient/control groups.

3.13 Immunohistochemistry

Briefly both 3xTg and WT mice at 3, 6, 12 and 18 months of age (n=3 per group, per genotype) were intra-cardioventricularly perfused with saline followed by fixation solution (4% paraformaldehyde in PBS 0.1 M, pH 7.4) at a flow rate of 36 ml min^{-1} [234]. Brains were post-fixed in the fixation solution for 1 day and then transferred in 0.02% sodium azide in PBS. Free-floating coronal sections of 50 μm thickness were obtained using a vibratome slicing system (microM, Walldorf, Germany) and stored at 4°C in 0.02% sodium azide in PBS. The endogenous peroxidase activity was quenched for 30 min in 0.3% H_2O_2. Sections were then pretreated in 90% formic acid and incubated overnight at 4°C either with the monoclonal 6E10 antibody (1:3000, Signet Laboratorie– Covance, Emeryville, CA, USA, #sig-39320) for Aβ staining, or with the human-specific anti-tau antibody, HT7 (1:2000, Thermo Scientific Pierce Product, Rockford, IL, USA, #MN1000). After removing the primary antibody in excess, sections were incubated with the appropriate secondary antibody and developed with diaminobenzidine substrate using the avidin-biotin horseradish peroxidase system (Vector Laboratories, Inc, Burlingame, CA, USA, #SK-4100; #PK-6100). All stained slices were viewed using a Nikon 80i Eclipse microscope equipped with a DS-U1 digital camera, and NIS-elements BR software (Nikon, Tokyo, Japan). The intensity of Aβ and tau immunostaining was measured semi-quantitatively as regional optical density using the Scion Image software, as previously reported [234-236]. Per each animal, measurements were obtained in at least 3 consecutive sections containing the region of interest. The averaged optical densities of non-immunoreactive regions of each section were used for background normalization.

3.14 Statistical Analysis

Statistical analysis was performed using Graphpad Prism® 5.0 software (Graphpad software Inc., La Jolla, CA, USA).

In the first project all data are expressed as means ± SD per group. All statistical analyses were performed using a nonparametric one-way ANOVA with post hoc Bonferroni t tests. $p < 0.05$ was considered significant.

In the second project the two-way ANOVA followed by the Bonferonni's post hoc test was used to analyze the effect of the Ts65Dn trisomy or the APP-PS1 mutation and age on the expression of miRNAs and their targets in Ts65Dn or APP-PS1 mice. To compare Alzheimer's patient samples of different Braak stages, a non-parametric Kruskal–Wallis test was used, followed by the Mann-Whitney U test to assess differences between individual groups. Correlations between miRNAs and their targets was assessed using the Spearman's rank test. A P value of < 0.05 was considered significant.

In the third project all data are presented as means ± SEM of n independent samples per group. Student's t test or a nonparametric one-way ANOVA with post hoc Turkey's t –tests were applied for statistical analysis. $P < 0.05$ was considered significantly different from the reference value.

4 RESULTS

4.1 Project 1: Increased mTOR Signaling Contributes to the Accumulation of Protein Oxidative Damage in Ts65Dn Mice

As previously described, an impairment in mTOR signaling causes the alteration of the autophagy-lysosome pathway (the major cellular pathway for the removal of Aβ and tau aggregates) resulting in abnormal protein aggregates, which characterizes both AD and DS pathology. Recent studies from our laboratory reported, in human DS samples, an early accumulation of protein oxidative damage concomitant with the alteration of mTOR/ autophagy signaling. However, the relationship between OS and mTOR/autophagy signaling is intricate and needs to be clarified. To this purpose, we analyzed the protein oxidation levels and the integrity of the mTOR axis in Ts65Dn mice at different ages compared with age-matched euploid mice as well as the effects of autophagy inhibition by blocking mTOR on protein oxidative damage in the SH-SY5Y cell line.

4.1.1 mTOR/autophagy axis and protein oxidation in Ts65Dn Mice

We evaluated, by Western Blot, the levels of mTOR and the levels of mTOR phosphorylated on Ser 2448 (which reflects the activation of the mTOR) in the hippocampus of Ts65Dn mice at 6 and 12 months of age. An increase of both expression and phosphorylation of mTOR was observed in Ts65Dn mice at 6 months of age compared with age-matched euploid controls (about 1.3-fold, $p<0.05$, and 1.4-fold, $p<0.05$, respectively; Fig. 14). In contrast, at 12 months mTOR did not show significant differences in the expression levels, between the two groups of comparison, but demonstrated alterations in the phosphorylation levels (about 1.35-fold, $p < 0.05$; Fig. 14). Based on the fact that mTOR controls in a negative manner the autophagy activity by inhibiting the autophagosome

formation, we evaluated by Western Blot the LC3 II/I ratio, which it is used as marker of autophagosome formation. Our data demonstrate that increased mTOR phosphorylation is associated with a significant decrease in the LC3 II/I ratio in Ts65Dn mice at both ages compared with euploid mice (about 0.8-fold, $p < 0.05$; Fig. 14). The evaluation of protein oxidation by slot blot showed an increase in protein nitration and protein-bound 4-hydroxynonenal but not of protein carbonyls in 12 months-old Ts65Dn mice compared with age-matched euploid mice (about 1.5-fold, $p < 0.05$; Fig. 14). These results indicate that, despite the early aberrant hyperphosphorylation of mTOR coupled with the reduction of autophagosome formation, protein oxidative damage become significant only in adult animals suggesting that the accumulation of oxidative damage become consistent only after chronic impairment of the mTOR/autophagy axis.

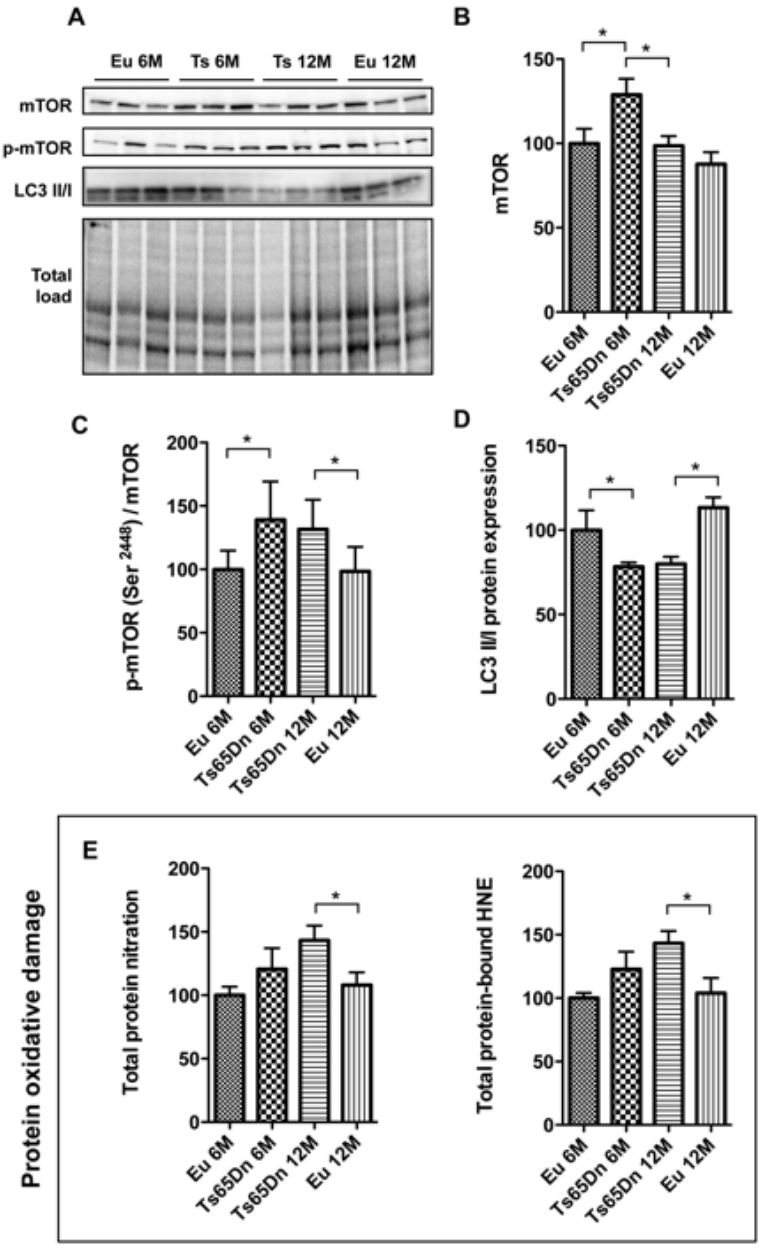

Fig. 14. mTOR signaling and protein oxidation in the Ts65Dn mouse hippocampus after 6 (6M) and 12 months (12M). (A) representative Western blot image with protein bands for mTOR expression levels, mTOR phosphorylation (Ser 2448) levels and LC3 (I and II) levels of samples from euploid (Eu) and Ts65Dn (Ts) mouse hippocampi at 6 and 12 months of age is shown. The analysis of experimental data is reported by histograms for mTOR expression (B), phosphorylated mTOR (pmTOR)/level ratio (C) and LC3 II/I ratio (D). (E) Data of total protein oxidation (protein-bound HNE and protein-bound 3-NT) obtained by slot blot analysis of euploid and Ts65Dn samples. Densitometric values shown in all the histograms are the mean of 8 individual samples per group normalized per total protein load and are displayed as percentage of euploid 6-month samples, set as 100%; * $p < 0.05$.

4.1.1 Effects of Rapamycin Treatment on Protein Oxidation in SH-SY5Y Cells

To confirm the involvement of the mTOR in the accumulation of the oxidative damage we evaluated the levels of protein oxidative modifications with inhibited mTOR in SH-SY5Y cell line treated with rapamycin for 24, 48 and 72h. The cells were cultured in DMEM with 10% FBS in control group, in DMEM with 1% FBS in the starved group (St) and in in DMEM with 1% FBS and 1μM of rapamycin added daily in rapamycin-treated group (Rp). Data on cell viability by MTT assay demonstrated no significant alterations in St and Rp group compared to controls (data not shown). The Western Blot data showed that rapamycin administration decreased mTOR expression when compared with control and St group after 24, 48 and 72h (about 0.6-, 0.55- and 0.5-fold, $p < 0.05$; Fig. 15). However only after a 72h treatment the levels of mTOR phosphorylated on Ser 2448 were reduced in the Rp group compared to St group. Nonetheless the autophagosome formation, as indexed by the LC3 II/I ratio, was increased in Rp group compared to St group already after 48h (about 1.7-fold, $p < 0.05$; Fig. 15) and 72h (about 1.3-fold, $p < 0.05$; Fig. 15) that was consistently with the decreased expression and phosphorylation of mTOR in Rp group at 24, 48 and 72h. Finally, a significant decrease of protein-bound 3-NT and protein-bound HNE levels were showed respectively at 48 h (about 0.8-fold, $p < 0.05$; Fig. 15) and 72 h (about 0.7-fold, $p < 0.05$; Fig. 15) and only at 72 h (about 0.8-fold, $p < 0.05$; Fig. 15) in Rp group compared to St group. Protein oxidation data were further confirmed by the analysis of total ROS production from the 2′,7′-dichlorofluorescein assay. Overall, our results prove that the rapamycin treatment, by inhibiting mTOR and enhancing the autophagosome formation, is able to reduce protein oxidative damage, thus confirming the involvement of the mTOR/autophagy axis in the protein oxidative buildup.

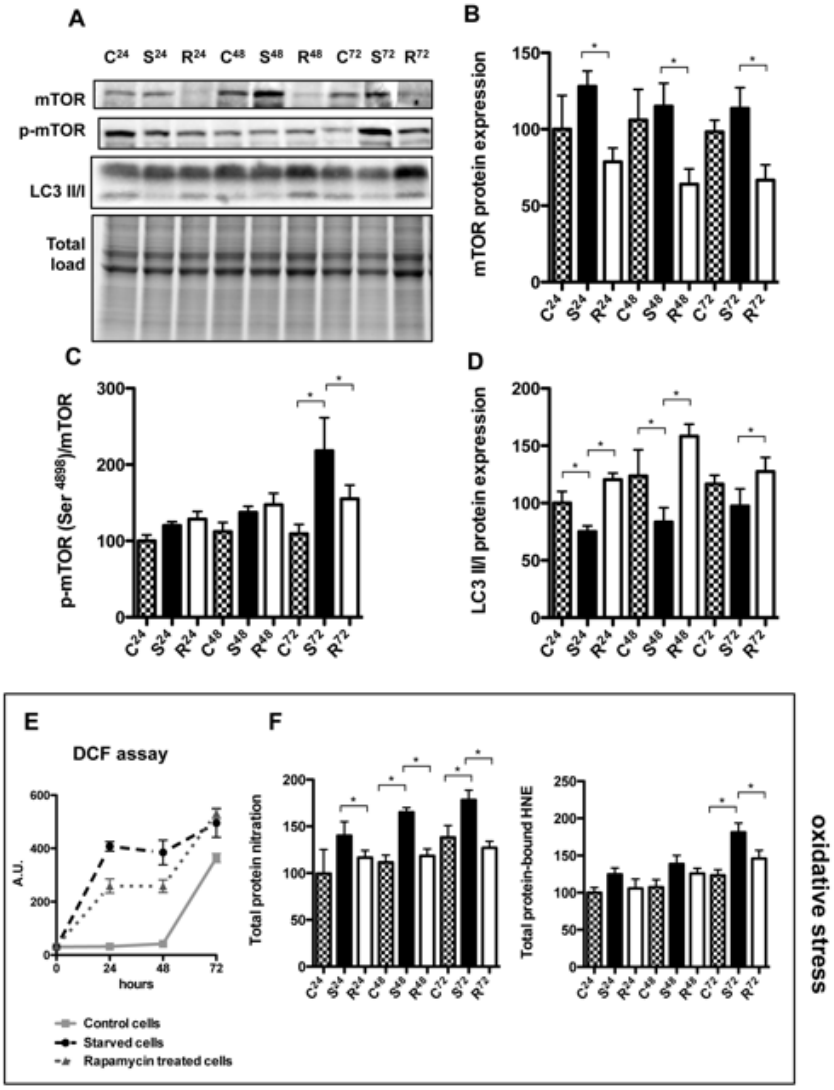

Fig. 15. mTOR signaling and protein oxidation in SH-SY5Y cells treated with rapamycin. (A) representative Western blot image with protein bands for mTOR expression levels, mTOR phosphorylation (Ser 2448) levels and LC3 (I and II) levels of SH-SY5Y samples from control cells (C), starved cells (S) and rapamycin-treated (R) groups is shown. The analysis of experimental data is reported by histograms for mTOR expression (B), phosphorylated mTOR (p-mTOR)/level ratio (C) and LC3 II/I ratio (D). (E) Data of total ROS production from the 2′,7′-dichlorofluorescein assay. (F) Data of total protein oxidation (protein-bound HNE and protein-bound 3-NT) obtained by slot blot analysis of cells treated or not with rapamycin. Densitometric values shown in all the histograms are the mean of 3 individual samples per group normalized per total protein load and are displayed as percentage of control at 24 h, set as 100%; * $p < 0.05$.

4.2 Project 2: Developmental expression and dysregulation of miR146a and miR155 in Down's syndrome and and Alzheimer's disease

As previously described, miRNAs are key post-transcriptional regulators of gene expression. Increasing evidence support their involvement in neural development and function under physiological and pathological conditions [237-239]. Therefore, their dysregulation can contribute to the development of neurobehavioral and neurodegenerative abnormalities.

miR146a and miR155 are two NF-κB-inducible miRNAs, associated with the activation of the IL-1β pathway and able to modulate astrocyte-mediated inflammation in culture. However little is known about their expression pattern in both development and aging of human brain. We hypothesized that the inflammation-mediated dysregulation of both miR146a and miR155 in fetal brain (i.e. in DS) could contribute to the development of neurobehavioral abnormalities, as well as, to age-related inflammatory neurodegenerative disorders including AD pathology. In order to clarify the potential link between deregulation of inflammation-related miRNAs, neurobehavioral deficits and AD-pathology; we investigated the expression and cell-specific distribution of both miR146a and miR155 in the developing hippocampus of healthy subjects, of patients with DS and in patients with DS-AD pathology. In addition, we evaluated the levels of these miRNAs, their putative targets as well as the levels of IL-1β in human hippocampus from sAD, at different stages of the disease, and in experimental mouse models of DS (Ts65Dn) and AD (APP/PS1).

4.2.1 miR146a and miR155 expression in the developing control hippocampus

By in situ hybridization, the hippocampal expression of miR146a and miR155 was investigated at different prenatal (from 13 to 41 GW) and postnatal ages (from day 1 to 8 months and 1-15 yrs; Table 1). The analysis showed that both miR146a (Fig. 16) and miR155 (Fig. 17) are detectable in the hippocampus in the second trimester of gestation. At GW 22 both miRNAs are expressed in neurons of the stratum pyramidale (CA1-CA3) and dentate gyrus (DG). Their expression persisted at later prenatal and postnatal age. In the second trimester of gestation, miR146a was also detected in the ventricular/subventicular zone (VZ/SVZ; Fig. 16) and co-localized with neuronal precursor markers (vimentin and GFAPδ). In adult control hippocampus both miRNAs are mainly detected in neuronal cells of the stratum pyramidale and in DG, whereas expression in astroglial cells within the hippocampal region was low or under detection level (Fig. 19A, Fig. 20A and Fig. 21 A-B).

4.2.1 miR146a and miR155 expression in the developing Down's syndrome hippocampus

In DS hippocampus, the expression pattern of miR146a and miR155 was similar to that observed in age-matched controls. Indeed both miR146a (Fig. 18) and miR155 (Fig. 16) were detectable in the second trimester of gestation in neurons of the stratum pyramidale (CA1-CA3) and in neurons of the DG, and their expression persisted at later prenatal and postnatal age. Similarly to controls also DS hippocampus showed miR146a in the VZ/SVZ (Fig. 18B,E). However, around mid-gestation we observed higher level of miR146a expression in astroglial cells within the hippocampal white matter, which persisted postnatally (Fig. 18G-H and Fig. 21 A-B).

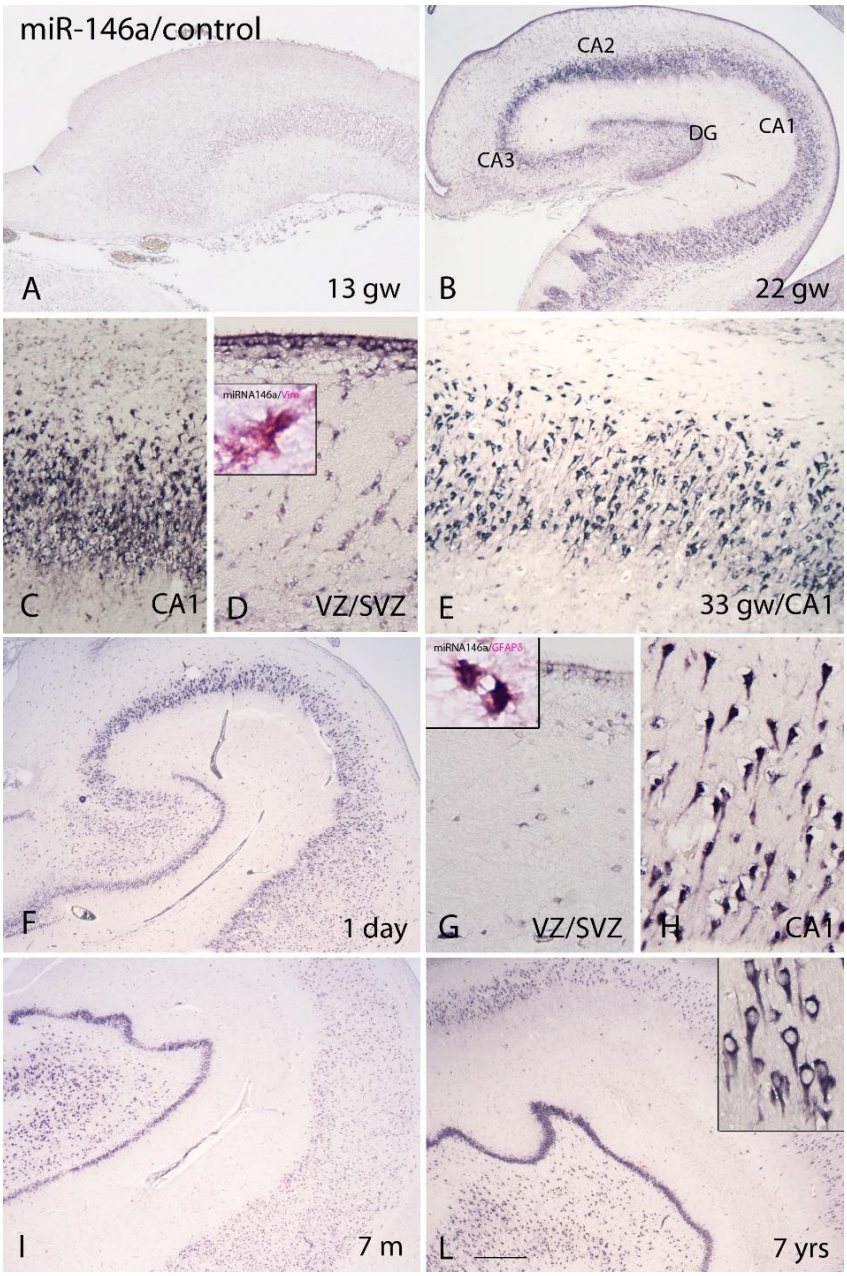

Fig. 16. *In situ* hybridization of miR146a at different developmental ages in the hippocampus. (A) miR146a expression in the hippocampus at 13 GW. (B-D**)**: miR146a at 22 GW, showing strong expression in the stratum pyramidale (CA1-CA3) and dentate gyrus; expression was also observed in the VZ/SVZ; insert in (D): co-localization with vimentin (Vim, red). (E): miR146a expression in the CA1 at 33 GW. (F-L) miR146a expression in the hippocampus at 1 day (F-H) 7 months (I) and 7 years (L; insert: high magnification of positive pyramidal neurons; CA1); insert in (G): co-localization with GFAPδ (red) in SVZ. Scale bar in (L). A: 200 µm; B, F, I,L: 400 µm; C,D,E,G: 80 µm; H: 45 µm.

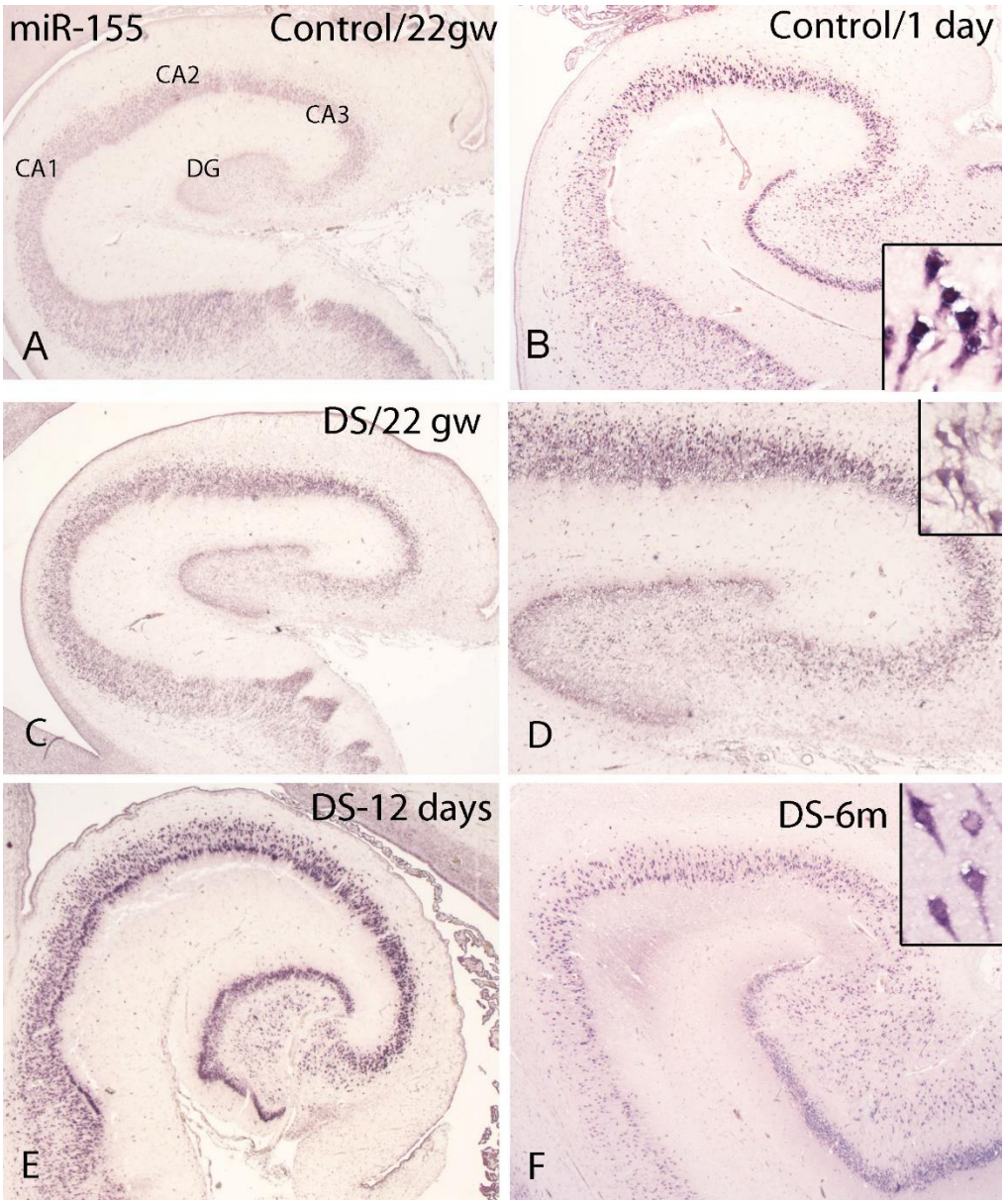

Fig. 17. *In situ* hybridization of miR155 at different developmental ages in control and DS hippocampus. (A-B): miR155 expression in the hippocampus at 22 GW (A) and at 1 day (B) with expression the stratum pyramidale (CA1-CA3) and dentate gyrus; (C-F): miR155 expression in the DS hippocampus at 22 GW (C-D) 12 days (E) 6 months (F; insert, CA1) showing neuronal miR155 expression throughout the different hippocampal subfields. Scale bar in (F). A-C, E, F: 400 µm; D: 200 µm.

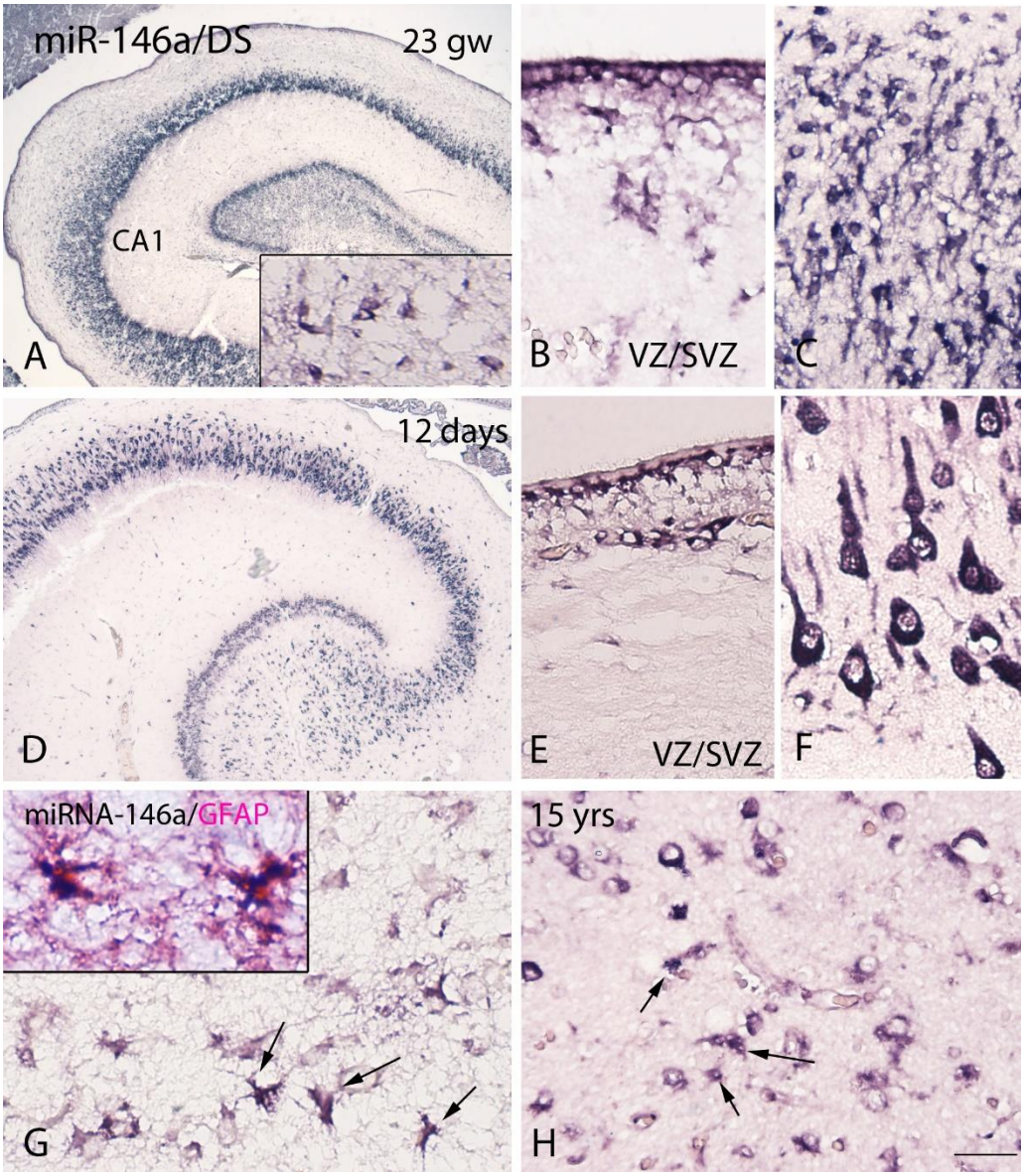

Fig. 18. *In situ* hybridization of miR146a at different gestational ages in DS hippocampus. (A-C): miR146a expression in the DS hippocampus at 22 GW; (A): the hippocampus shows strong expression in the stratum pyramidale and dentate gyrus (insert shows positive glial cells in the white matter,alveus.); (B): expression was also observed in VZ/SVZ; (C): neuronal expression in CA1. (D-G): postnatal DS hippocampus at 12 days showing miR146a expression throughout the different hippocampal subfields (D); expression was also observed in VZ/SVZ (E); F: neuronal expression in CA1; (G): glial expression in the white matter (arrows); insert: co-localization with GFAP (red). (H): miR146a expression in the DS hippocampus at 15 years (arrows indicate positive glial cells). Scale bar in (H). A, D: 400 µm; B,C, E, H: 40 µm; F,G: 30 µm.

4.2.2 miR146a and miR155 expression in Down's syndrome hippocampus with Alzheimer's disease pathology

In the hippocampus of DS adult with AD pathology we observed, compared to controls, increased expression of miR146a and miR155 in astrocytes throughout the different hippocampal regions, particularly in regions with Aβ deposits (Fig. 19, Fig. 20 and Fig. 21 A-B). Double labeling experiments confirmed the increased expression of both miR146a and miR155 in astrocytes of DS-AD patients (Fig. 19 and Fig. 20). Focally co-localization with a microglial marker (HLA-DR) was observed for miR146a (Fig. 19F); we also observed expression of miR155 in blood vessels (Fig. 20E-G; co-localization with CD34). Similar patterns of expression has been observed in specimens of sAD (Fig. 21C-D). qPCR analysis of miR146a and miR155 in cortical specimens from DS-AS (early stages of AD) did not show any difference in the level of expression compared to adult controls (not shown).

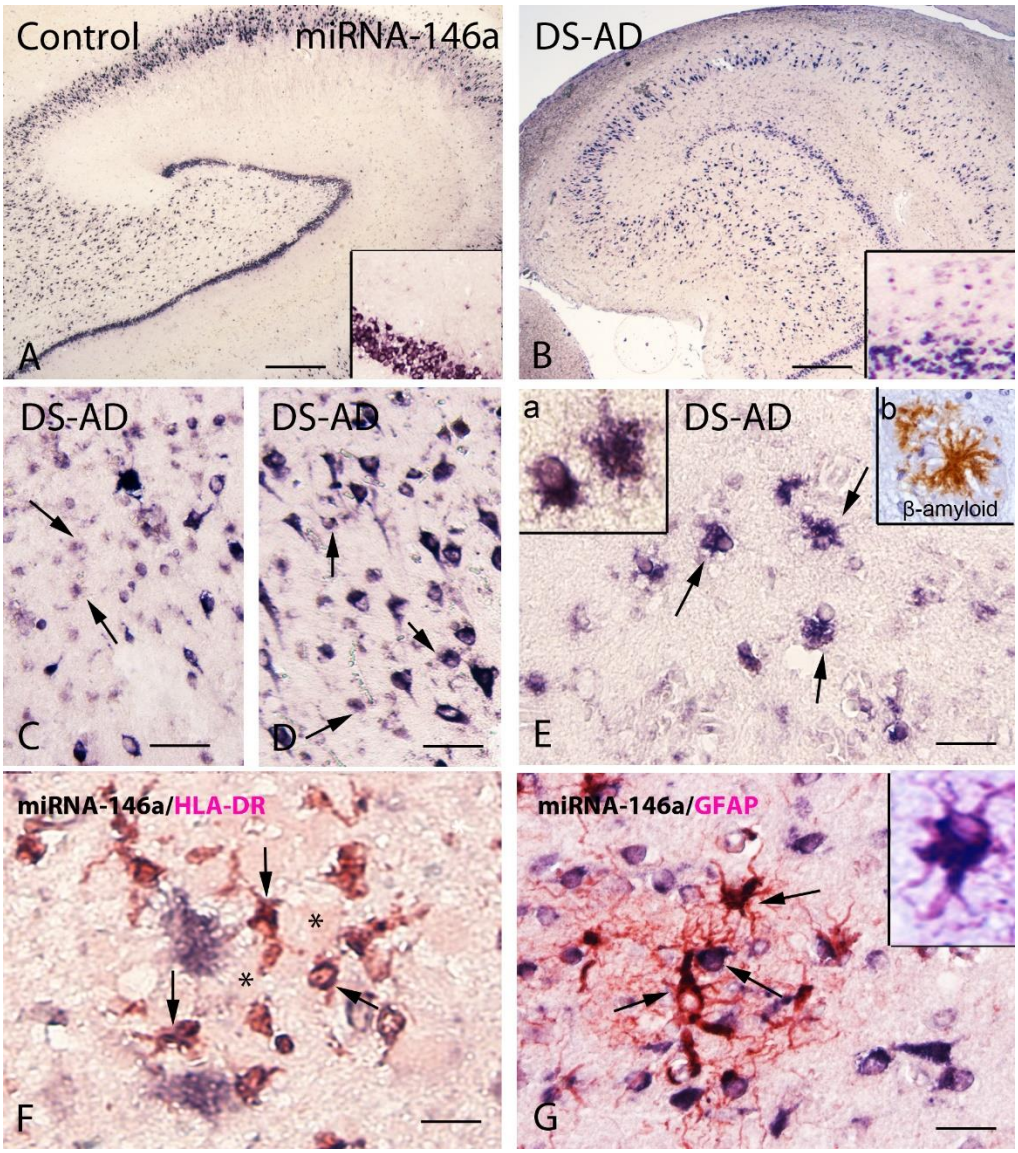

Fig. 19. *In situ* hybridization of miR146a in adult hippocampus of control and Down's syndrome with Alzheimer's disease pathology. (A) miR-146a expression in adult control hippocampus (insert: dentate gyrus). (B-E) miR-146a expression in adult DS-AD hippocampus; in DS-AD increased expression was observed in cells with glial morphology throughout the hippocampus (arrows in CA4, C; CA1, D, white matter E, high magnification in insert a; insert in B shows dentate gyrus with increased expression in the molecular layer; insert b in E, amyloid plaque). (F) miR-146a was focally detectable in HLA-DR positive cells (red, arrows; around amyloid deposits, asterisks). (G): expression of miR-146a was observed in GFAP positive cells (red; arrows and insert). Scale bar in G. A, B: 400 µm; C, D, F: 80 µm; E, G: 40 µm; F: 20 µm.

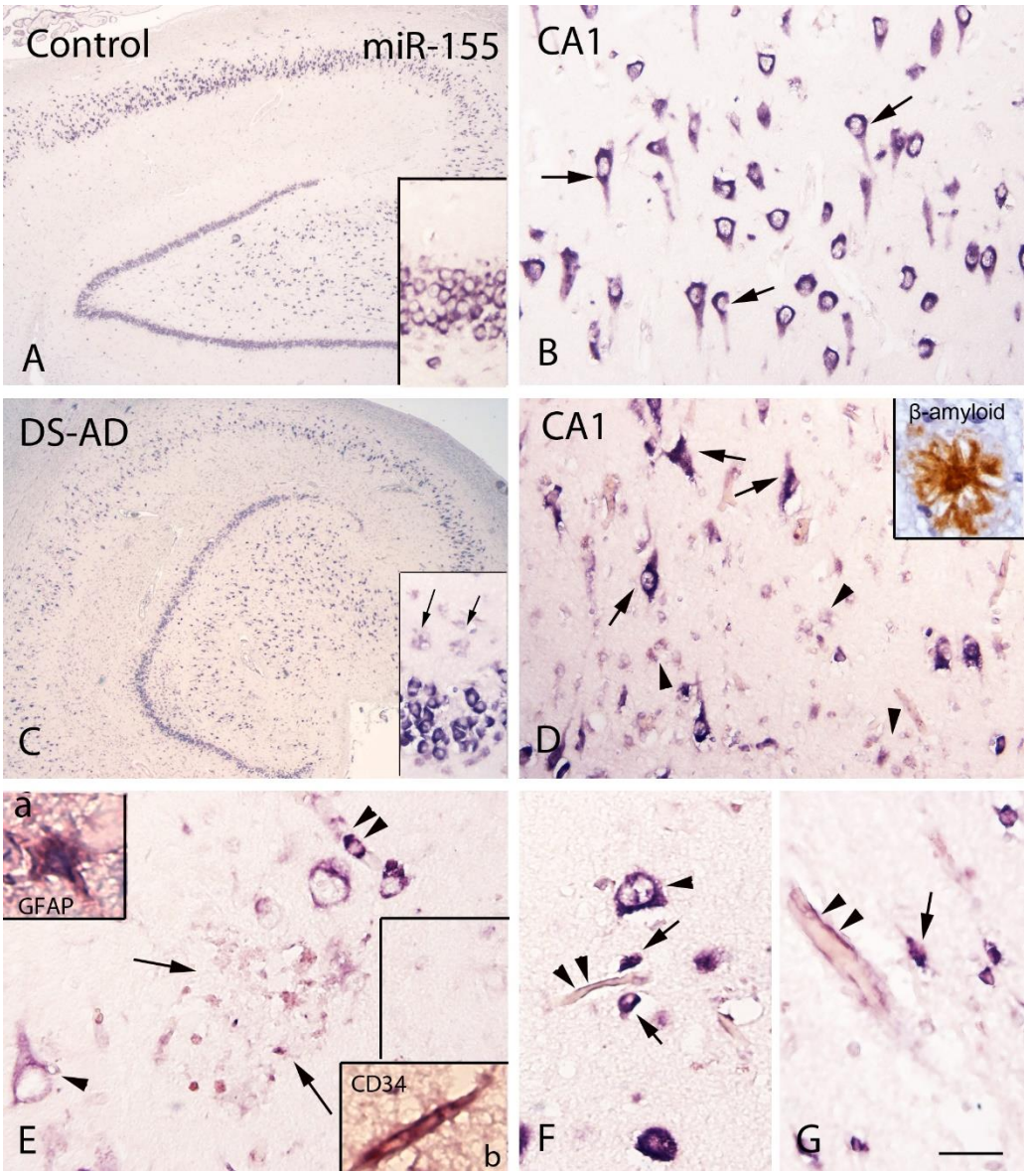

Fig. 20. *In situ* hybridization of miR155 in adult hippocampus of control and Down's syndrome with Alzheimer's disease pathology. (A-B): miR-155 expression in adult control; neuronal expression is detected throughout the different hippocampal subfields (insert in A: dentate gyrus, DG; arrows in B pyramidal neurons of CA1). (C-G) DS-AD hippocampus with slightly increased expression in cells with glial morphology in the molecular layer of the DG (insert in C) and in CA1 (D); insert D, amyloid plaque. Panels (E-G) show expression in glial cells (arrows), neurons arrowheads and in endothelial cells (double arrowheads); insert (a) in € shows expression in GFAP positive cells (red) and insert (b) in E colocalisation with CD34in a blood vessel. Scale bar in G. A, C: 400 µm; B, D: 80 µm; E-G: 40 µm.

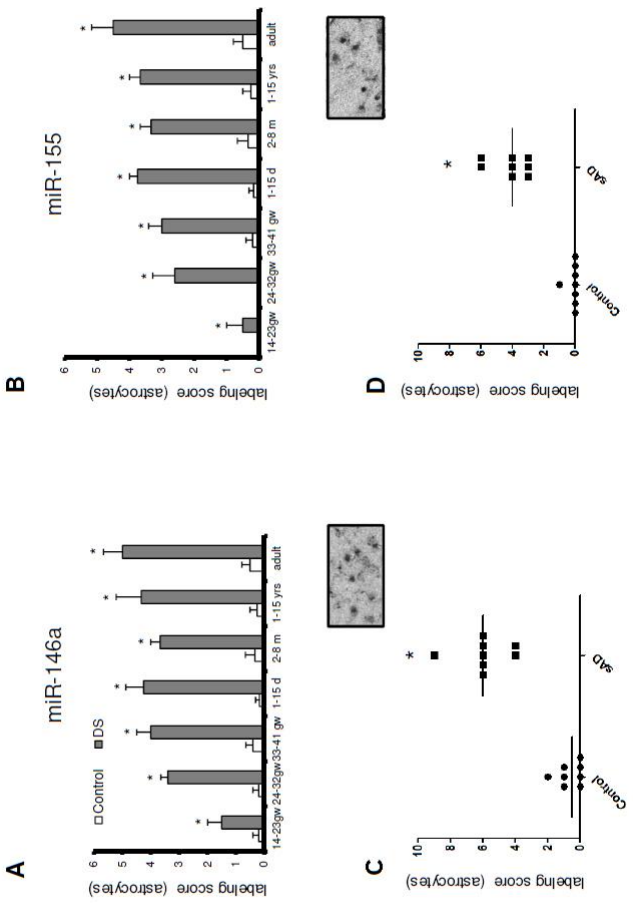

Fig 21. Evaluation of miR-146a and miR-155 astroglial expression. (A-B): labeling score of miR146a (A) and miR155 (B) in controls and DS during development and adult DS with AD pathology. (C-D) labeling score of miR-146a (C) and miR-155 (D) in controls (n= 8), and sAD (n= 8, stage III); inserts in (C-D) show positive astrocytes in sAD; Values represent the mean ± SEM of samples at ages. *p < 0.05, compared to control.

4.2.3 miR146a and miR155 expression in the Ts65Dn mice

The expression of miR146a and miR155 was analyzed by q-PCR in the hippocampus and frontal cortex of Ts65Dn mice. miR146a expression showed an age-dependent decrease in both Ts65Dn and control euploid mice with lower expression at 6-18 months compared to 4-5 week old mice in hippocampus and cortex (Fig. 22A,D). miR155 showed a different age-depend changes in both Ts65Dn and control euploid mice with lower expression at 6-18 months compared to 4-5 weeks in hippocampus (Fig. 22B) and higher expression at 6-18 months compared to the 4-5 weeks in cortex (Fig. 22E). Two-way ANOVA analysis showed a contribution of age to the expression of both miR146a (cortex: $F(3,41) = 24.08$, $P<0.0001$; hippocampus: $F(3,39) = 9.91$, $P<0.0001$) and miR155 (cortex: $F(3,39) = 45.2$, $P<0.0001$; hippocampus: $F(3,30) = 17.84$, $P<0.0001$) and also the interaction between Ts65Dn trisomy and age ($F(3,39) = 3.12$, $P=0.037$). In both hippocampus and cortex, IL-1β showed higher level of expression in older animals (6-18 months compared to 4-5 weeks) and at 18 months we observed increased expression of IL-1β in Ts65Dn compared to control euploid mice (Fig. 22C,F). Two-way ANOVA analysis showed a significant contribution of age (cortex: $F(3,41) = 33.85$, $P<0.0001$; hippocampus: $F(3,41) = 22.88$, $P<0.0001$) and the interaction between Ts65Dn trisomy and age (cortex: $F(3,41) = 8.00$, $P = 0.0003$; hippocampus: $F(3,41) = 3.13$, $P=0.36$) to the expression levels of IL1β. The Bonferroni's post-test showed a significantly increased expression of IL1β ($P<0.001$) in the Ts65Dn compared to control euploid mice at 18 months in the cortex only). Evaluation of the expression levels of downstream targets of miR146a (Irak1 and Traf6) and of miR155 (Ship1), showed higher expression of Traf6 in the cortex at 6-12 months compared to 4-5 week old mice (Fig. 22G). Two-way ANOVA analysis showed a significant contribution of age ($F(3,41) = 8.65$, $P=0.0001$), of trisomy ($F(1,41) = 5.75$, $P=0.21$) and a significant interaction of age and trisomy ($F(3,41) = 2.99$, $P=0.042$) to the expression of Traf6 in the

cortex. The Bonferroni's post-test showed significantly increased Traf6 expression in Ts65Dn compared to control euploid mice at 12 months ($P<0.05$). Expression of miR146a was negatively correlated (Spearman's rank correlation coefficient $r = -0.651$, $P=0.0008$) with the downstream target Traf6 in the cortex in the Ts65Dn mouse (Fig. 22H). Ship1 showed a trend towards increased expression with increasing age in the hippocampus and cortex in both control euploid and Ts65Dn mice (Fig. 23). Two-way ANOVA analysis of the hippocampus samples showed a significant contribution of trisomy ($F(1,41) = 4.11$, $P=0.049$) and age ($F(3,41) = 14.67$, $P<0.0001$) and the interaction between the two factors ($F(3,41) = 5.94$, $P=0.002$). Moreover, the Bonferroni's post-test showed significantly increased expression ($P<0.001$) of Ship1 in the Ts65Dn compared to control euploid mice at 6 months of age. Interestingly, in the cortex, although a significant contribution of age could be inferred ($F(3,41) = 8.48$, $P=0.0002$), there was neither an effect of the Ts65Dn trisomy nor an interaction effect. The Bonferroni's post-test did not reveal any significant differences between Ts65Dn and control euploid mice. Two-way ANOVA analysis showed a significant interaction effect of age and Ts65Dn trisomy on the expression of Irak2 in the hippocampi of Ts65Dn and control euploid mice ($F(3,41) = 6.88$, $P=0.0007$). Bonferroni's post-test showed a significant increase ($P<0.05$) in the expression of Irak2 in Ts65Dn compared to WT mice at 6 months age whereas a significant decrease ($p<0.05$) was observed at 18 months. No difference was observed in the expression of Irak2 in the cortex of Ts65Dn compared to control euploid control mice (Fig. 23). Furthermore, no differences were observed in the expression of Cfh in the hippocampus and cortex of Ts65Dn compared to euploid control mice (Fig. 23).

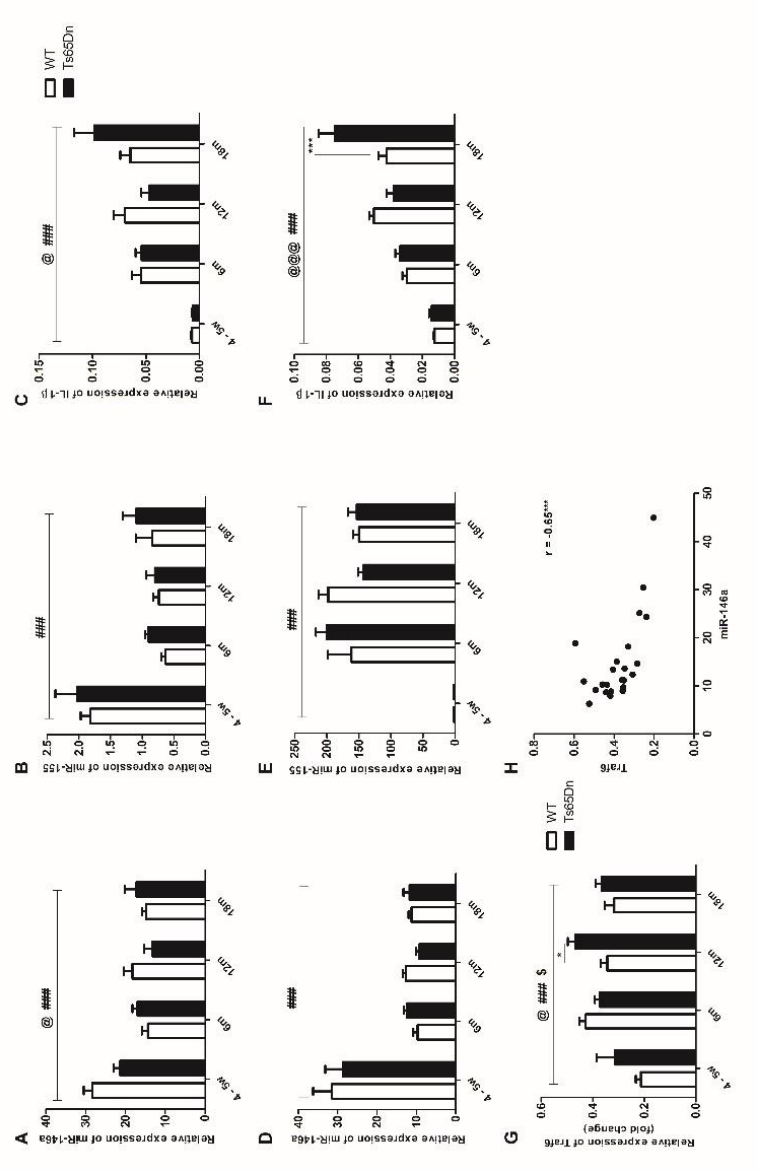

Fig. 22. Expression of miR146a, miR155, IL-1β and the miR146a target Traf6 in the Ts65Dn mouse. (A-G): qPCR of miR146a (A), miR155 (B), IL-1β (C) and Traf6 (G) in the hippocampus (A-C) and cortex (D-G) of the Ts65Dn mouse at 4– 5 weeks (n = 5) and 6 (n=6), 12 (n=6) and 18 months (n = 6) of age compared to age-matched euploid animals (n = 8 for 4-5weeks; n = 6 for 6, 12, 18 months). Data are expressed relative to the reference genes (geometric mean of Rnu6B and Rnu44 for the miRNAs and Tbp and Hprt for IL-1β and Traf6, respectively). The error bars represent standard error mean (SEM). Statistical significance : $ $p<0.05$ showing the effect of Ts65Dn segmental trisomy; ### $p<0.001$ showing the effect of age and @@, $P<0.01$ showing the interaction of Ts65Dn*age in a two-way ANOVA analysis. * $P<0.05$, ** $P<0.01$ and *** $P<0.001$ show statistical significance assessed by the Bonferroni's post-test (H): Scatter plots showing the significant negative correlation between miR146a and Traf6 in the cortex in the Ts65Dn mouse model; r = Spearman's rank correlation coefficient, ***$P<0.001$.

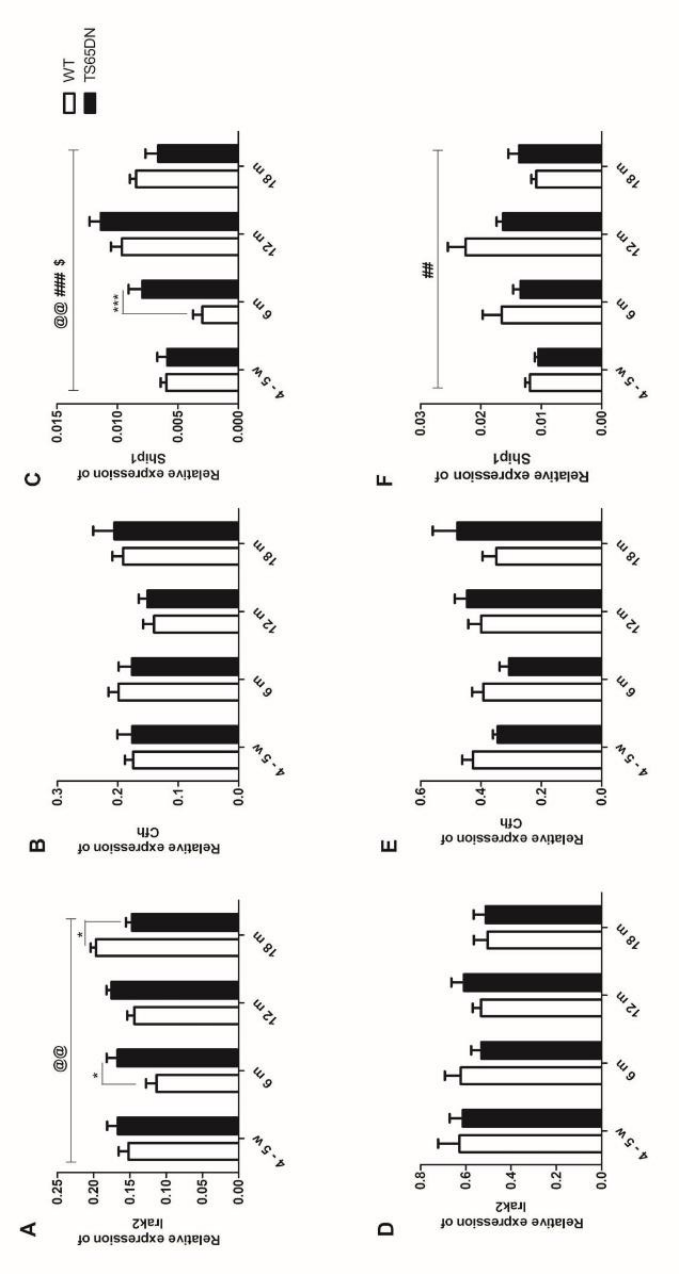

Fig. 23. Expression of Irak2, Cfh and Ship1 in the Ts65Dn mouse. (A-F): qPCR of Irak2, Cfh and Ship1 in the hippocampus (A-C) and cortex (D-F) of the Ts65Dn mouse at 4 – 5 weeks (n = 5) and 6 (n=6), 12 (n=6) and 18 months (n = 6) of age compared to age-matched euploid animals (n = 8 for 4/5weeks; n = 6 for 6, 12, 18 months). Data are expressed relative to the reference genes (geometric mean of Tbp and Hprt respectively). The error bars represent standard error of mean (SEM). Statistical significance : $, P<0.05 showing the effect of Ts65Dn segmental trisomy; ##, P<0.01, ###, P<0.001 showing the effect of age and @@, P<0.01 showing the interaction of Ts65Dn*age in a two-way ANOVA analysis. * P<0.05, ** P<0.01 and *** P<0.001 show statistical significance assessed by the Bonferroni's post-test.

4.2.4 miR146a and miR155 expression in the APP-PS1 mice

We analyzed the expression of miR146a and miR155 in the hippocampus of APP/PS1 mice using q-PCR (Fig. 24). At 3 months of age no difference in expression of miR146a and miR155 was seen between APP/PS1 and WT mice. APP/PS1 mice showed an increase in expression of both miR146a and miR155 at 11-13 months of age as compared to both WT and 3 months-old APP/PS1 mice (Fig. 24A-B). The expression decreased for the two miRNAs at 19-21 months of age, however it remained higher than both WT and APP/PS1 mice at 3 months of age, although this difference was not statistically significant. Two-way ANOVA showed a significant contribution of the APP/PS1 mutations (miR146a: $F(1,30) = 5.90, P<0.05$; miR155: $F(1,30) = 4.95$, $P<0.05$) and age (miR146a: $F(2,30) = 10.67, P<0.001$; miR155: $F(2,30) = 11.39$, $P<0.001$) to the increased expression of both miRNAs, but no interaction of the two factors. The Bonferroni's post-test showed increased expression of both miR146a and miR155 in APP/PS1 as compared to WT mice at 11-13 months of age ($P<0.05$). Increased expression of IL-1β was observed in the APP/PS1, compared to WT, at 11-13 months of age ($P<0.01$) persisting up to 19-21 months ($P<0.001$) (Fig. 24C). Two-way ANOVA showed a significant contribution of the APP/PS1 mutations ($F(1,30) = 20.29$, $P<0.0001$) and age ($F(2,30) = 8.11$, $P=0.0015$), and a significant interaction of the two factors ($F(2,30) = 6.98$, $P=0.0032$) to the increased IL-1β expression. A strong positive correlation ($r=0.8769$; $P<0.0001$) was observed between the expression of miR146a and miR155 within all the groups of mice (Fig. 24D). Positive correlation was also detected between both miR146a and miR155 and IL-1β (miR146, $r=0.459$; miR155, $r=0.579$; $P<0.05$; Fig. 24E-F). In addition, we also studied, by qPCR, the expression of Irak1 and Traf6 (targets of miR146a) and Ship1 (target of miR155) in APP/PS1 compared to WT mice. Irak1 and Traf6 showed a lower expression in APP/PS1 compared to WT mice already at 3 months of age ($P<0.05$ and $P<0.01$ respectively). The expression further declined at 11-13 months of age

as compared to 3 months in both APP/PS1 and WT mice (Fig. 24G-H). Two-way ANOVA showed a significant contribution of age (Irak1: $F(2,30) = 7.69$, $P=0.002$; Traf6: $F(2,30) = 21.06$, $P<0.0001$) and of the APP/PS1 (Irak1: $F(1,30) = 13.39$, $P=0.001$; Traf6: $F(1,30) = 10.81$, $P=0.0026$) mutation to this decrease without any significant interaction. Ship1 (target of miR155) showed a time-dependent increased expression in the APP/PS1 mice, with significantly higher expression levels when compared to WT mice at 19-21 months of age ($P<0.001$). Two-way ANOVA demonstrated a strong effect of both age (Irak1: $F(2,30) = 7.69$, $P=0.002$; Traf6: $F(2,30) = 21.06$, $P<0.0001$) and APP/PS1 mutation (Irak1: $F(1,30) = 13.39$, $P=0.001$; Traf6: $F(1,30) = 10.81$, $P=0.0026$) (Fig 25). A strong negative correlation was observed between the expression levels of miR146a and Traf6 (Spearman's rank correlation coefficient, $r=-0.427$, $P=0.009$) whereas Irak1 showed a trend towards negative correlation ($r=-0.275$) (Fig. 24I-J). No difference in expression of Irak2 and Cfh was observed in the hippocampi of APP/PS1 compared to control mice, although two-way ANOVA showed an age effect for Irak2 across the samples ($F(2,30 = 7.53$, $P=0.002$) (Fig. 25).

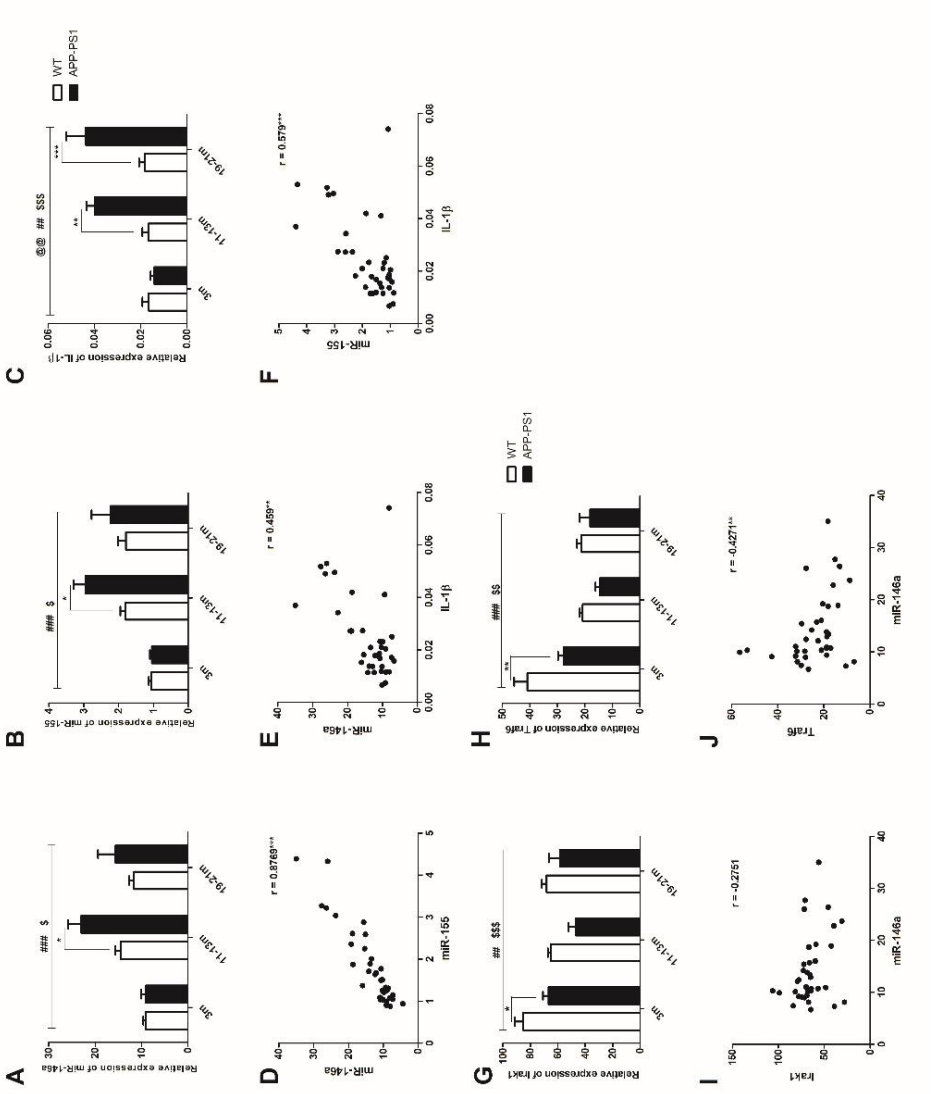

Fig.24.Expression of miR146a, miR155, IL-1β and the miR146a target Irak1 and Traf6 in the APP-PS1 mouse. (A-C), (G), (H): qPCR of miR146a (A), miR155 (B), IL-1β (C), Irak1 (G) and Traf6 (H) in the hippocampi of APP-PS1 mice at 3 (n=6), 11-13 (n=6) and 19-21 months (n=6) compared to WT mice (n=6 for 3, 11-13 and 19-21 months respectively). Data are expressed relative to the reference genes (geometric mean of Rnu6B and Rnu44 for the miRNAs and Tbp and Hprt for IL-1β, Irak1 and Traf6 respectively). The error bars represent standard error of mean (SEM). Statistical significance: $, p<0.05, $$$, P<0.001 showing the effect of APP-PS1 mutations, ## P<0.01 ### P<0.001 showing the effect of age, and @@, P<0.01 showing the interaction of APP-PS1*age in a two-way ANOVA analysis. *P<0.05, **P<0.01 and ***P<0.001 show statistical significance assessed by the Bonferroni's post-test (D-F): Scatter plots showing significant correlation of miR146a with miR155 (D) and each miRNA with IL-1β expression (E-F). r = Spearman's rank correlation coefficient; *P<0.05, **P<0.01, ***P<0.001. (I-J) Scatter plots showing the negative correlation between miR146a and its targets Irak1 and Traf6. r = Spearman's rank correlation coefficient; **P<0.01.

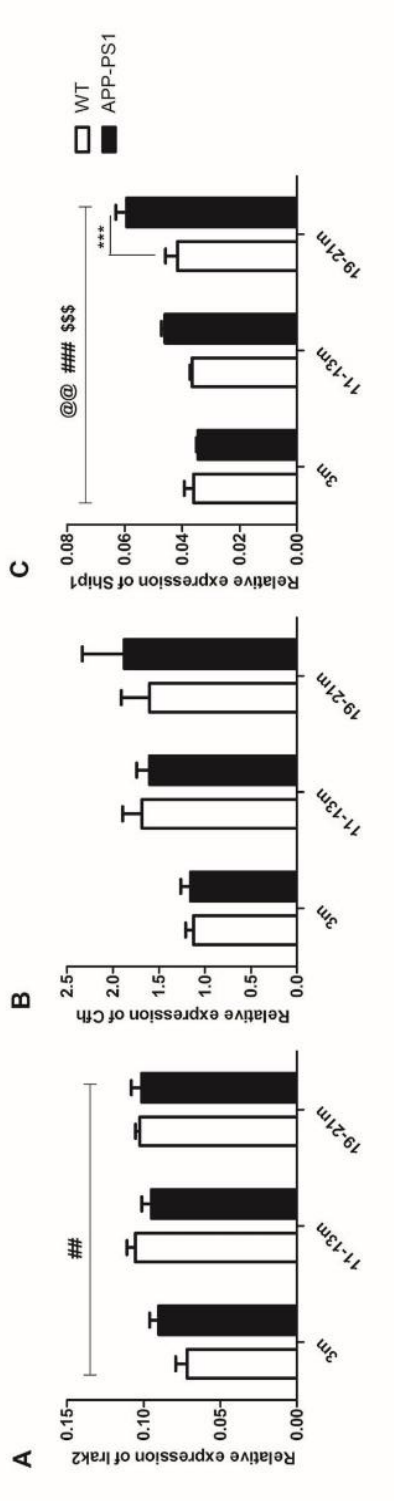

Fig. 25. Expression of Irak2, Cfh and Ship1 in the APP-PS1 mouse. (A-C): qPCR of Irak2 (A), Cfh (B), Ship1 (C) in the hippocampi of APP-PS1 mice at 3 (n=6), 11-13 (n=6) and 19-21 months (n=6) compared to WT mice (n=6 for 3, 11-13 and 19-21 months respectively). Data are expressed relative to the reference genes (geometric mean of Tbp and Hprt respectively). The error bars represent standard error of mean (SEM). Statistical significance: $$$, P<0.001 showing the effect of APP-PS1 mutations, ## P<0.01 ### P<0.001 showing the effect of age, and @@, P<0.01 showing the interaction of APP-PS1*age in a two-way ANOVA analysis. *** P<0.001, shows statistical significance assessed by the Bonferroni's post-test.

4.2.5 miR146a and miR155 expression in Alzheimer's Disease at different stages of the disease

The expression levels of both miR146a and miR155 were analyzed, by qPCR, in hippocampal specimens of subjects with AD pathology covering Stages II-IV and healthy controls. The expression of miRNA146a (but not miR155) was increased in AD specimens (Braak stage IV), compared to controls (Fig. 26A-B). In these same specimens we observed the increased expression of IL-1β (Fig. 26C). The expression of both miR146a and miR155 showed a positive correlation (r=0.327, P=0.042 and r=0.466, P=0.002) with IL-1β (Fig. 26D-E). A negative correlation was observed between the expression levels of miR146a and its target Irak1 (r=-0.355; p=0.027; Fig. 26G). No difference was observed in expression of Irak2 and Cfh whereas Ship1 (target of miR155) showed increased expression in AD specimens (Braak II, P=0.007 and Braak IV, P=0.017) compared to controls (Fig. 27).

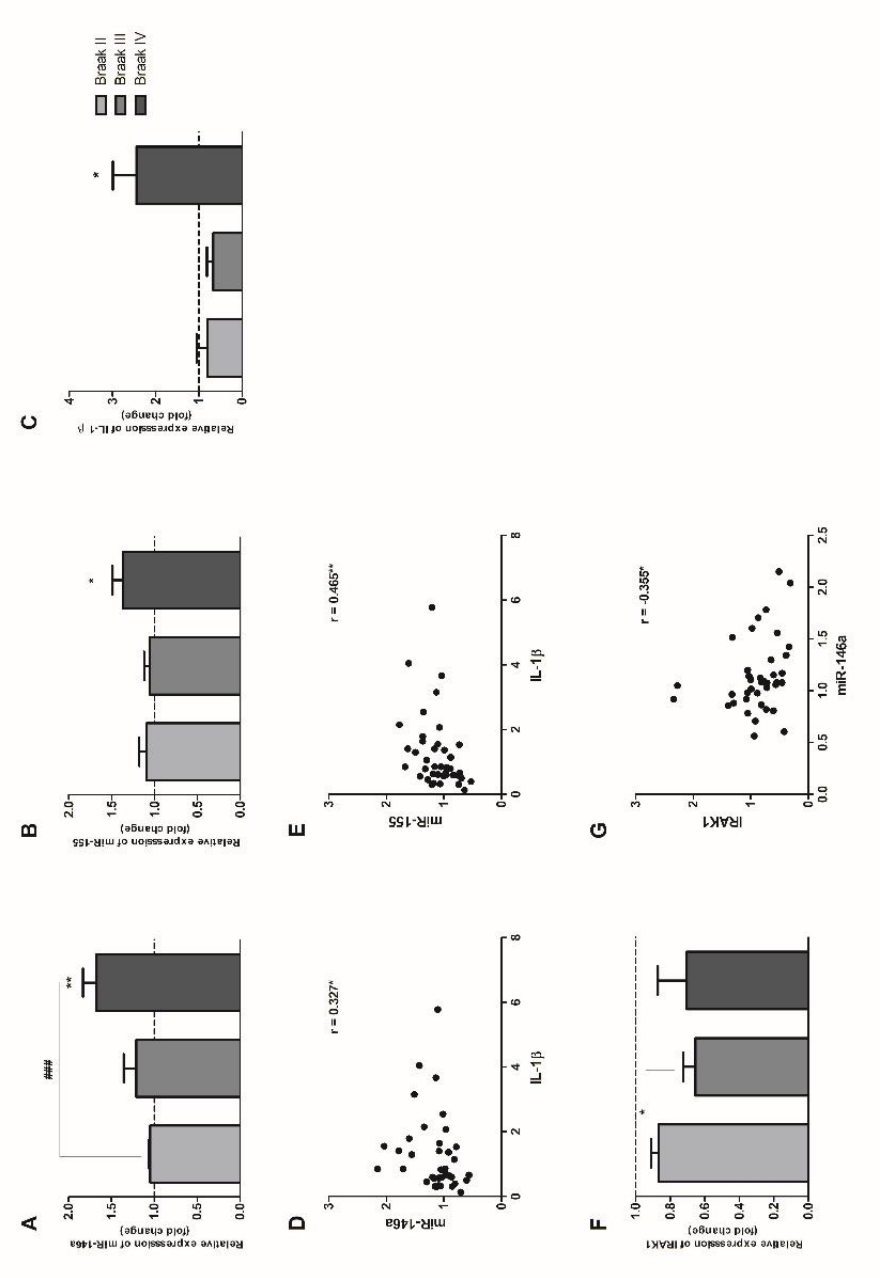

Fig. 26. Expression of miR146a, miR155, IL-1β and Irak1 in sAD. (A-C), (F): qPCR of miR146a, miR155, IL-1β, Irak1 in A. Data are expressed relative to levels observed in control hippocampus (n=9, represented by the dashed line). The error bars represent standard error of mean (SEM). Statistical significance: * P<0.05, **P<0.01 relative to controls; ### P<0.001 Braak II vs Braak III. (D-E), (G): Scatter plots showing significant correlation of miR146a and miR155 with IL-1β expression and miR146a with its target Irak1. r = Spearman's rank correlation coefficient; *P<0.05, **P<0.01.

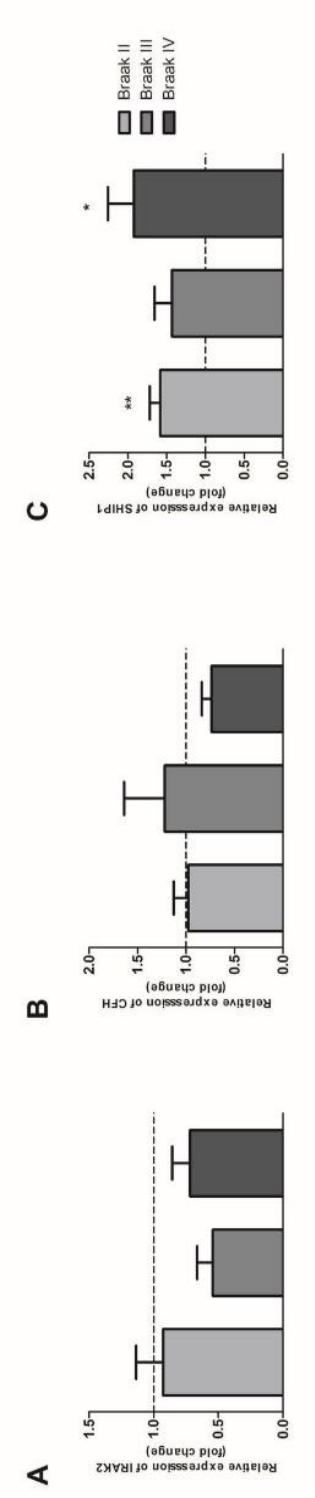

Fig. 27. Expression of Irak2, Cfh and Ship1 in sAD (A-C): qPCR of Irak2, Cfh and Ship1 in AD. Data are expressed relative to levels observed in control hippocampi (n=9, represented by the dashed line). The error bars represent standard error of mean (SEM). Statistical significance: * $P<0.05$, ** $P<0.01$ relative to controls.

4.3 Project 3: Impairment of BVR-A promotes brain insulin resistance in Alzheimer disease

AD brain is characterized by an inadequate response to insulin, formerly known as BIR; it has been proposed a link between insulin resistance and cognitive dysfunction. However, the mechanisms that underlie this process are not fully elucidated. Since BVR-A represents an upstream inhibitory regulator of the insulin signaling cascade and because we previously demonstrated the OS-induced impairment of BVR-A in human AD brain, we hypothesized the involvement of BVR-A dysregulation in the onset of BIR. To this purpose we analyzed the age dependent changes of (i) BVR-A levels and activation, (ii) total amount of OS markers levels (PC, HNE, 3-NT), (iii) IR/IRS1 levels and activation in the hippocampus of 3xTg-AD mice. Furthermore, *ad hoc* experiments have been performed in SH-SY5Y cells to clarify the molecular mechanism(s) underlying changes observed in mice, focusing on the contribution of oxidative/nitrosative stress on insulin resistance. Finally, because mTOR is able to phosphorylate IRS1 on critical Ser residues we investigated whether in our models (mice and cellular) insulin resistance can be associated with mTOR hyper-activation.

4.3.1 Oxidative stress correlates with AD pathology in 3xTg-AD mice

We evaluated by slot blot the changes of oxidative/nitrosative stress markers as total PC, total HNE adducts and total 3-NT levels in the hippocampus of 3xTg-AD mice at 3, 6, 12 and 18 months of age. We found a significant elevation of 3-NT levels since 6 months of age which further rises at 12 months and remains still elevated at 18 months in 3xTg-AD mice compared with age-matched WT mice (Fig. 28A). While PC and HNE levels showed a significant elevation only at 12 and 18 months in 3xTg-AD mice of age compared with age-matched WT mice (Fig. 28A). In addition, age-associated changes related with the neuropathological

AD alterations occured in the same time-frame in the hippocampus of 3xTg-AD mice (Fig. 28B). The results obtained from the semi-quantitative analyses of Aβ and tau immunostaining showed a significant increase in Aβ in the hippocampus of 3xTg-AD mice at 6-month compared to age-matched WT mice, while no difference was found in tau immunoreactivity at the same age. At 12 months of age 3xTg-AD mice showed Aβ deposits and human tau-reactive neurons in the hippocampus. Finally, we found dense Aβ deposit and extensive human tau immunoreactivity in the 18 month old 3xTg-AD mice. None of these immunoreactive structures were detected in the WT brains (Fig. 28B). These results agree with previous results, which demonstrated, in 3xTg-AD mice brain, the gradual accumulation of Aβ and tau pathology [240].

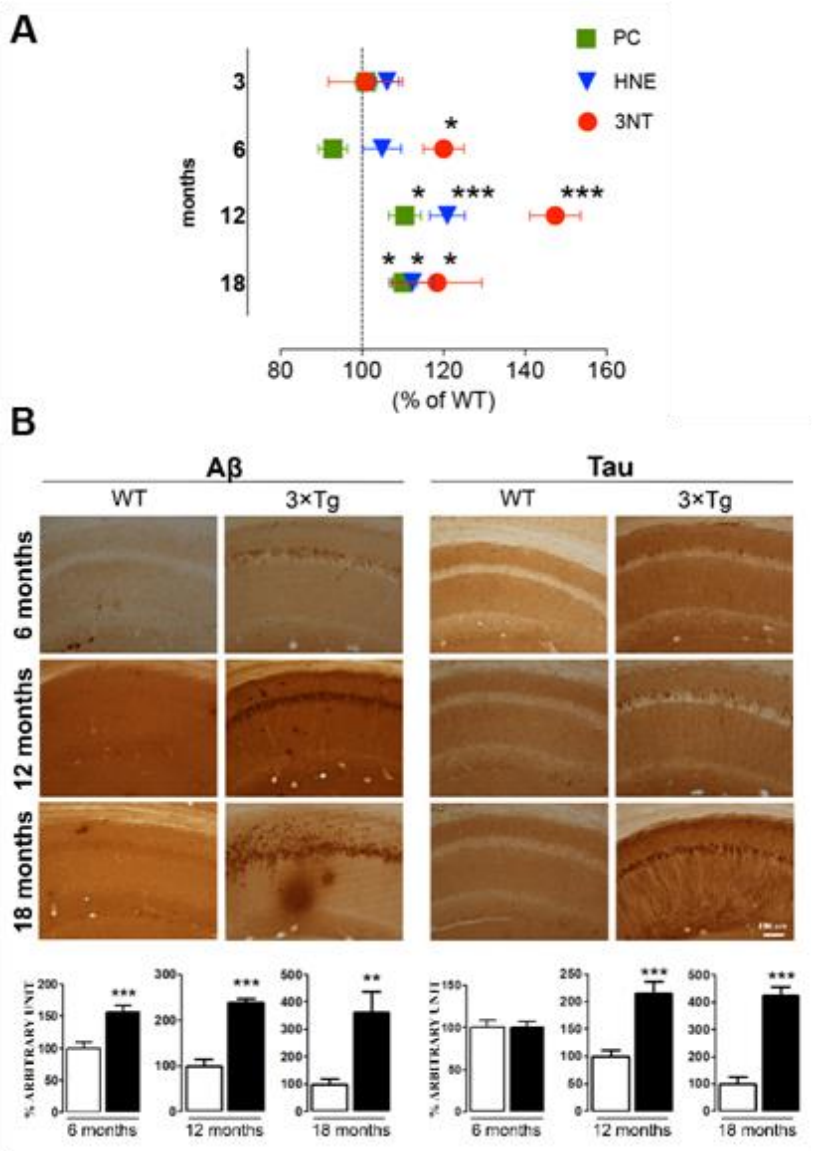

Fig. 28. Increased oxidative and nitrosative stress levels progresses with AD pathology in the hippocampus of 3xTg-AD mice. (A) PC levels (green squares), protein-bound HNE levels (blue triangles) and 3-NT levels (red dots) evaluated in the hippocampus of 3xTg-AD mice at 3 (n=6), 6 (n=6), 12 (n=6) and 18 (n=6) months of age. Densitometric values shown are given as percentage of the age-matched WT mice (n=6/group), set as 100%. Means ± SEM of three replicates of each individual sample per group. *p<0.05 and **p<0.01 versus WT (Student's t-test). (B) Representative microphotographs (10 magnification, scale bar 100 μm) and results obtained from the semi-quantitative analyses of Aβ and tau immunostaining from WT (n=3, white bars) and 3xTg-AD (n=3, black bars) mice. The data are mean ± SEM **p<0.01 and ***p<0.001 versus age-matched WT mice (Unpaired Student's t-test, n=3).

4.3.2 The impairment of BVR-A occurs early in the 3xTg-AD mice

To evaluate the potential contribution of oxidative/nitrosative stress on BVR-A function, we analyzed the age associated changes of BVR-A protein levels, BVR-A activation (pTyr-BVR-A) and 3-NT adducts on BVR-A protein (3-NT-BVR-A) from hippocampus of 3xTg-AD mice at different ages. Western blot analysis showed a significant reduction of BVR-A protein levels from 3 to 12 months in 3xTg-AD mice in respect to WT mice, whereas a significant increase was observed at 18 months (Fig. 29). With regard to BVR-A activation we observed a significant early increase at 3 months followed by a reduction from 6 to 18 months. However, only at 6 months we observed a drastic reduction of pTyr-BVR-A, indeed at both 12 and 18 months of age changes of pTyr-BVR-A levels did not reach the statistical significance (25% and 20%, respectively at 12 and 18 months of age, Fig. 29). In addition, in older 3xTg-AD mice (corresponding to the advanced stages of AD pathology) we observed that the altered BVR-A activation was coupled to a significant increase of 3-NT modifications, which peaked at 12 months, reaching 150% in the 3xTg-AD mice compared to the relative control group (Fig. 29). Furthermore, we also investigated whether in 3xTg-AD mice the BVR-A reductase activity was impaired as reported in human AD brain [226]. We observed that the reductase activity was significantly reduced only at 12 months coincidently with the maximal increase of 3-NT-BVR-A at this time point, which is probably responsible of a general impairment of the protein (Fig. 29). These results highlight an early dysregulation of BVR-A either in terms of protein levels or activity, which worsen with the progression of AD pathology in these mice. Furthermore, the reduction of BVR-A activation coupled with increased total oxidative/nitrosative stress levels from 6 to 18 months suggests a probable link between these events in the progression of AD pathology.

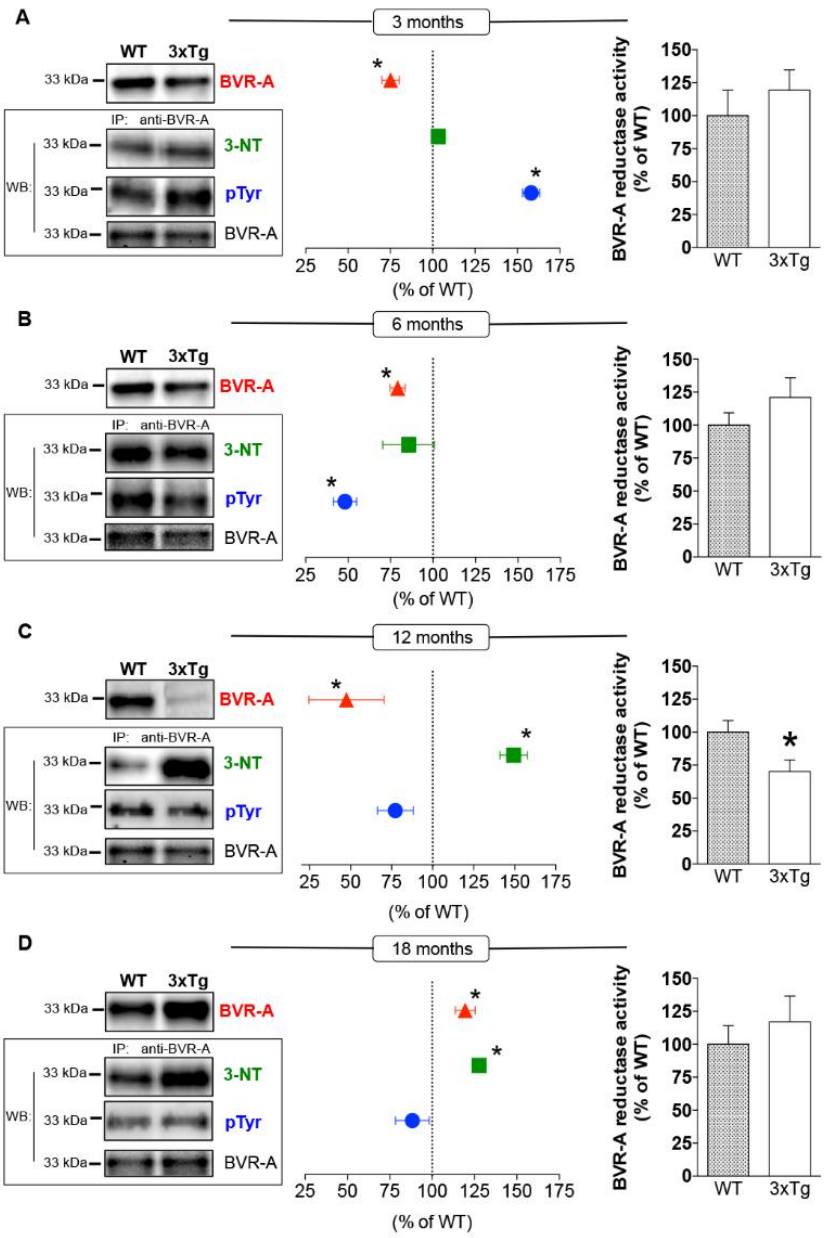

Fig. 29. Early impairment of BVR-A is observed during the progression of AD pathology in the hippocampus of 3xTg-AD mice. BVR-A (i) protein levels (red triangles), (ii) 3-NT modifications (green squares), (iii) Tyr phosphorylation (pTyr) (blue dots) and (iv) reductase activity (right columns) evaluated in the hippocampus of 3xTg-AD mice at (A) 3 (n=6), (B) 6 (n=6), (C) 12 (n=6) and (D) 18 (n=6) months of age. Left panels: western blot analyses. Representative bands are shown. Middle panels: densitometric analyses of wester blot protein bands. BVR-A protein levels were normalized per total protein load. 3-NT modifications and pTyr levels on BVR-A were normalized by using total BVR-A as loading control [215, 219]. Densitometric values shown are given as percentage of WT mice (n=6/group) set as 100%. Right panels: BVR-A reductase activity expressed as percent of WT mice (n=6/group) and evaluated as described in Materials and Methods. Means ± SEM, *p<0.05 vs WT mice (Student's t-test).

4.3.3 BVR-A impairment leads to BIR in the 3xTg-AD mice

To unravel the mechanisms through which the BVR-A dysregulation might impact the insulin signaling in AD, we evaluated changes with regard to IR and IRS1 protein levels/activation in the hippocampus of 3xTg-AD mice at 3, 6, 12 and 18 months of age. Through the evaluation of IR protein levels and activation [pIR(Tyr1662/1163)] as well as IRS1 protein levels and both activation [pIRS1(Tyr632)] and inactivation [pIRS1(Ser307)] in the hippocampus of 3xTg-AD mice we highlighted two distinct phases (3-6 and 12-18 months). At 3 months of age we observed a significant reduction of IR protein levels (Fig. 30A) associated with a consistent elevation of IR activation (Fig. 30A) without significant changes of IRS1 protein levels or activation (Fig. 30A). At 6 months of age, both IR and IRS1 protein levels were reduced, while they appeared to be consistently activated (Fig. 30B). At 12 months of age, we observed a completely opposite scenario characterized by a reduction of IR protein levels and activation (Fig. 30C) together with a consistent increase of IRS1 inactivation (Fig. 30C), supporting the onset of the BIR state. Finally, at 18 months of age, 3xTg-AD mice are characterized by a persistent state of BIR as demonstrated by the elevated levels of IRS1 Ser307 phosphorylation (Fig. 30D). These results allow identifying different phases along the progression of AD pathology, which finally led to insulin resistance in the hippocampus of elder 3xTg-AD mice. Noteworthy, the strong reduction of BVR-A activation at 6 months of age is associated with the consistent increase of IRS1 activation; whereas the persistent impairment of BVR-A at 12 months is associated with a clear inactivation of IRS1. These evidences are in agreement with our hypothesis suggesting that the lack of control exerted by BVR-A on IRS1 is firstly associated with IRS1 hyperactivation, which in turn leads to BIR probably through feedback mechanisms aimed to turn-off IRS1 hyperactivity.

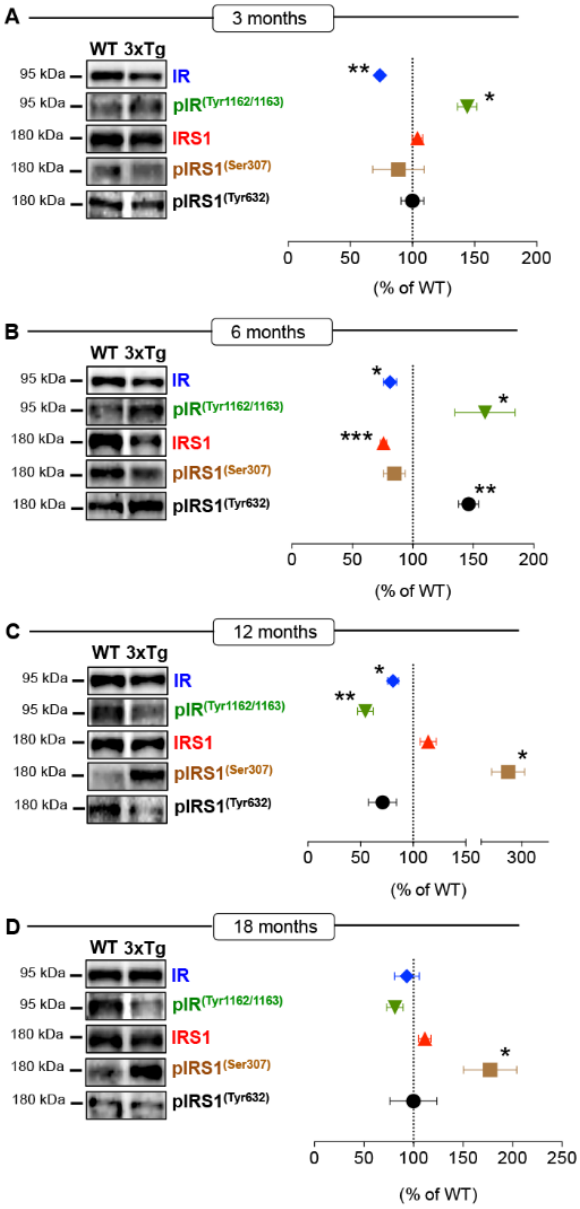

Fig. 30. Hyper-activation of the insulin signaling precedes BIR in the hippocampus of 3xTg-AD mice. IR protein levels (blue diamonds), IR activation [pIR(Tyr1162/1163), green triangles], IRS1 protein levels (red triangles), IRS1 inactivation [pIRS1(Ser307), brown squares] and IRS1 activation [pIRS1(Tyr632), black dots] evaluated in the hippocampus of 3xTg-AD mice at (A) 3 (n=6), (B) 6 (n=6), (C) 12 (n=6) and (D) 18 (n=6) months of age. Left panels: western blot analyses. Representative bands are shown. Right panels: densitometric analyses of western blot protein bands. Protein levels were normalized per total protein load. IR- and IRS1-associated phosphorylations were normalized by taking into account the respective protein levels and are expressed as the ratio between the phosphorylated form and the total protein levels: pIR(Tyr1162/1163)/IR, pIRS1(Ser307)/IRS1 and pIRS1(Tyr632)/IRS1. Densitometric values shown are given as percentage of WT mice (n=6/group) set as 100%. Means ± SEM, *p<0.05, **p<0.01 and ***p<0.001 vs WT mice (Student's t-test).

4.3.4 BVR-A impairment precedes TNF-α elevation in the 3xTg-AD mice

Because TNF-α is known to inhibit BVR-A [241] we investigated whether reduced BVR-A protein levels could result from increased TNF-α level in the hippocampus of 3xTg-AD mice. To this purpose, we evaluated, by western blot analysis, the TNF-α protein levels in 3xTg-AD mice at 3, 6, 12 and 18 months of age (Fig. 31). In agreement with previous data [242, 243] we found a significant reduction of TNF- α levels from 3 to 12 months of age followed by a consistent increase in 3xTg-AD mice with respect to WT at 18 months (Fig. 31). These results suggest that the reduction of BVR-A protein levels in 3xTg-AD mice is independent from TNF-α since it occurs before of the TNF-α elevation.

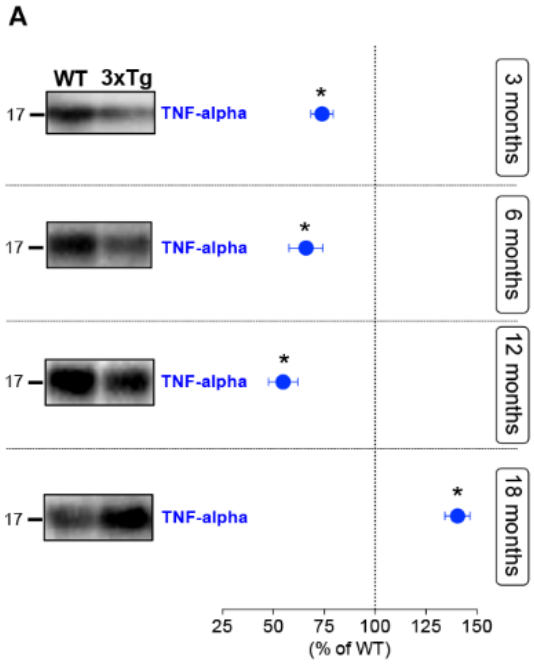

Fig. 31. Age-associated changes of TNF-α protein levels in the hippocampus of 3xTgAD. TNF-α protein levels (blue dots) in the hippocampus of 3xTg-AD mice at 3 (n=6), 6 (n=6) and 12 (n=6) and 18 (n=6) months of age. Left panels: western blot analyses. Representative bands are shown. Right panels: densitometric analyses of western blot protein bands. TNF-α protein levels were normalized per total protein load. Densitometric values shown are given as percentage of WT mice (n=6/group) set as 100%. Means ± SEM, *p<0.05 vs WT mice (Student's t-test).

4.3.5 BVR-A impairment and BIR in normal aging

In order to identify whether BIR occurring during normal aging was associated with a dysregulation of BVR-A, we analyzed changes of IR/IRS1 protein levels and activation in light of the changes occurring with regard to BVR-A in the hippocampus of WT mice aged from 3 to 18 months. Western blot analysis showed a reduction of BVR-A protein levels both at 12 and 18 months; furthermore, it was associated to a reduction of BVR-A activation although this value did not reach statistical significance (Fig. 32A). At 18 months of age WT mice exhibited a significant increase of 3-NT-BVR-A (Fig. 32A) together with a significant decrease of BVR-A reductase activity (Fig. 33A), thus supporting a general age-associated impairment of BVR-A. While with regard to TNF-α levels, the hippocampus of WT mice was characterized by a significant increase at 12 months followed by a consistent reduction at 18 months (Fig. 33C). The analysis of IR protein levels did not reveal any significant change (Fig. 32B), whereas with regard to IR activation we found a consistent increase from 3 to 12 months, followed by a fall at 18 months (Fig. 32B). A decrease of IRS1 protein levels together with a consistent IRS1 inactivation has been found with age (Fig. 32B). Indeed, while at 6 months of age increased IR activation is not associated with IRS1 hyperactivation, probably because BVRA is still functioning, at 12 and 18 months of age, reduced BVR-A protein levels and activation are associated with the inactivation of IRS1, and thus BIR. These results recall what we have observed in 3xTg-AD mice and suggest that the impairment of BVR-A could represent a bridge in the transition from normal aging to AD.

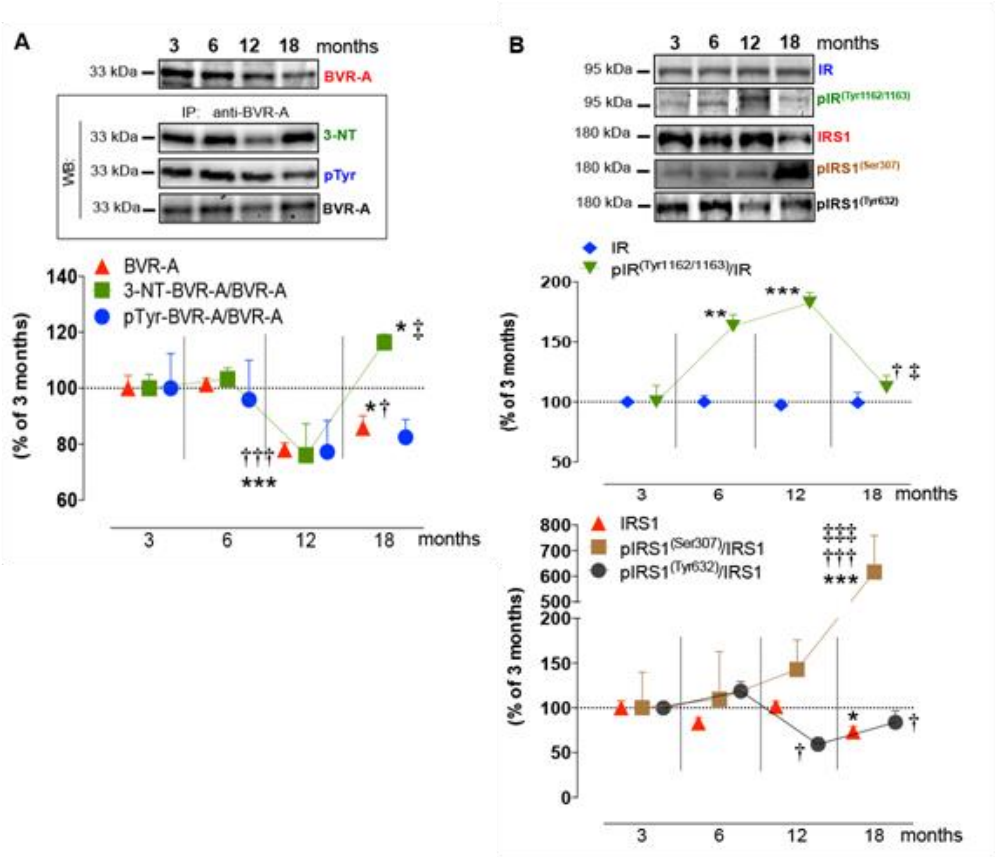

Fig. 32. BVR-A impairment parallels BIR during normal aging in the hippocampus of WT mice. (A) BVR-A (i) protein levels (red triangles), (ii) 3-NT modifications (green squares) and (iii) Tyr phosphorylation (pTyr) (blue dots) evaluated in the hippocampus of WT mice at 3 (n=6), 6 (n=6), 12 (n=6) and18 (n=6) months of age. Upper panels: western blot analyses. Representative bands are shown. Lower panels: densitometric analyses of western blot protein bands. BVR-A protein levels were normalized per total protein load. 3-NT modifications and pTyr levels on BVR-A were normalized by using total BVR-A as loading control [215, 219]. (B) IR protein levels (blue diamonds), IR activation [pIR(Tyr1162/1163), green triangles], IRS1 protein levels (red triangles), IRS1 inactivation [pIRS1(Ser307), brown squares] and IRS1 activation [pIRS1(Tyr632), black dots] evaluated in the hippocampus of WT mice at 3 (n=6), 6 (n=6), 12 (n=6) and 18 (n=6) months of age. Upper panels: western blot analyses. Representative bands are shown. Lower panels: densitometric analyses of western blot protein bands. Protein levels were normalized per total protein load. IR- and IRS1-associated phosphorylations were normalized by taking into account the respective protein levels and are expressed as the ratio between the phosphorylated form and the total protein levels: pIR(Tyr1162/1163)/IR, pIRS1(Ser307)/IRS1 and pIRS1(Tyr632)/IRS1. Densitometric values shown are given as percentage of 3 months-old mice set as 100%. Means7SEM, *p<0.05, **p<0.01 and ***p<0.001 vs 3 months; †p<0.05 and †††p<0.001 vs 6 months; ‡p<0.05 vs 12 months (ANOVA with post hoc Turkey t-test).

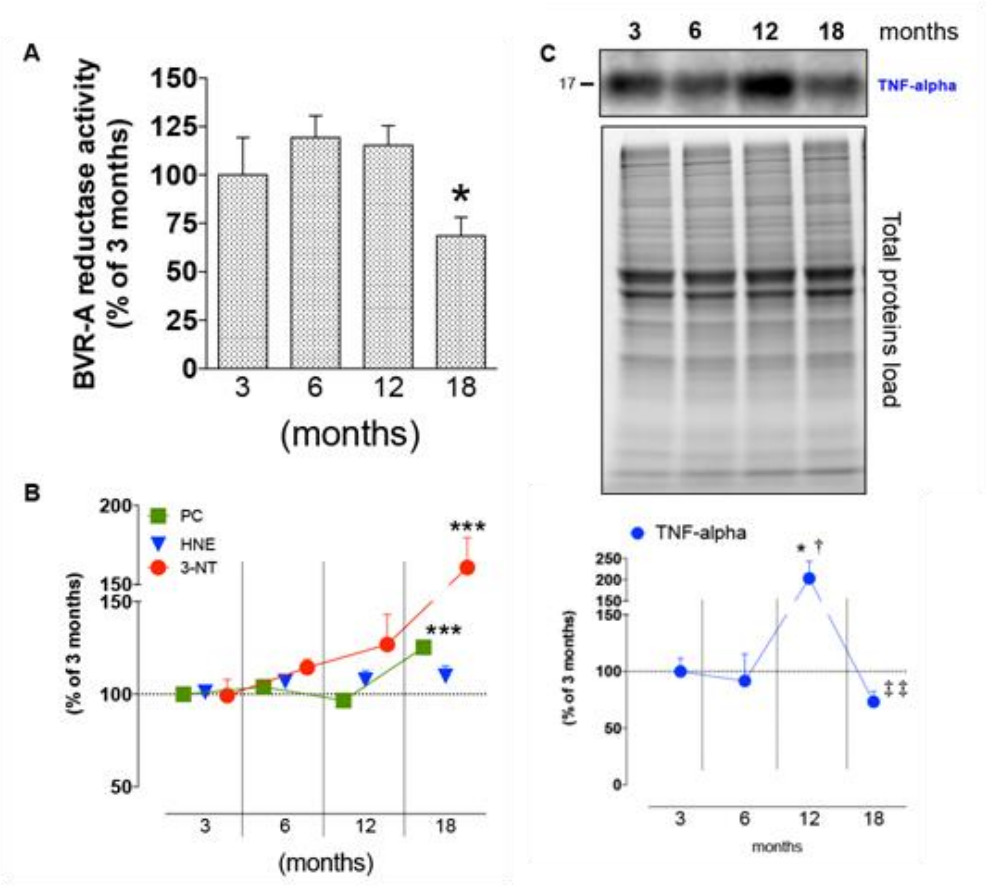

Fig. 33. Changes of BVR-A reductase activity, oxidative/nitrosative stress levels and TNF-α during normal aging in the hippocampus of WT mice. (A) BVR-A reductase activity expressed as units (U)/mL (n=6/group) as described in Materials and Methods. Means ± SEM, *p<0.05 vs 3-months old mice (ANOVA with post hoc Turkey t-test). (B) PC levels (green squares), protein-bound HNE levels (blue triangles) and 3-NT levels (red dots) evaluated in the hippocampus of WT mice at 3 (n=6), 6 (n=6), 12 (n=6) and 18 (n=6) months of age. Densitometric values shown are given as percentage of 3 months old mice set as 100%. Means ± SEM of three replicates of each individual sample per group. ***p<0.001 versus 3 months old mice (ANOVA with post hoc Turkey t-test). (C) TNF-α protein levels evaluated in the hippocampus of WT mice at 3 (n=6), 6 (n=6), 12 (n=6) and 18 (n=6) months of age. Upper panels: western blot analyses. Representative bands are shown. Lower panel: densitometric analyses of western blot protein bands. Protein levels were normalized per total protein load. Densitometric values shown are given as percentage of 3 months old mice set as 100%. Means ± SEM, *p<0.05 vs 3 months; †p<0.05 vs 6 months; ‡‡p<0.05 vs 12 months (ANOVA with post hoc Turkey t-test).

4.3.6 BVR-A impairment is associated with BIR in SH-SY5Y cells

In order to demonstrate that BVR-A is effectively involved in the onset of BIR through an upstream inhibitory control on IRS1, we evaluated the BVR-A protein levels, pTyr-BVR-A as well as IR/IRS1 protein levels and activation in SH-SY5Y neuroblastoma cells under different conditions: normal insulin signaling, BIR and the over-induced insulin signaling. First, we investigated about the experimental condition to recreate *in vitro* the different state of insulin signaling. Thus in a preliminary set of experiments, we investigated whether insulin 0.1 µM administered for 24 h was able to activate the insulin signaling and whether the administration of additional increasing doses of insulin (0.1–5 µM for 1h) aimed to mimic insulin overexposure would promote BIR in our cellular model. As expected, insulin pre-treatment (0.1 µM for 24 h) promotes a significant increase of both IR and IRS1 activation (Fig. 34A and Fig. 35). By re-challenging pre-treated cells with increasing doses of insulin (0.1–5 µM), we observed two opposite effects: increased IRS1 inactivation with insulin 0.1 µM and 0.5 µM (Fig. 34A and Fig. 35) and increased IRS1 activation with insulin 5 µM (Fig. 34A and Fig. 35). Interestingly, none of these conditions were characterized by changes of BVR-A protein levels (Fig. 35). Therefore we investigated about the BVR-A activation levels because the activation, rather than the expression levels, would provide more information about the molecular mechanisms underlying insulin-mediated effects. Thus we evaluated the BVR-A activation at 3 different conditions: normal insulin signaling (Ins 0.1 µM for 24 h), BIR (Ins 0.1 µM for 24 h + Ins 0.1 µM for 1 h) and the over-induced insulin signaling (Ins 0.1 µM for 24 h + Ins 5 µM for 1 h). As shown in Fig. 34A, normal insulin signaling is associated with a significant increase of pTyrBVR-A as expected, whereas BIR is characterized by a reduction of BVR-A activation. Surprisingly in condition of over-induced insulin signaling (Ins 5 µM for 1h) we observed a remarkable increase of BVR-A activation (Fig. 34A). Finally, we found that BIR also parallels

a significant reduction of the BVR-A reductase activity (Fig. 34D). All together these observations suggest that BIR is associated with a decreased BVR-A activation and that this phenomenon could be overwhelmed by higher doses of insulin, which, instead, promote an increase of BVR-A activation and IRS1 Tyr phosphorylation.

Fig. 34. BVR-A impairment is associated with BIR in SH-SY5Y neuroblastoma cells. (A) Insulin 0.1 µM for 24h induced both IRS1 activation (pIRS1(Tyr632), black dots) and BVRA activation (pTyr-BVR-A, blue dots) in SH-SY5Y neuroblastoma cells thus mirroring the physiological insulin signaling. Instead, pre-treated cells further treated with insulin (0.1 or 5 µM) for an additional hour to mimic insulin over-exposure, showed dose-dependent effects. Indeed, insulin 0.1 µM was associated with BIR (increased pIRS1(Ser307), brown squares) and BVR-A inactivation, whereas insulin 5 µM treatment by-passed BIR and was associated with increased activation of both IRS1 and BVR-A. *p<0.05, vs Ctr; †p<0.05, ††p<0.01 and †††p<0.001 vs Ins 0.1 µM (ANOVA with post hoc Tukey t-test). (B) ONOO (50-500 µM) for 24 h dose-dependenlty promoted BIR (increased pIRS1(Ser307), brown squares) and BVR-A inactivation (reduced pTyr-BVR-A, blue dots) in SH-SY5Y neuroblastoma cells. Decreased pIRS1(Tyr632) was also observed. *p<0.05 and **p<0.01 vs Ctr (ANOVA ANOVA with post hoc Tukey t-test). (C) H_2O_2 50 µM for 24 h promoted BIR (increased pIRS1(Ser307), brown squares) and BVR-A inactivation (reduced pTyr-BVR-A, blue dots) in SH-SY5Y neuroblastoma cells. Increased pIRS1(Tyr632) was also observed, but IRS1 inactivation overcomes this effect. *p<0.05, vs Ctr (Student's t-test). (D) BVR-A reductase activity relative to A, B and C evaluated as described in Materials and Methods and expressed as percent of Ctr (n=3 independent cultures/group). Means ± SEM, *p<0.05 and **p<0.01 vs Ctr mice; †p<0.05, vs Ins 0.1 µM (ANOVA with post hoc Tukey t-test for Ins and ONOO- related experiments; Student's t-test for H_2O_2 related experiment). For A, B and C: Upper panels: western blot analyses. Representative bands are shown. Lower panels: densitometric analyses of western blot protein bands. Protein levels were normalized per total protein load. IR- and IRS1-associated phosphorylations were normalized by taking into account the respective protein levels and are expressed as the ratio between the phosphorylated form and the total protein levels: pIR(Tyr1162/1163)/IR, pIRS1(Ser307)/IRS1 and pIRS1(Tyr632)/IRS1. pTyr levels on BVR-A were normalized by using total BVR-A as loading control [215, 219]. Densitometric values shown are given as percentage of control cells (Ctr) set as 100%. Means ± SEM (n=3 independent cultures/group). →

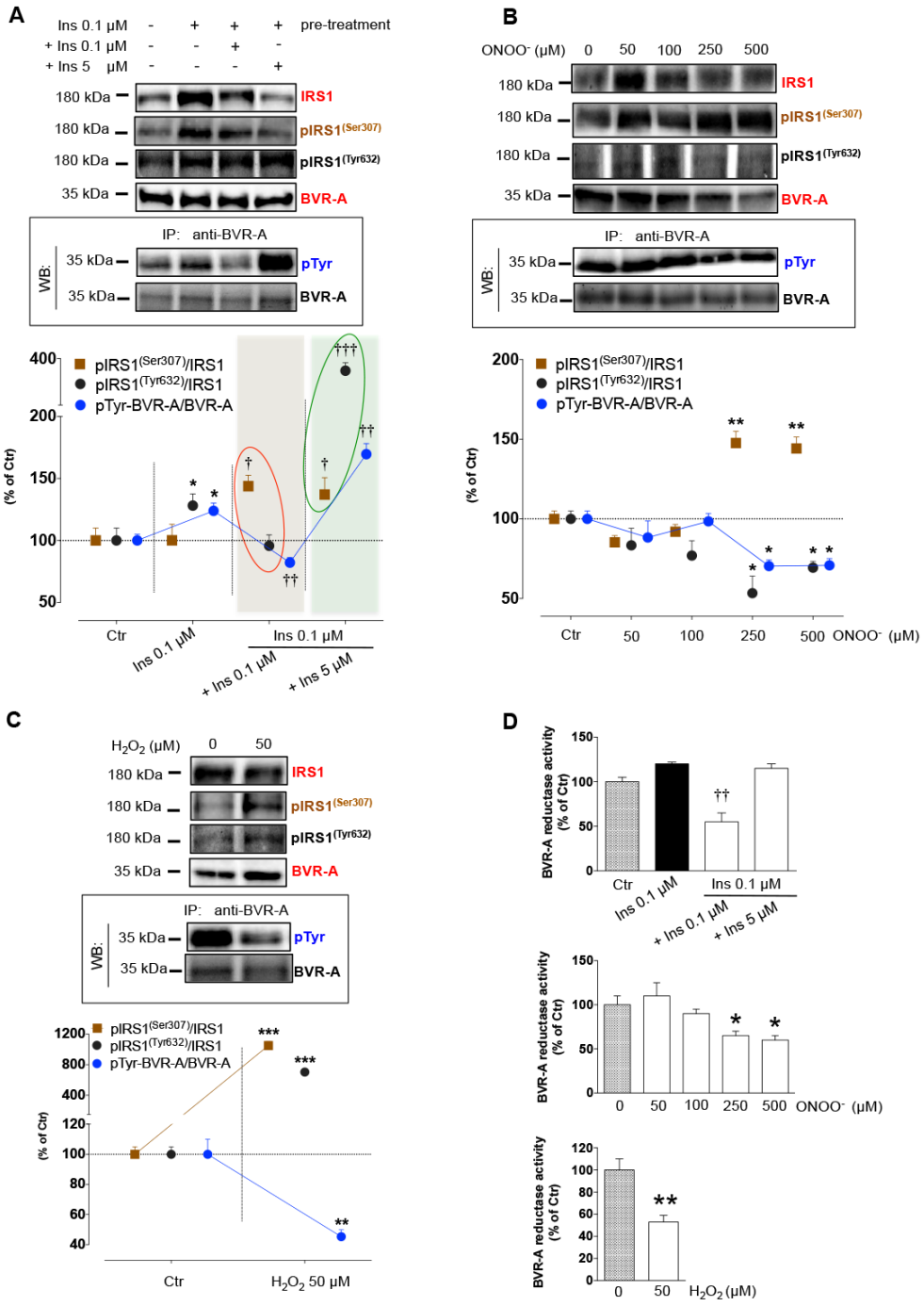
A
Ins 0.1 μM - + + + pre-treatment
+ Ins 0.1 μM - - + -
+ Ins 5 μM - - - +
180 kDa IRS1
180 kDa pIRS1(Ser307)
180 kDa pIRS1(Tyr632)
35 kDa BVR-A
IP: anti-BVR-A
WB:
35 kDa pTyr
35 kDa BVR-A
pIRS1(Ser307)/IRS1
pIRS1(Tyr632)/IRS1
pTyr-BVR-A/BVR-A
(% of Ctr)
Ctr
Ins 0.1 μM
+ Ins 0.1 μM
+ Ins 5 μM
B
ONOO- (μM) 0 50 100 250 500
180 kDa IRS1
180 kDa pIRS1(Ser307)
180 kDa pIRS1(Tyr632)
35 kDa BVR-A
IP: anti-BVR-A
WB:
35 kDa pTyr
35 kDa BVR-A
pIRS1(Ser307)/IRS1
pIRS1(Tyr632)/IRS1
pTyr-BVR-A/BVR-A
(% of Ctr)
Ctr 50 100 250 500 ONOO- (μM)
C
H2O2 (μM) 0 50
180 kDa IRS1
180 kDa pIRS1(Ser307)
180 kDa pIRS1(Tyr632)
35 kDa BVR-A
IP: anti-BVR-A
WB:
35 kDa pTyr
35 kDa BVR-A
pIRS1(Ser307)/IRS1
pIRS1(Tyr632)/IRS1
pTyr-BVR-A/BVR-A
(% of Ctr)
Ctr
H2O2 50 μM
D
BVR-A reductase activity (% of Ctr)
Ctr
Ins 0.1 μM
+ Ins 0.1 μM
+ Ins 5 μM
BVR-A reductase activity (% of Ctr)
0 50 100 250 500 ONOO- (μM)
BVR-A reductase activity (% of Ctr)
0 50 H2O2 (μM)

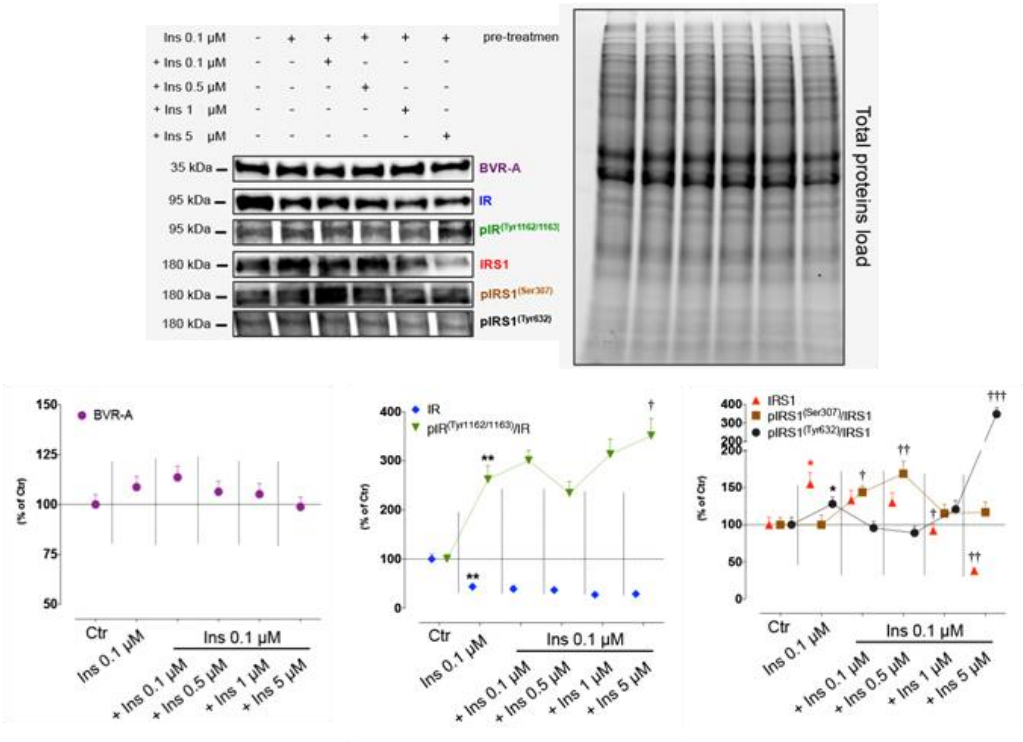

Fig. 35. Insulin over-exposure mimics brain insulin resistance (BIR) in SH-SY5Y neuroblastoma cells. SH-SY5Y cells were pre-treated with insulin 0.1 µM for 24 h to induce the activation of the insulin signaling. No significant changes have been observed for BVR-A protein levels with the tested doses (purple dots). Rather, insulin treatment was associated with a reduction of IR protein levels (blue diamonds) together with a consistent IR activation (pIR(Tyr1162/1163)/IR, green triangles). As expected, increased IR activation was coupled with increased IRS1 protein levels (red triangles) and IRS1 activation (pIRS1(Tyr632)/IRS1, black dots). No significant changes have been observed for BVR-A protein levels (purple dots). At the end of the 24 h cells were rechallenged with increasing doses of insulin (0.1-0.5-1-5 µM) for an additional hour, to test the effects produced by insulin over-exposure. Additional insulin did not produce changes of IR protein levels or IR activation with regard to pre-treated cells, except at the dose of 5 µM, which promoted a further elevation of IR activation (pIR(Tyr1162/1163)/IR, green triangles). Instead, we observed a dose-dependent decrease of IRS1 protein levels together with modifications of its activation state. Moreover, a significant elevation of IRS1 inhibition (pIRS1(Ser307)/IRS1, brown squares) occurs at the doses of insulin 0.1 µM and 0.5 µM with respect to pre-treated cells. This effect was accompanied by a reduction of IRS1 activation (pIRS1(Tyr632)/IRS1, black dots), which rises-up at the dose of 1 µM to finally overcome BIR at the dose of 5 µM. Upper panels: western blot analyses. Representative bands are shown. Lower panels: densitometric analyses of western blot protein bands. Protein levels were normalized per total protein load. IR- and IRS1-associated phosphorylations were normalized by taking into account the respective protein levels and are expressed as the ratio between the phosphorylated form and the total protein levels: pIR(Tyr1162/1163)/IR, pIRS1(Ser307)/IRS1 and pIRS1(Tyr632)/IRS1. Densitometric values shown are given as percentage of control cells (Ctr) (n=3 independent cultures/group) set as 100%. Means ± SEM, *p<0.05, **p<0.01 vs Ctr; †p<0.05, ††p<0.01 and †††p<0.001 vs Ins 0.1 µM (ANOVA with post hoc Turkey t-test).

4.3.7 Increased oxidative and nitrosative stress levels promote BVR-A impairment and BIR in SHSY5Y cells

Since oxidative and nitrosative stress elevation is associated with reduced BVR-A Tyr phosphorylation and BIR during both AD and normal aging in mice, we evaluated the effects of a nitrosative agent (ONOO, 50–500 µM for 24h) and a pro-oxidant agent (H_2O_2, 0–50 µM for 24h) on SH-SY5Y cells with the aim to unravel whether oxidative/nitrosative stress could be a cause of the observed BVR-A impairment and BIR. We observed that the treatment with the nitrosative agent ONOO was associated with a significant elevation of IR protein levels at all the doses tested. Whereas only at the highest doses (250 and 500 µM) ONOO promotes a decrease of IR activation (Fig. 36), a significant increase of IRS1 inhibition (Fig. 34B) and a reduction of BVR-A protein levels (Fig. 36) and activation (Fig. 34B). At all the doses tested the treatment with H_2O_2 did not produce changes of IR protein levels, while at both 10 µM and 50 µM an increase of IR activation, a decrease of IRS1 protein levels and an enhance of IRS1 inhibition were observed (Fig. 37). Furthermore, 50µM H_2O_2 promoted a significantly increased of BVR-A protein levels (Fig. 37). Because the treatment with H_2O_2 at 50µM recreated the conditions previously observed in human AD brain and in 3xTg-AD mice, in which elevated OS levels co-exist with increased BVR-A protein levels and BIR, we then analyzed the BVR-A activation in this condition. Interestingly, we observed a consistent decrease of BVR-A Tyr phosphorylation (Fig. 34B). In accordance with findings in human and mice, these observations suggest that both ONOO and H_2O_2 at the highest doses promote a significant reduction of BVR-A reductase activity (Fig. 34D). These evidence clearly suggests that increased oxidative and nitrosative stress levels finally promote a reduction of BVR-A activation and BIR. Intriguingly, increased nitrosative stress levels could be among the mechanisms responsible for the

observed reduction of BVR-A protein levels and activation in the early phases of AD pathology, in 3xTg-AD mice.

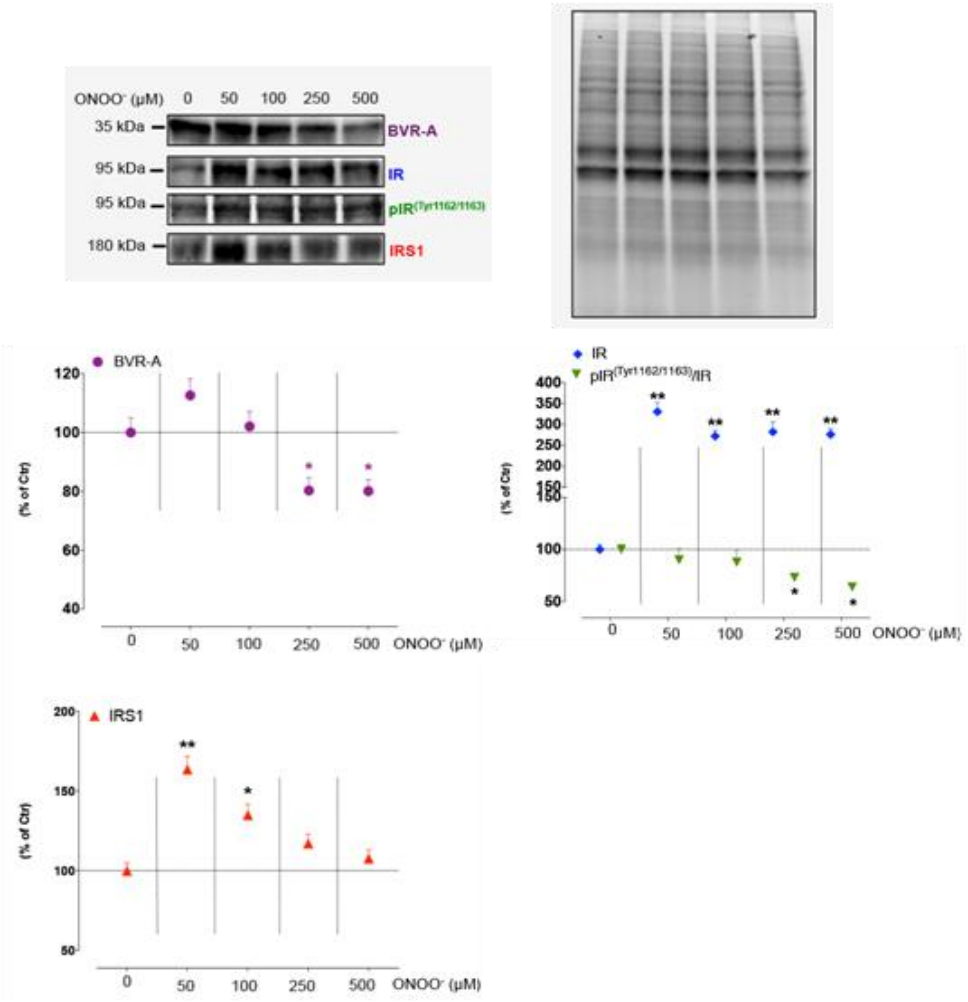

Fig. 36. Nitrosative stress promotes brain insulin resistance (BIR) in SH-SY5Y cells. To test whether nitrosative stress promotes BIR, SH-SY5Y cells were treated with increasing doses (50-500 μM) of peroxynitrite (ONOO-) for 24h. We observed a significant decrease of BVR-A protein levels (purple dots) with ONOO- 250 and 500 μM. Furthermore, ONOO- treatment promoted a significant elevation of IR protein levels (blue diamonds) along with a decreased IR activation (pIR(Tyr1162/1163)/IR, green triangles) at the highest doses. IRS1 protein levels (red triangles) are significantly elevated with ONOO- 50 and 100 μM, while we did not find significant changes with the highest doses. Upper panels: western blot analyses. Representative bands are shown. Lower panels: densitometric analyses of western blot protein bands. Protein levels were normalized per total protein load. IR-associated phosphorylation was normalized by taking into account the respective protein levels and is expressed as the ratio between the phosphorylated form and the total protein levels: pIR(Tyr1162/1163)/IR. Densitometric values shown are given as percentage of Ctr (n=3 independent cultures/group) set as 100%. Means ± SEM, *p<0.05, **p<0.01 vs Ctr (ANOVA with post hoc Turkey t-test).

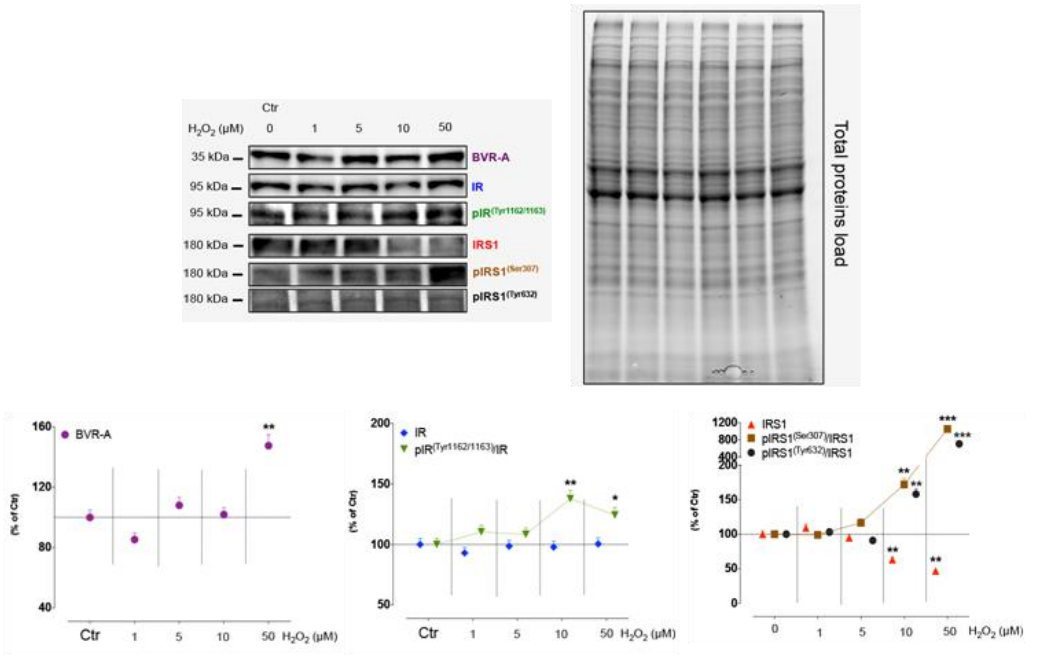

Fig. 37. Oxidative stress promotes brain insulin resistance (BIR) in SH-SY5Y cells. To test whether oxidative stress promotes BIR, SH-SY5Y cells were treated with increasing doses (1-50 μM) of hydrogen peroxide (H_2O_2) for 24 h. BVR-A protein levels (purple dots) were significantly elevated in cells treated with H_2O_2 50 μM. We observed a significant increase of IR activation ($pIR^{(Tyr1162/1163)}$/IR, green triangles) with both H_2O_2 10 and 50 μM, without changes of IR protein levels (blue diamonds). IRS1 protein levels are consistently decreased at higher doses, while a significant increase of both activatory ($pIRS1^{(Tyr632)}$/IRS1, black dots) and inhibitory ($pIRS1^{(Ser307)}$/IRS1, brown squares) phosphorylation was observed. Despite of that, the extent of the inhibitory phosphorylation reach those of the activatory phosphorylation at the dose of 10 μM to be finally prominent at the dose of 50 μM, thus indicating a condition of BIR [$pIRS1^{(Ser307)}$/$pIRS1^{(Tyr632)}$ ratio expressed as percentage of control cells (Ctr) setted as 100% is: 95% (1 μM); 115% (5 μM); 108% (10 μM) and 150% (50 μM)]. Upper panels: western blot analyses. Representative bands are shown. Lower panels: densitometric analyses of western blot protein bands. Protein levels were normalized per total protein load. IR- and IRS1-associated phosphorylations were normalized by taking into account the respective protein levels and are expressed as the ratio between the phosphorylated form and the total protein levels: $pIR^{(Tyr1162/1163)}$/IR, $pIRS1^{(Ser307)}$/IRS1 and $pIRS1^{(Tyr632)}$/IRS1. Densitometric values shown are given as percentage of Ctr (n=3 independent cultures/group) set as 100%. Means ± SEM, *p<0.05, **p<0.01 *vs* Ctr (ANOVA with post hoc Turkey t-test).

4.3.8 Lack of BVR-A promotes BIR in SH-SY5Y cells

Given that (i) BIR is associated with a reduced BVR-A activation and that (ii) both increased oxidative and nitrosative stress levels promote a decrease of BVR-A activation, we evaluated the effects produced on IR and IRS1 by BVR-A knock-down in SH-SY5Y neuroblastoma cells. Interestingly, the silencing of BVR-A (siRNA) was associated with reduced IR protein levels and increased IR activation (Fig. 38). Despite of that, a clear inactivation of IRS1 was observed (Fig. 38). To note, the effects produced by insulin, in cells in which BVR-A was consistently silenced, differ from those produced under normal conditions. Indeed, we observed a dramatic increase of IRS1 inhibition after insulin treatment, which was even higher compared to siRNA alone (Fig. 38). These results indicate that reduced BVR-A activation, here mimicked by knocking-down the protein, leads to BIR, and that the effect normally produced by insulin would be shifted toward a condition of BIR when BVR-A does not function properly.

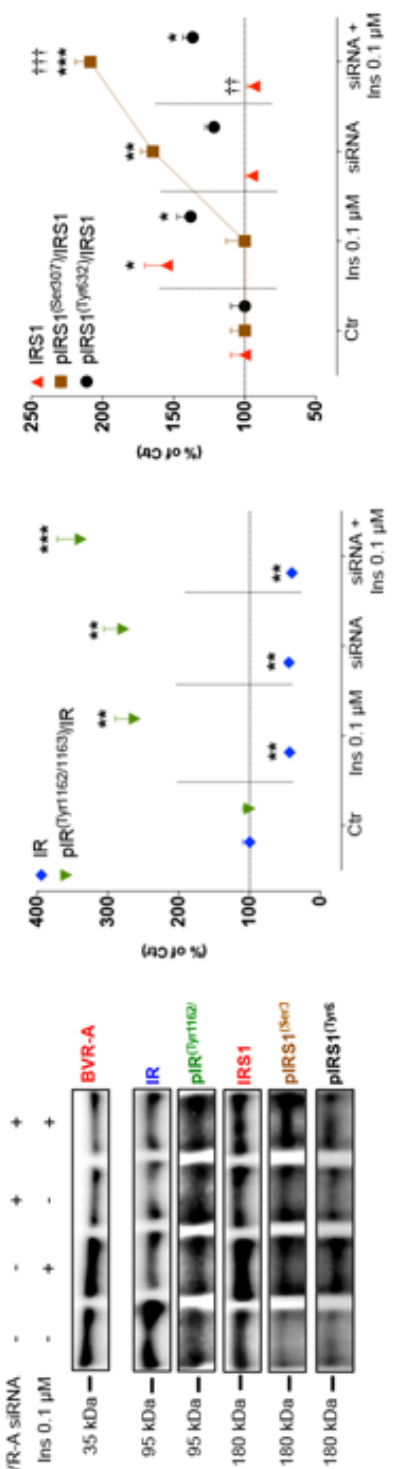

Fig. 29. Lack of BVR-A promotes BIR in SH-SY5Y cells. Silencing BVR-A with a specific siRNA for 24 h was associated with IR activation (increased pIR(Tyr1162/1163)/IR ratio, green triangles) but promoted BIR (increased pIRS1(Ser307), brown squares) in SH-SY5Y neuroblastoma cells. Insulin 0.1 µM was not able to promote the activation of the insulin signaling, but, rather, worsened BIR in cells lacking BVR-A. Increased pIRS1(Tyr632) was also observed, but IRS1 inactivation overcomes this effect. *p<0.05, **p<0.01 and ***p<0.001 vs Ctr; †p<0.05, ††p<0.01 and †††p<0.001 vs Ins 0.1 µM (ANOVA with post hoc Tukey t-test). Left panels: western blot analyses. Representative bands are shown. Right panels: densitometric analyses of western blot protein bands. Protein levels were normalized per total protein load. IR- and IRS1-associated phosphorylations were normalized by taking into account the respective protein levels and are expressed as the ratio between the phosphorylated form and the total protein levels: pIR(Tyr1162/1163)/IR, pIRS1(Ser307)/IRS1 and pIRS1(Tyr632)/IRS1. Densitometric values shown are given as percentage of control cells (Ctr) set as 100%. Means ± SEM (n¼3 independent cultures/group).

4.3.9 BVR-A impairment causes BIR through mTOR

Based on the fact that mTOR, once persistently stimulated, is able to phosphorylate IRS1 on Ser residues, including Ser307, critical for BIR development [244, 245] and because previous studies reported in AD the hyperactivation of mTOR [62, 246-250]; we investigated whether also in our cellular model the BIR was associated with mTOR hyper-activation. To this purpose we evaluated mTOR protein levels and activation (measured by the levels of Ser2448 phosphorylation) in SH-SY5Y cells treated with insulin. We found that insulin treatment does not promote significant changes with regard to mTOR protein levels or activation (Fig. 39A). Interestingly, by re-challenging pre-treated cells with increasing doses of insulin (0.1– 5 μM for 1 h), we further observed a significant increase of mTOR with insulin 0.1 μM and 0.5 μM and a subsequent decrease at the doses of 1 μM and 5 μM (Fig. 39A). These changes parallel either BIR or IRS1 activation and are consistent with changes of BVR-A activation in the same cells (Fig. 34A and Fig. 35). Furthermore, to better clarify the impact of increased oxidative/nitrosative stress levels and BVR-A reduction on mTOR activation, we evaluated the effects produced by ONOO, H_2O_2 or BVR-A silencing in SH-SY5Y neuroblastoma cells. Interestingly, although ONOO and H_2O_2 treatments dose-dependently increased mTOR protein levels (Figs. 39B-C) they produced different outcomes on mTOR activation. Indeed, in accordance with previous findings [251], ONOO promoted a decrease of mTOR phosphorylation (Fig. 39B), whereas a consistent elevation of p-mTOR at Ser2448 was observed after the treatment with 50 μM H_2O_2 (Fig. 39C). Surprisingly, in a subsequent set of experiments, the knock-down of BVR-A was associated with a strong activation of mTOR (Fig. 40), while was further elevated in cells treated with both BVR-A siRNA and 0.1 μM insulin for 24 h (Fig. 40). To note, H_2O_2-induced elevation of p-mTOR at Ser2448 is concomitant with the inactivation of BVR-A (Fig. 32C) and the increased IRS1 phosphorylation levels at Ser307 in the same samples (Fig. 34C). To check whether also in our mice

model BIR was associated with mTOR hyper-activation we then analyzed changes occurring both as effect of AD pathology and normal aging. We found that 3xTg-AD mice are characterized by a significant elevation of p-mTOR (Ser2448) at 12 months (Fig. 41A), which is consistent with increased pIRS1 (Ser307) levels observed at the same age (Fig. 30C). Furthermore, changes associated with normal aging highlight that despite a reduction of mTOR activity occurs from 3 to 12 months, a significant increase at 18 months of age is evident with respect to both 6 and 12 months (Fig. 41B). Although the extent of mTOR phosphorylation at 18 months is still lower than those observed at 3 months of age, it is, however higher than those at both 6 and 12 months of age. Therefore, we think that the raise found at 18 months could be responsible at least in part of IRS1 inactivation. Indeed, in terms of percentage, this increase occurs at a similar extent of those observed in 3xTg-AD mice or SH-SY5Y neuroblastoma cells characterized by BIR. Taken together, these findings denote that increased mTOR activation parallels either BVR-A impairment or insulin resistance in mice and cells, thus strengthening our hypothesis that dysregulation of BVR-A would lead to IRS1 hyperactivation, which is then turned-off by feed-back mechanism(s) including mTOR. Once again, the effects produced by nitrosative stress could be prominent in the early phase of the pathology or the aging process, whereas a major effect of oxidative stress is evident later.

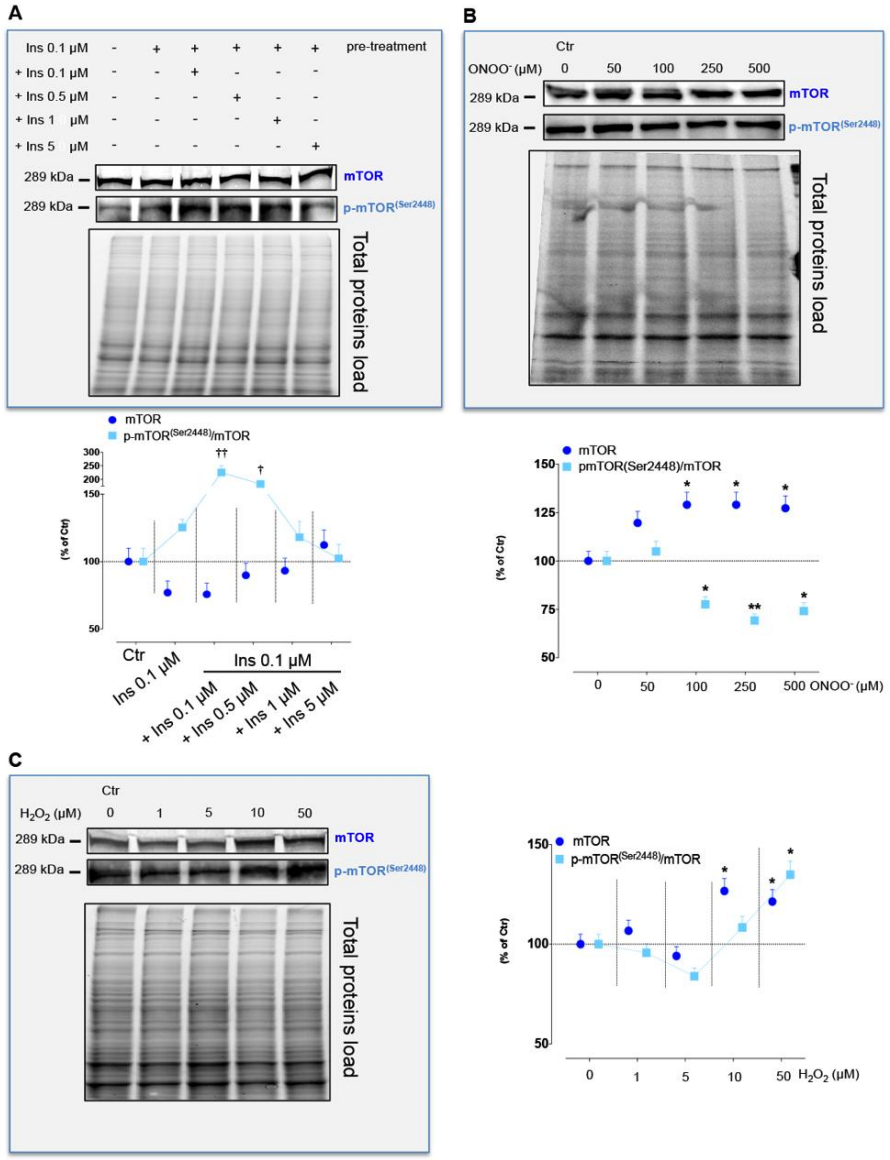

Fig. 39. Aberrant mTOR activation is associated with a state of brain insulin resistance (BIR) in SH-SY5Y cells overexposed to insulin or undergoing increased oxidative and nitrosative stress levels. mTOR protein levels (blue dots) and activation (p-mTOR$^{(Ser2448)}$/mTOR, blue squares) in SH-SY5Y cells treated with insulin (A), $ONOO^-$ (B) or H_2O_2 (C) as previously described. For (A) and (B) Upper panels: western blot analyses. Representative bands are shown. Lower panels: densitometric analyses of western blot protein bands. For (C), left panels: western blot analyses. Representative bands are shown. Right panel: densitometric analyses of western blot protein bands. For (A), (B) and (C) protein levels were normalized per total protein load. mTOR phosphorylation was normalized per total mTOR protein levels and is expressed as p-mTOR$^{(Ser2448)}$/mTOR ratio. Densitometric values shown are given as percentage of control cells (Ctr) set as 100%. Means ± SEM (n=3 independent cultures/group), *p<0.05 and **p<0.01 *vs* Ctr; ††p<0.01 and †††p<0.001 *vs* Ins 0.1 µM (ANOVA with post hoc Tukey t-test).

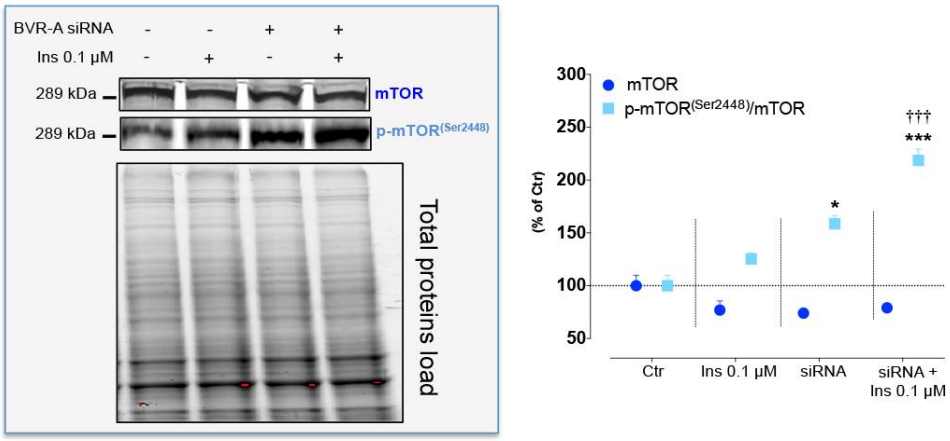

Fig. 40. Lack of BVR-A promotes mTOR hyper-activation in SH-SY5Y cells. mTOR protein levels (blue dots) and activation (p-mTOR$^{(Ser2448)}$/mTOR, blue squares) were evaluated in SH-SY5Y cells knocked-down for BVR-A (BVR-A siRNA). Silencing BVR-A is associated with mTOR hyper-activation. Interestingly, insulin 0.1 µM further increases mTOR hyper-activation in cells lacking BVR-A. *p<0.05 and ***p<0.001 *vs* Ctr; †††p<0.001 *vs* Ins 0.1 µM (ANOVA with post hoc Tukey t-test). Left panels: western blot analyses. Representative bands are shown. Right panels: densitometric analyses of western blot protein bands. Protein levels were normalized per total protein load. mTOR phosphorylation was normalized per total mTOR protein levels and is expressed as p-mTOR$^{(Ser2448)}$/mTOR ratio. Densitometric values shown are given as percentage of control cells (Ctr) set as 100%. Means ± SEM (n=3 independent cultures/group), *p<0.05 and **p<0.01 *vs* Ctr; ††p<0.01 and †††p<0.001 *vs* Ins 0.1 µM (ANOVA with post hoc Tukey t-test).

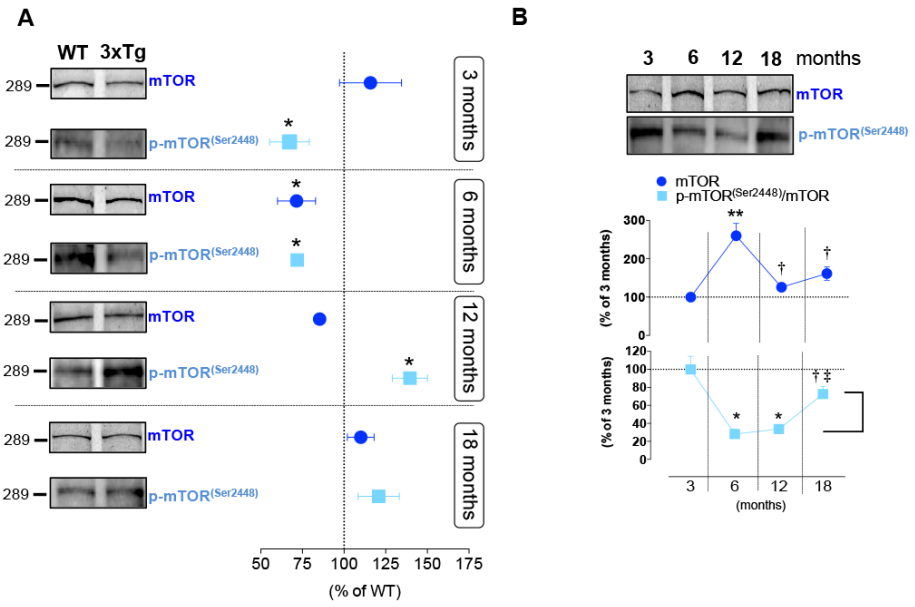

Fig. 41. Hyper-activation of mTOR parallels BIR both during AD and normal aging. (A) mTOR protein levels (blue dots) and activation [p-mTOR(Ser2448), blue squares] evaluated in the hippocampus of 3xTg-AD mice at 3 (n=6), 6 (n=6), 12 (n=6), and 18 (n=6) months of age. Left panels: western blot analyses. Representative bands are shown. Right panels: densitometric analyses of western blot protein bands. Protein levels were normalized per total protein load. mTOR phosphorylation was normalized per total mTOR protein levels and is expressed as p-mTOR(Ser2448)/mTOR ratio. Densitometric values shown are given as percentage of WT mice (n=6/group) set as 100%. Means ± SEM, *p<0.05, vs WT mice (Student's t-test). (B) mTOR protein levels (blue dots) and activation [p-mTOR(Ser2448), blue squares] evaluated in the hippocampus of WT mice as effect of normal aging at 3 (n=6), 6 (n=6), 12 (n=6), and 18 (n=6) months of age. Upper panels: western blot analyses. Representative bands are shown. Lower panels: densitometric analyses of western blot protein bands. Protein levels were normalized per total protein load. mTOR phosphorylation was normalized per total mTOR protein levels and is expressed as p-mTOR(Ser2448)/mTOR ratio. Densitometric values shown are given as percentage of 3 months-old mice set as 100%. Means ± SEM, *p<0.05 and **p<0.01 vs 3 months; †p<0.05 vs 6 months; ‡p<0.05 vs 12 months (ANOVA with post hoc Tukey t-test).

5 DISCUSSION

DS is caused by the anomalous presence of three copies of Chr 21 and characterized by a greatly increased risk of early-onset AD pathology. Indeed, after the age of 40 years, the majority of DS individuals develop a type of dementia with deposition of Aβ plaques and NFTs that are the most prominent and detrimental neuropathological change in AD brain. Inflammation and OS are known to occur in the brains of both AD and DS patients in response to the presence of Aβ plaques and NFTs [6, 13] and several studies demonstrated the involvement of OS and inflammation in accelerated senescence. In addition, the impairment in autophagy-lysosome pathway, resulting in abnormal accumulation of proteins, play a critical role in both AD and DS pathology. Our recent study reported that the early accumulation of protein oxidative damage in human DS is concomitant with the alteration of mTOR/autophagy signaling. Furthermore, the development of BIR is considered a crucial event, impinging on mTOR/autophagy signaling, which contributes to the progression of AD-like pathology. Within this scenario, we focused our attention on the dysregulation of autophagy, insulin signaling and inflammation in DS and AD, human brain samples and animal models, to gain new insights in their role in the onset and progression of the neurodegenerative process. Finally, we propose that OS, as cause and/or consequence of increased free radical burden, represents the "leitmotif" shared by these altered pathways. In particular, a mutual relationship between redox homeostasis and mTOR/autophagy axis activity has been postulated. mTOR is a ser/thr protein kinase and involves in many cellular pathways that regulate neuronal development, synaptic plasticity, cellular aging and neurodegeneration processing. During embryonic development, mTOR signaling acts as a potent neuronal survival and division signal responding to growth factors. While in the adult brain, mTOR controls the synaptic plasticity,

neuronal polarity, neurotransmission and processes underlying memory and learning [252-256]. In the aged brain instead, mTOR is involved in the regulation of the proteostasis network because it is directly involved in the on/off switch of autophagy regulating phagophore formation [48]. Therefore, it is conceivable that the disturbance of mTOR signaling could lead to the alteration of autophagy and to the abnormal accumulation of protein aggregates, which characterizes both AD and DS pathology [42, 249, 252, 257, 258]. Increasing evidence suggests that the mTOR/autophagy axis plays a dual role in the cellular response to OS. Indeed, *in vitro* studies showed that increased levels of OS cause a reduction of mTOR activity, thus inducing the formation of autophagosomes in order to remove potential ROS-induced damage [259-261]. On the other hand, increased mTOR and reduced autophagy, due to aging and age-related disorders, can lead to ROS accumulation and the increase in oxidized proteins including the components of the protein degradative system, thus exacerbating the damage [57, 258, 262, 263]. AD and DS neuropathology are characterized by increased OS and in particular, our group demonstrated that DS cases reported increased oxidative damage to several components of autophagy and proteasome systems confirming a close connection between altered proteostasis network and increased OS [50, 264]. In addition, it has been demonstrated in DS brain the early mTOR hyperactivation coupled with the impairment of autophagy, insulin cascade and increased Aβ load, suggesting that all these events could trigger the appearance of AD symptoms in DS [62, 246, 252, 265]. In order to clarify the relationship between OS and mTOR/autophagy signaling, we analyzed the age-related accumulation of protein oxidation together with the integrity of the mTOR axis in Ts65Dn mice at different ages compared with age-matched euploid mice. In parallel, by blocking mTOR with rapamycin treatment in SH-SY5Ycells, we evaluated the effects of autophagy inhibition on protein oxidative damage. We hypothesize that the overexpression of human Chr 21 genes, such as Sod1, App or Bach1 (encoded on Chr 17 in mice),

might lead to increased 'subchronic' levels of OS in Ts65Dn mice [266, 267]. However, we show that despite the potential early genotype-dependent increase of OS in Ts65Dn mice the total levels of protein oxidation, indexed by both protein-bound HNE and protein-bound 3-NT, start to rise at 6 months but become significantly increased only at 12 months compared with age-matched euploid mice. The analysis of mTOR expression, in Ts65Dn mice, shows an increase at 6 months but unchanged levels at 12 months of age compared with age-matched euploid controls. Instead, the levels of mTOR phosphorylation on Ser 2448, which reflects the activation of mTOR, show increased levels at 6 and 12 months of age in Ts65Dn mice compared with age-matched euploid mice. These results support a genotype-dependent alteration of the mTOR pathway in Ts65Dn mice starting at 6 months of age that persists at 12 months of age. Because mTOR inhibits the formation of autophagosomes, we evaluated LC3 II/I ratio demonstrating that increased mTOR phosphorylation is associated with a significant decrease in the LC3 II/I ratio in Ts65Dn mice both at 6 and 12 months of age compared with euploid mice. All together these results support that, despite the early alteration of the mTOR/autophagy pathway in Ts65Dn mice, protein oxidative damage becomes significant only in old animals, suggesting that the accumulation of oxidative damage depend on the prolonged impairment of the mTOR/autophagy axis. To confirm our hypothesis, we evaluated the effect of rapamycin (mTOR inhibitor) on protein oxidation in SH-SY5Ycells H_2O_2-treated. Our data show that rapamycin administration decreased mTOR expression after 24, 48 and 72h when compared with control group, but only at 72h we measured a concomitant reduction of mTOR phosphorylation levels. Interestingly, the evaluation of autophagosome formation, as indexed by the LC3 II/I ratio, displayed an increase in the rapamycin treated group already after 48h compared to control. The evaluation of total protein oxidation, in the Rp group, showed a significant decrease in protein bound 3-NT levels at 48 and 72h and a significant decrease in

protein-bound HNE levels at only 72h compared to St group. Overall, these data demonstrate that mTOR inhibition induces autophagosome formation and reduces the protein oxidative damage. This study provides further insights into the role of mTOR hyperactivation and autophagy reduction in the progression of neurodegenerative diseases characterized by the buildup of oxidized proteins such as AD and DS pathology. Hyperactivation of mTOR signaling has also been associated with increased OS and elevated inflammatory response. Among putative regulators involved in the inflammatory response we focalized our attention on miRNAs.

miRNAs are post-transcriptional regulators of gene expression and increasing evidence support their involvement in neural development and neural function under physiological and pathological conditions [237-239]. In particular, miR146a and miR155 are two miRNAs associated with IL-1β pathway that differently modulate the inflammatory response astrocyte-mediated. miR146a acts as negative-inflammatory regulator by suppressing NF-κB transcriptional activity and sequentially blocks the TLR-signaling, while miR155 acts as pro-inflammatory regulator through the inhibition of SHIP1, a negative regulator of TLR-signaling [186, 268]. Interestingly it has been reported the early upregulation of miR155 in 3xTg AD mice, in microglial and astrocytes exposed to Aβ [269], as well as the up-regulation of miR146a in human AD brain and in different AD mouse models [36, 37, 270]. Based on these observations we hypothesized that an inflammation-mediated dysregulation of both miR146a and miR155 in fetal brain (i.e. in DS) could contribute to development of neurobehavioral abnormalities, as well as, could contribute to age-related inflammatory neurodegenerative disorders, including AD pathology. Thus, in the present study we provide the first description of the expression pattern and cellular localization of both miR146a and miR155 in control and DS hippocampus during pre- and early postnatal development, as well as, in adults with DS-AD pathology. In order to provide supportive evidence of

age and pathology related dysregulation of miR146a and miR155, we evaluated the levels of these miRNAs, their putative targets and the levels of IL-1β in human hippocampus from sporadic AD and in Ts65Dn mice and APP/PS1 mice. We showed a similar developmental pattern of miR146a and miR155 expression in DS and control hippocampus with prenatal expression of miR146a in VS/SVZ and persistent neuronal expression at later prenatal and postnatal ages. However, at mid-gestation, we observed, higher level of miRNA146a expression in DS astroglial cells compared to control within the hippocampal white matter. Such astroglial expression persisted also postnatally. Since in a recent study using the same cohort, we could not detect significant differences in the number of astrocytes between DS patients and controls [271], and because miR146a is potently induced by IL-1β in astrocytes [186, 197], we think that this local upregulation of miR146a in DS hippocampus may be the result of a proinflammatory microenvironment involving IL-1β-mediated astroglial activation. Interestingly, a recent study identified miR146a as one of the miRNAs deregulated in autism spectrum disorders, as well as in patients with intellectual disability without autistic features, suggesting that miR146a upregulation could represent a common hallmark of different neurodevelopmental disorders [272]. Moreover, *in vitro* experiments indicate that an overexpression of miR146a may critically affect both neuronal and glial cells biology, resulting in an impaired neuronal dendritic arborization and increased astrocyte glutamate uptake [272]. We evaluated the expression of both miR155 and miR146a in Ts65Dn at different age (from 4-5 weeks to 18 months) in both cortex and hippocampus. While Keck-Wherley et al. [273] revealed increased expression (using qPCR) of miR155 in Ts65Dn hippocampus of 5 to 6 weeks of age we failed to detect differences for both miR146a and miR155 at 4-5 weeks but also in older Ts65Dn (6-18 months) and the target of miR155 (Ship1) was even increased in the Ts65Dn compared to control euploid mice at 6 months of age. We detected the upregulation of IL-1β mRNA in Ts65Dn at 18 months

compared to control euploid mice, indicating an increased activation of IL-1β pathway. While a previous study reported a reduction of IL-1β protein level in Ts65Dn hippocampus from 8 to 10 months of age [274], we didn't detect significant differences in IL-1β expression between 4-5 weeks and 12 months in Ts65Dn compared to control euploid mice. Despite the higher level of IL-1β, we observed an age depend reduction of miR146a (hippocampus and cortex) and of miR155 (hippocampus) compared to young animals (4-5 weeks). In the cortex, the expression of miR146 was negatively correlated with its target Traf6, suggesting a modulation of the IL-1β pathway. The mechanisms underlying these age and region specific changes of miR146a and miR155 are still unclear and deserve further investigation. We observed a significant increase in expression of both miR146a and miR155 in APP/PS1 mice at 11-13 months of age as compared to both WT and APP/PS1 mice at 3 months. We also measured the increased expression of IL-1β in the APP/PS1 mice, compared to WT, confirming the activation of neuroinflammatory signals in this model [274]. Interestingly, a positive correlation was also detected between both miR146a, miR155 and IL-1β, in agreement with their known regulation via NF-κB signaling [185, 186, 228, 268, 275]. Moreover, we observed a negative correlation between the level of miR146a and the expression of its target Traf6. The more prominent deregulation of miR146a and miR155 observed in APP/PS1 AD model, compared to Ts65Dn DS model, may suggest the contribution of Aβ to the regulation of these miRNA, as supported by *in vitro* studies in glial cells [72, 276]. Accordingly, miR146a and miR155 were both upregulated in glial cells within the hippocampus of DS with AD pathology, particularly in the vicinity of Aβ deposits. In agreement with the involvement of miR155 in endothelial cell function and angiogenesis we also detected its expression in endothelial cells suggesting a role of miR155 in BBB dysfunction, which has been reported in AD [277, 278]. Furthermore, we reported the upregulation of miR146a in AD at late-stage and also showed a negative

correlation between miR146a and its target Irak1. This is in line with a recent study, which show the reduction of Irak1 mRNA levels in human astrocytes transfected with miR146a mimic after stimulation with IL-1β [186]. Another potential target of both miR146a and miR155 is the complement factor H (CFH), which acts as negative regulator of the innate immune and inflammatory response [279, 280]. Thus, the possible repression of CFH, has to be taken into account with respect to the interpretation of the ultimate effects of changes in the expression of miR146a and miR155. However, under our experimental conditions, we did not detect significant changes in the expression of CFH after overexpression or knockdown experiments targeting both miR146a and miR155 [186].

An emerging link between peripheral metabolic disorder and AD has been proposed by recent epidemiological studies [199-202, 281, 282]. In particular, AD patients are characterized by impaired glucose metabolism and postmortem analyses in AD brain demonstrated an inadequate response to insulin known BIR. This condition is mainly due to reduced IR activation and increased levels of inhibitory phosphorylation of IRS1. However, the onset of BIR in AD is a matter still under debate. Because BVR-A represents an upstream regulator of the insulin cascade [214] and because we previously demonstrated that OS induces the impairment of BVR-A in human AD brain, we hypothesize that the OS-induced BVR-A dysregulation could be associated with the onset of BIR. The involvement of BVR-A in the insulin signaling is interesting for two main reasons: BVR-A is a direct target of IR kinase activity and once IR-phosphorylated is able to phosphorylate IRS1 on Ser inhibitory domains critical for insulin signaling [214] and (ii) BVR-A contains specific motifs in its sequence through which modulates IR kinase activity both negatively and positively [283]. Our work provides for the first time evidence (i) about a dysfunction of insulin signaling produced by the impairment of a member of the signaling itself, i.e., BVR-A, and (ii) on how the identified mechanism develops with AD pathology and normal aging. In order to

confirm our hypothesis and clarify the mechanisms underlying BIR we analyzed the age dependent changes of (i) BVR-A protein levels, (ii) BVR-A activation indexed by pTyr-BVR-A, (iii) total OS markers levels (PC, HNE, 3-NT) as well as (iv) IR/IRS1 levels and activation in 3xTg-AD mice. Furthermore, *ad hoc* in-vitro experiments have been performed to decipher the contribution of increased oxidative/nitrosative stress on BVR-A impairment and insulin resistance. Finally, because mTOR is able to phosphorylate IRS1 we investigated also if the BIR could be associated with mTOR hyper-activation in both mice and in vitro model. Unexpectedly we found reduced BVR-A protein levels in the hippocampus of 3xTg-AD mice aged from 3 to 12 months with respect to WT controls (Fig. 29A–C). While, increased BVR-A protein levels have been found at 18 months of age (Fig. 28B) [284]. In agree with previous studies, the semi-quantitative analyses of Aβ and tau immunostaining demonstrated a gradually accumulation of Aβ and tau pathology in 3xTg-AD mice characterized by dense Aβ deposit and extensive human tau immunoreactivity at 18 months of age [240]. Furthermore, because TNF-α is known to inhibit BVR-A [241] we investigated whether reduced BVR-A protein levels, observed from 3 to 12 months of age in 3xTg-AD mice, can result from increased TNF-α level. We found a significant reduction of TNF-α levels from 3 to 12 months of age followed by a consistent increase at 18 months in 3xTg-AD mice with respect to WT (Fig. 31). All together these results suggest that the reduction of BVR-A protein levels, already evident at 3 months, seems to be a specific event, which occurs independently of TNF-α elevation (Fig. 31) and prior Aß and tau accumulation (Fig. 28B). In order to decode the potential contribution of oxidative/nitrosative stress to the alterations of BVR-A function, we evaluated the levels of oxidative/nitrosative stress markers and of pTyr-BVR-A in the hippocampus of 3xTg-AD mice at 3, 6, 12 and 18 months of age. This analysis allowed us to identify three different phases of BVR-A activation: a first phase at 3 months of age characterized by an increased pTyr-BVR-A, a second phase at 6

months of age characterized by a drastic decrease of pTyr-BVR-A and a third phase from 12 to 18 months characterized by a consistent increase of 3-NT-BVR-A. These results suggest that the reduction of BVR-A activation at 6 months is due to reduced phosphorylation on Tyr residues (Fig. 29B) rather than increased 3-NT modifications, which becomes consistent at 12 months (Fig. 29C). It is important to highlight that both phosphorylation and nitration reactions share the same Tyr residues and are mutually exclusive events [285] therefore one conceivable explanation for this control on BVR-A activation is that the increased total 3-NT levels observed at 6 months (Fig. 28A) affect redox sensitive signaling pathways, such as phosphorylation cascades [286]. Data obtained on cells treated with ONOO reinforced such hypothesis. Furthermore, we investigated whether in 3xTg-AD mice the BVR-A reductase activity was impaired as reported in human AD brain [226]. Interestingly, we observed a significant reduction of BVR-A reductase activity at 12 months, which coincides with increased levels of 3-NT modifications (Fig. 29), suggesting that increased oxidative/nitrosative stress levels promote the impairment of both BVR-A activities (reductase and kinase) with the progression of AD pathology. To unravel the mechanisms through which the BVR-A dysregulation might impact insulin signaling in AD, we evaluated changes with regard to IR and IRS1 protein levels/activation in the hippocampus of 3xTg-AD mice. We found the early increased activation of both IR and IRS1 from 3 to 6 months followed by reduction of IR activation together with a consistent IRS1 inactivation starting at 12 months of age (Fig. 30). These two phases are consistent with changes of BVR-A activation state suggesting that the lack of control exerted by BVR-A on IRS1 is primarily associated with IRS1 hyperactivation. This, in turn, leads to BIR probably through feedback mechanisms aimed to turn-off IRS1 hyperactivity. Indeed, while at 3 months of age it is conceivable that IR hyper-activation could be blunted by increased BVR-A activation, which would avoid IRS1 hyper-activation (Fig. 29A and Fig. 30A), at 6 months of age reduced BVR-

A activation is associated with IRS1 hyper-activation (Fig. 29B and Fig. 30C–D). We propose that the period included between 6 and 12 months of age represents the time-frame for the switch from activated insulin signaling to BIR in the hippocampus of 3xTg-AD mice. Considering that insulin signaling positively modulate the synaptic plasticity and long-term potentiation (LTP) [287, 288], the dramatic decline of cognitive functions in 3xTg-AD from 6 to 12 months of age [284] correlates positively with our data on the impairment of the insulin signaling which mainly occurring in the same time-frame, supporting a role of defective insulin signaling in the decline of cognitive functions [284]. Surprisingly we observed that BIR occurs in the hippocampus of WT mice with normal aging and is associated with reduced BVR-A protein levels and with increased 3-NT modifications of BVR-A (Fig. 32A–B). Data about TNF-α levels only partially explain the reduction of BVR-A protein levels at 12 months of age, which precedes the appearance of the BIR at 18 months in WT mice (Fig. 32A–B). Indeed, whether increased TNF-α levels could contribute to BVR-A reduction at 12 months (Fig. 32A and Fig. 33C)[241], reduced TNF-α levels at 18 months would not explain either the persistent reduction of BVR-A protein levels or the huge increase of IRS1 phosphorylation (Fig. 32A–B and Fig. 33C). With regard to 3-NT-BVR-A levels we observed a significant increase in WT mice at 18 months of age (Fig. 34A) associated with a significant decrease of BVR-A reductase activity (Fig. 44A). Essentially what emerges from our data on WT mice is that, during normal aging, BIR parallels with increased oxidative/nitrosative stress levels (Fig. 32B) and BVR-A impairment (Fig. 32A–B). These results strengthen the role of BVR-A in the onset of BIR and we propose the impairment of BVR-A as a bridge connecting aging and AD. From a molecular point of view our cell-based experiments clearly highlight that insulin resistance is associated with a reduction of BVR-A activation and that oxidative and nitrosative stress promotes insulin resistance and BVR-A inactivation. Considering that in the brain the regulation of

glucose uptake and energy metabolism differs from peripheral tissues indeed the activation of insulin signaling cascade mainly exerts neurotrophic functions we demonstrated that silencing BVR-A in neurons promotes IRS1 inactivation and negatively impacts the effects produced by insulin itself (Fig. 38). We hypothesize that the persistent inactivation of BVR-A can initially sustain insulin signaling by IRS1 hyper-activation and subsequently promote BIR by unknown feedback mechanisms that turn-off IRS1-associated downstream effects. Because mTOR, once persistently stimulated, is able to phosphorylate IRS1 on Ser inhibitory domains, [244, 245] and because recent studies suggest the involvement of mTOR hyperactivation in AD [62, 246-250]; we propose mTOR as putative kinase implicated in BIR development causing IRS1 inhibitory phosphorylation. To this purpose we investigated in SH-SY5Y cells line whether insulin resistance and increased oxidative/nitrosative stress levels are associated with an aberrant activation of mTOR. We showed the aberrant activation of mTOR either following insulin over-exposure or H_2O_2 treatment. Instead, ONOO treatment was associated with a reduction of mTOR activation. Noteworthy, the silencing of BVR-A is associated with mTOR hyper-activation (Fig. 40). However, whether the observed increased mTOR activation is a direct effect of BVR-A inactivation or the results of the sustained activation of the insulin signaling has to be clarified. The fact that BVR-A could regulate mTOR activation [97] appear very fascinating and proposed by previous report that show high doses of biliverdin (the substrate of BVR-A) promote the activation of mTOR pathway [289]. However, because biliverdin does not directly regulate mTOR activation, and because biliverdin is known to inhibit BVR-A expression [241], our findings suggest that the effect of biliverdin on mTOR pathway can be an event secondary mediated by a down-regulation of BVR-A. The idea that the reduction of BVR-A activity results in the hyper-activation of mTOR could represents one of the mechanisms responsible of IRS1 inactivation is further confirmed by data obtained in mice both during AD-

like pathology and normal aging. Indeed, in 3xTg-AD mice mTOR hyperactivation occurs at 12 months of age (Fig. 41A), exactly when we observed significant IRS1 inhibition (Fig. 30C), as well as in WT mice, but at 18 months of age (Fig. 32B and Fig. 41B). Taken together, these observations support our hypothesis that the persistent inactivation of BVR-A contributes to BIR in AD by mTOR hyperactivation. Furthermore, considering TNF-α as mediator of BIR in AD [290] and based on our results in 3xTg-AD mice, that showed increased levels of TNF-α only at 18 months of age, we may hypothesize that the impairment of BVR-A coupled with the hyper-activation of mTOR are early events contributing to BIR. Finally, another interesting result is that the administration of high doses of insulin (5 μM) to SH-SY5Y cells, previously stimulated with insulin 0.1 μM, is able to overcomes insulin resistance (Fig. 34A) associated with the increased activation of BVR-A (Fig. 43A) and the reduction of p-mTOR to control levels (Fig. 39A).

6 CONCLUSION

In this study we focused our attention on the dysfunction of molecular pathways including autophagy, insulin signaling and inflammation that are closely related with increased OS and that might be involved in the development of Alzheimer-like dementia. A mutual relationship between redox homeostasis and mTOR/autophagy axis activity has been postulated and our results collected in Ts65Dn and SH-SY5Y neuroblastoma cell line support the idea that the defects of mTOR signaling contribute to the buildup of protein oxidative damage and that a protective role is played by autophagy in reducing protein oxidation. Further, a link between inflammation and OS exists and the hyperactivation of mTOR signaling has been associated with both increased OS and elevated inflammatory response. miR146a and miR155 are two inflammation-related miRNAs NF-κB-inducible associated with IL-1β pathway. Increasing evidence supports the involvement of miRNAs in neural development and function under physiological and pathological conditions [237-239]. Interestingly, it has been reported the upregulation of miR155 and miR146a in AD brain and in different AD mouse models [280, 291]. Based on these observations we hypothesized that an inflammation-mediated dysregulation of both miR146a and miR155 in fetal brain (i.e. in DS) could contribute to development of neurobehavioral abnormalities as well as could contribute to age-related inflammatory neurodegenerative disorders including AD pathology. Our findings suggest a possible involvement of both miR146a and miR155 in the hippocampus during brain development and provide evidence of a dysregulation of these two immunomodulatory miRNAs in DS and AD pathology. In addition, the more prominent deregulation of miR146a and miR155 observed in APP/PS1 AD model, compared to Ts65Dn DS model, may suggest the contribution of Aβ to the regulation of these miRNA. Post-mortem

analyses in AD demonstrated BIR, due to reduced IR activation and increased inhibitory phosphorylation of IRS1, proposing a role for cognitive deficits. Because BVR-A is a direct target of IR kinase activity and once IR-phosphorylated is able to phosphorylate IRS1 on Ser inhibitory, and because we previously demonstrated that OS induces impairment of BVR-A in human AD brain, we suggest that BVR-A dysregulation could be associated with the onset of BIR. Furthermore, because mTOR, as BVR-A, is able to phosphorylate IRS1 on Ser inhibitory domains [244, 245] and because recent studies suggest the involvement of mTOR hyperactivation in AD [62, 246-250]; we investigated also if the BIR could be associated with mTOR hyper-activation. The results obtained suggest that the OS-induced inactivation of BVR-A initially sustain insulin signaling by IRS1 hyper-activation. Such over-activation of the insulin signaling, for a time longer than normal, promote BIR by hyper-activation of mTOR that turn-off IRS1 hyper-activity (Fig. 42).

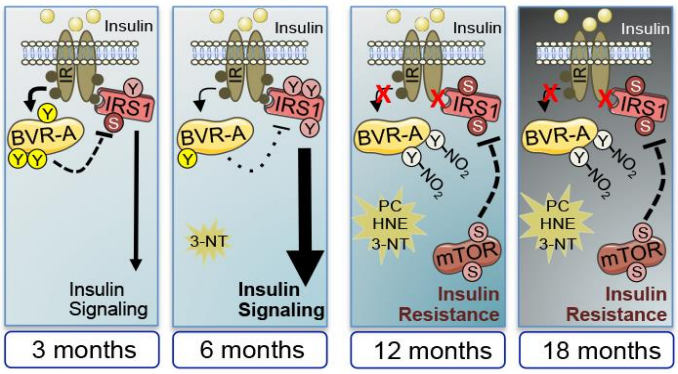

Fig. 42. Temporal profile of the events promoting BIR in the hippocampus 3xTg-AD mice. Proposed mechanism leading to BIR in AD. At 3 months of age the insulin binding to IR promotes IR phosphorylation on Tyr residues, which leads to a consistent activation of BVR-A. This latter, in turn, probably blunts IRS1 hyper-activation thus allowing a still normal activation of the insulin signaling. At 6 months of age while IR appears to be still activated, BVR-A does not probably because increased 3-NT levels. Lacking BVR-A activity promotes IRS1 hyper-activation, which sustains the activation of the insulin signaling for a time perhaps longer than normal. Between 6 and 12 months of age, the further rise of the oxidative/nitrosative stress levels (PC, HNE and 3-NT) result in the oxidative stress-induced impairment of BVR-A, which contributes to maintain IRS1 hyperactive. IRS1 hyperactivation leads to the aberrant activation of mTOR, which through a feedback mechanism turn-off IRS1 thus leading to BIR. Finally, 18 months of age are characterized by the persistence of the same modifications observed at 12 months, which contribute to the maintenance of an BIR profile. Arrows, promotion; dotted lines, inhibition; Y, phosphor-Tyr residues; S, phospho-Ser residues; Y-NO2, 3-NT modifications.

7 APPENDIX

Appendix A

Developmental expression and dysregulation of miR-146a and miR-155 in Down's syndrome and mouse models of Down's syndrome and Alzheimer's disease

A. Arena[1,2*], A.M. Iyer[1*], I. Milenkovic[3], G. G. Kovács[3], I. Ferrer[4], M. Perluigi[2], E. Aronica[1,5*]

[1]Department of (Neuro)Pathology, Academic Medical Center, University of Amsterdam, The Netherlands

[2]Department of Biochemical Sciences, Sapienza University of Rome, Rome, Italy

[3] Institute of Neurology, Medical University of Vienna, Austria

[4]Institute of Neuropathology, Bellvitge University Hospital, University of Barcelona Hospitalet de Llobregat, Spain

[5]Swammerdam Institute for Life Sciences, Center for Neuroscience, University of Amsterdam and Stichting Epilepsie Instellingen Nederland (SEIN), The Netherlands

** contributed equally to this work.*

Correspondence should be addressed to: Dr. E. Aronica
Dept. (Neuro) Pathology,
Academic Medical Center,
Meibergdreef 9
1105 AZ Amsterdam, The Netherlands
Phone: 31-20-5662943
FAX: 31-20- 5669522
E-mail: e.aronica@amc.uva.nl

Key Words: hippocampus – development- Down's syndrome - Alzheimer's disease – Ts65DN- APP/PS1- microRNAs

Running title: miR-146a and miR-155 in development and Down's syndrome

Appendix B

Publisher: Taylor & Francis

Journal: *Expert Review of Neurotherapeutics*

DOI: 10.1080/14737175.2017.1246183

Review

Modulation of GLP-1 signaling as a novel therapeutic approach in the treatment of Alzheimer's disease pathology

Antonella Tramutola[1], Andrea Arena[1], Chiara Cini[1], D. Allan Butterfield[2] and Eugenio Barone[1,3,*]

[1] *Department of Biochemical Sciences "A. Rossi-Fanelli", Sapienza University of Rome, Piazzale A. Moro 5, 00185 Roma, Italy;*
[2]*Department of Chemistry and Sanders-Brown Center on Aging, University of Kentucky, Lexington, KY 40506-0055, USA.*
[3]*Universidad Autónoma de Chile, Instituto de Ciencias Biomédicas, Facultad de Salud, Avenida Pedro de Valdivia 425, Providencia, Santiago, Chile.*

*Corresponding author: Eugenio Barone, Department of Biochemical Sciences "A. Rossi-Fanelli", Sapienza University of Rome, Piazzale A. Moro 5, 00185 Roma, Italy;
phone: +39 064991 0885
e-mail: eugenio.barone@uniroma1.it

Appendix C

ANTIOXIDANTS & REDOX SIGNALING
Volume 00, Number 00, 2016

DOI: 10.1089/ars.2016.6686

FORUM ORIGINAL RESEARCH COMMUNICATION

Polyubiquitinylation Profile in Down Syndrome Brain Before and After the Development of Alzheimer Neuropathology

Antonella Tramutola,[1] Fabio Di Domenico,[1] Eugenio Barone,[1] Andrea Arena,[1] Alessandra Giorgi,[1] Laura di Francesco,[1] Maria Eugenia Schininà,[1] Raffaella Coccia,[1] Elizabeth Head,[2,3] David Allan Butterfield,[2,4] and Marzia Perluigi[1]

Abstract

Aims: Among the putative mechanisms proposed to be common factors in Down syndrome (DS) and Alzheimer's disease (AD) neuropathology, deficits in protein quality control (PQC) have emerged as a unifying mechanism of neurodegeneration. Considering that disturbance of protein degradation systems is present in DS and that oxidized/misfolded proteins require polyubiquitinylation for degradation *via* the ubiquitin proteasome system, this study investigated if dysregulation of protein polyubiquitinylation is associated with AD neurodegeneration in DS. ***Results:*** Postmortem brains from DS cases before and after development of AD neuropathology and age-matched controls were analyzed. By selectively isolating polyubiquitinated proteins, we were able to identify specific proteins with an altered pattern of polyubiquitinylation as a function of age. Interestingly, we found that oxidation is coupled with polyubiquitinylation for most proteins mainly involved in PQC and energy metabolism. ***Innovation:*** This is the first study showing alteration of the polyubiquitinylation profile as a function of aging in DS brain compared with healthy controls. Understanding the onset of the altered ubiquitome profile in DS brain may contribute to identification of key molecular regulators of age-associated cognitive decline. ***Conclusions:*** Disturbance of the polyubiquitinylation machinery may be a key feature of aging and neurodegeneration. In DS, age-associated deficits of the proteolytic system may further exacerbate the accumulation of oxidized/misfolded/polyubiquitinated proteins, which is not efficiently degraded and may become harmful to neurons and contribute to AD neuropathology. *Antioxid. Redox Signal*. 00, 000–000.

Keywords: Alzheimer disease, Down syndrome, proteasome, proteomics, trisomy21, ubiquitin

Introduction

DOWN SYNDROME (DS) IS the most frequent genetic cause of intellectual disability caused by the presence of three copies of chromosome 21 (Chr21). Several studies reveal that DS and Alzheimer's disease (AD) neuropathology have many common features that include deposition of senile plaques and neurofibrillary tangles, together with cellular dysfunction such as mitochondrial defects, increased oxidative stress, and impairment of protein quality control (PQC) (4, 27, 51, 53, 57). Around two-thirds of individuals with DS develop dementia in their 50s, but the severity of neuropathology and dementia varies significantly among DS population. Triplication of APP is considered the major pathological event to which converge both AD-DS and normal AD, but it is clear that several other genes contribute to the neurodegenerative process. Moreover, understanding the cross-talk between genetic and environmental factors could provide insights into the molecular mechanisms responsible of early onset AD in DS. Thus, DS offers a unique model to investigate the early molecular changes that disturb neuronal homeostasis and that with age lead slowly, but irreversibly, to neuronal death [reviewed in Wiseman *et al.* (72)].

[1]Department of Biochemical Sciences, Sapienza University of Rome, Italy, Rome.
[2]Sanders-Brown Center on Aging, University of Kentucky, Lexington, Kentucky.
Departments of [3]Pharmacology and Nutritional Sciences and [4]Chemistry, University of Kentucky, Lexington, Kentucky.

Appendix D

HHS Public Access
Author manuscript
J Alzheimers Dis. Author manuscript; available in PMC 2016 August 01.

Published in final edited form as:
J Alzheimers Dis. 2016 ; 52(1): 359–371. doi:10.3233/JAD-151105.

ACTIVATION OF p53 IN DOWN SYNDROME AND IN THE Ts65Dn MOUSE BRAIN IS ASSOCIATED WITH A PRO-APOPTOTIC PHENOTYPE

Antonella Tramutola[#1], **Gilda Pupo**[#1], **Fabio Di Domenico**[1], **Eugenio Barone**[1,2], **Andrea Arena**[1], **Chiara Lanzillotta**[1], **Diede Brokeaart**[3], **Carla Blarzino**[1], **Elizabeth Head**[4], **D Allan Butterfield**[4,5], and **Marzia Perluigi**[1,*]

[1] Department of Biochemical Sciences, Sapienza University of Rome, Italy

[2] Universidad Autónoma de Chile, Instituto de Ciencias Biomédicas, Facultad de Salud, Providencia, Santiago, Chile

[3] Department of Neuropathology, University of Amsterdam (NL)

[4] Sanders-Brown Center of Aging, University of Kentucky, Lexington KY, USA

[5] Department of Chemistry, University of Kentucky, Lexington KY, USA

[#] These authors contributed equally to this work.

Abstract

Down Syndrome (DS) is the most common genetic cause of intellectual disability resulting from trisomy of chromosome 21. The main feature of DS neuropathology includes early onset of Alzheimer's disease, with deposition of senile plaques and tangles. We hypothesized that apoptosis may be activated in the presence of AD neuropathology in DS, thus we measured proteins associated with upstream and downstream pathways of p53 in the frontal cortex from DS cases with and without AD pathology and from Ts65Dn mice, at different ages. We observed increased acetylation and phosphorylation of p53, coupled to reduced MDM2-mediated ubiquitination and lower levels of SIRT1. Activation of p53 was associated with a number of down-stream targets (bax, PARP1, caspase-3, heat shock proteins and PGC1α) that were modulated in both DS and DS/AD compared with age-matched controls. In particular, the most relevant changes (increased p-p53, acetyl-p53 and reduced formation of MDM2/p53 complex) were found to be modified only in the presence of AD pathology in DS. In addition, a similar pattern of alterations in the p53 pathway were found in Ts65Dn mice. These results suggest that p53 may integrate different signals, which can result in a pro-apoptotic-phenotype contributing to AD neuropathology in people with DS.

[*]Corresponding author: Marzia Perluigi, Department of Biochemical Sciences, Sapienza University of Rome, P.le Aldo Moro, 5 00185 Rome (IT), Phone: +39 0649910885, Fax: +39 064440062, Marzia.perluigi@uniroma1.it.

Contributions.
M.P., D.A.B and F.DD conceived and designed the experiments. A.T., G.P., D.B. and A.A. performed the experiments. E.B., C.L and C.B. performed statistics and analyzed the data. M.P. and A.T. wrote the paper. E.H. and D.A.B. critically revised the manuscript. All the authors read and discussed the manuscript. Study supervision: M.P. and F.DD.

Competing interests.
The authors declare no competing financial interests.

Appendix E

Free Radical Biology and Medicine 91 (2016) 127–142

Contents lists available at ScienceDirect

Free Radical Biology and Medicine

journal homepage: www.elsevier.com/locate/freeradbiomed

Original Contribution

Impairment of biliverdin reductase-A promotes brain insulin resistance in Alzheimer disease: A new paradigm

Eugenio Barone [a,b], Fabio Di Domenico [a], Tommaso Cassano [c], Andrea Arena [a], Antonella Tramutola [a], Michele Angelo Lavecchia [d], Raffaella Coccia [a], D. Allan Butterfield [e,*], Marzia Perluigi [a,*]

[a] Department of Biochemical Sciences "A. Rossi-Fanelli", Sapienza University of Rome, Piazzale A. Moro 5, 00185 Roma, Italy
[b] Universidad Autónoma de Chile, Instituto de Ciencias Biomédicas, Facultad de Salud, Avenida Pedro de Valdivia 425, Providencia, Santiago, Chile
[c] Department of Clinical and Experimental Medicine, University of Foggia, Via Napoli 20, 71122 Foggia, Italy
[d] Department of Physiology and Pharmacology "V. Erspamer", Sapienza University of Roma, Piazzale A. Moro 5, 00185 Roma, Italy
[e] Department of Chemistry, Markey Cancer Center, and Sanders-Brown Center on Aging, University of Kentucky, Lexington, KY 40506-0055, USA

ARTICLE INFO

Article history:
Received 5 October 2015
Received in revised form
10 December 2015
Accepted 12 December 2015
Available online 15 December 2015

Keywords:
Alzheimer disease
Biliverdin reductase-A
Oxidative stress
Insulin resistance
3xTg-AD mice

ABSTRACT

Clinical studies suggest a link between peripheral insulin resistance and cognitive dysfunction. Interestingly, post-mortem analyses of Alzheimer disease (AD) subjects demonstrated insulin resistance in the brain proposing a role for cognitive deficits observed in AD. However, the mechanisms responsible for the onset of brain insulin resistance (BIR) need further elucidations. Biliverdin reductase-A (BVR-A) emerged as a unique Ser/Thr/Tyr kinase directly involved in the insulin signaling and represents an upstream regulator of the insulin signaling cascade. Because we previously demonstrated the oxidative stress (OS)-induced impairment of BVR-A in human AD brain, we hypothesize that BVR-A dysregulation could be associated with the onset of BIR in AD. In the present work, we longitudinally analyze the age-dependent changes of (i) BVR-A protein levels and activation, (ii) total oxidative stress markers levels (PC, HNE, 3-NT) as well as (iii) IR/IRS1 levels and activation in the hippocampus of the triple transgenic model of AD (3xTg-AD) mice. Furthermore, *ad hoc* experiments have been performed in SH-SY5Y neuroblastoma cells to clarify the molecular mechanism(s) underlying changes observed in mice. Our results show that OS-induced impairment of BVR-A kinase activity is an early event, which starts prior the accumulation of Aβ and tau pathology or the elevation of TNF-α, and that greatly contribute to the onset of BIR along the progression of AD pathology in 3xTg-Ad mice. Based on these evidence we, therefore, propose a new paradigm for which: OS-induced impairment of BVR-A is firstly responsible for a sustained activation of IRS1, which then causes the stimulation of negative feedback mechanisms (i.e. mTOR) aimed to turn-off IRS1 hyper-activity and thus BIR. Similar alterations characterize also the normal aging process in mice, positing BVR-A impairment as a possible bridge in the transition from normal aging to AD.

1. Introduction

During the last years a growing number of observations highlighted a close interconnection between Alzheimer disease (AD) and common diseases of modern adulthood, including obesity and type 2 diabetes mellitus (T2DM) [1,2]. Furthermore, epidemiological studies showed that hallmarks of peripheral metabolic disorders, such as glucose intolerance and/or impairment of insulin secretion, are associated with a higher risk to develop dementia or AD [2–5], whereas patients with AD more frequently present with an impaired glucose metabolism or T2DM [6,7].

This clinical evidence raised doubts about the correct functioning of insulin signaling especially in light of the neurotrophic actions mediated by insulin [8]. Indeed, the activation of insulin signaling cascade does not induce a significant glucose uptake in the brain as it does in peripheral tissues [9,10], but, rather, it modulates other important functions through the activation of the two main pathways downstream to the insulin receptor (IR): (i) the phosphoinositide-3 kinase (PI3K) pathway, which is involved in the maintenance of synaptic plasticity and memory consolidation [11,12]; and (ii) the mitogen-activated protein kinase (MAPK) cascade, which is responsible both for the induction of several genes required for neuronal and synapse growth,

* Corresponding authors.
E-mail addresses: dabcns@uky.edu (D.A. Butterfield), marzia.perluigi@uniroma1.it (M. Perluigi).

http://dx.doi.org/10.1016/j.freeradbiomed.2015.12.012
0891-5849/

Appendix F

Original Paper

Neurodegener Dis 2016;16:62–68
DOI: 10.1159/000441419

Received: June 1, 2015
Accepted after revision: October 1, 2015
Published online: November 26, 2015

Increased Mammalian Target of Rapamycin Signaling Contributes to the Accumulation of Protein Oxidative Damage in a Mouse Model of Down's Syndrome

Antonella Tramutola[a] Chiara Lanzillotta[a] Andrea Arena[a] Eugenio Barone[a, b]
Marzia Perluigi[a] Fabio Di Domenico[a]

[a]Department of Biochemical Sciences, Sapienza University of Rome, Rome, Italy; [b]Instituto de Ciencias Biomédicas, Facultad de Salud, Universidad Autónoma de Chile, Santiago, Chile

Key Words
Mammalian target of rapamycin · Autophagy · Protein oxidation · Down's syndrome · Alzheimer's disease

Abstract
Background: Neurodegenerative diseases are characterized by increased levels of oxidative stress and an altered mammalian target of rapamycin (mTOR)/autophagy axis; however, the mutual relationship between these two events is controversial. Previous studies in Down's syndrome (DS) and Alzheimer's disease (AD) suggested that the accumulation of protein oxidative damage results from the increased free radical production, mainly related to metabolic alterations, mitochondrial degeneration and amyloid-β deposition, and aberrant activity of protein degradative systems. ***Summary:*** This study analyzed mTOR signaling in Ts65Dn mice, a model of DS, at 6 and 12 months of age compared with euploid mice showing the early aberrant hyperphosphorylation of mTOR coupled with the reduction of autophagosome formation. Moreover, the evaluation of protein oxidation shows an increase in protein nitration and protein-bound 4-hydroxynonenal in 12-month-old Ts65Dn mice suggesting the potential involvement of altered autophagy in the buildup of protein oxidative damage. In addition, data obtained on cell culture support the protective role of autophagy in reducing protein oxidation. ***Key Messages:*** Overall, this study provides further evidence for the role of mTOR hyperactivation and reduced autophagy in the accumulation of protein oxidative damage during DS and AD pathologies.

Introduction

The mammalian target of rapamycin (mTOR) is expressed at high levels in the brain, mainly in neurons but also in glial cells. mTOR is at the crossroads of many cellular pathways that regulate neuronal development and synaptic plasticity, as well as cellular aging and neurodegeneration. During embryonic development, mTOR signaling serves as a potent neuronal survival and division signal responding to growth factors and guidance cues, including insulin-like growth factor-1 and insulin. In the adult brain, the same system evolves to control synaptic plasticity, neuronal polarity, neurotransmission, metabolic control and processes underlying memory and learning [1–5]. In the aged brain, mTOR is deeply involved in the regulation of the proteostasis network, through the on/off switch of translation and autophagy, in order to avoid the accumulation of toxic protein aggregates that might result in brain degeneration [6]. Autophagy acts as a starvation

KARGER

© 2015 S. Karger AG, Basel
1660–2854/15/0162–0062$39.50/0

E-Mail karger@karger.com
www.karger.com/ndd

Dr. Fabio Di Domenico
Department of Biochemical Sciences A. Rossi Fanelli
Sapienza University of Rome, P.le Aldo Moro, 5, IT–00185 Rome (Italy)
E-Mail fabio.didomenico@uniroma1.it

Appendix G

HHS Public Access
Author manuscript
J Alzheimers Dis. Author manuscript; available in PMC 2015 December 14.

Published in final edited form as:
J Alzheimers Dis. 2015 ; 44(4): 1107–1120. doi:10.3233/JAD-141254.

Bach1 overexpression in Down syndrome correlates with the alteration of the HO-1/BVR-A system: insights for transition to Alzheimer Disease

Fabio Di Domenico[1], **Gilda Pupo**[1], **Cesare Mancuso**[2], **Eugenio Barone**[1], **Francesca Paolini**[3], **Andrea Arena**[1], **Carla Blarzino**[1], **Frederick A. Schmitt**[4,5], **Elizabeth Head**[4,6], **D. Allan Butterfield**[4,7], and **Marzia Perluigi**[1,*]

[1]Department of Biochemical Sciences, Sapienza University of Rome, Italy

[2]Institute of Pharmacology, Catholic University School of Medicine, Rome, Italy

[3]Laboratory of Virology, Regina Elena National Cancer Institute, Rome, Italy

[4]Sanders-Brown Centre of Aging, University of Kentucky, Lexington KY, USA

[5]Department of Neurology, University of Kentucky, Lexington KY, USA

[6]Department of Pharmacology & Nutritional Sciences, University of Kentucky, Lexington KY, USA

[7]Department of Chemistry, University of Kentucky, Lexington KY, USA

Abstract

Bach1, among the genes encoded on chromosome 21, is a transcription repressor, which binds to antioxidant response elements (AREs) of DNA thus inhibiting the transcription of specific genes involved in the cell stress response including heme oxygenase-1 (HO-1). HO-1 and its partner, biliverdin reductase-A (BVR-A), are up-regulated in response to oxidative stress (OS) in order to protect cells against further damage. Since OS is an early event in Down syndrome (DS) and might contribute to the development of multiple deleterious DS phenotypes, including AD pathology, we investigated the status of the Bach1/HO-1/BVR-A axis in DS and its possible implications for AD development. In the present study, we showed increased total Bach1 protein levels in the brain of all DS cases coupled with reduced induction of brain HO-1. Furthermore, increased OS could on one hand overcome the inhibitory effects of Bach1 and on the other hand, promote BVR-A impairment. Our data show that the development of AD in DS subjects is characterized by (i) increased Bach1 total and poly-ubiquitination; (ii) increased HO-1 protein levels; and (iii) increased nitration of BVR-A followed by reduced activity. To corroborate our findings we analyzed Bach1, HO-1 and BVR-A status in the Ts65Dn mouse model at 3 (young) and 15 (old) months of age. The above data support the hypothesis that the dysregulation of HO-1/BVR-A system contributes to the early increase of OS in DS and provide potential mechanistic paths involved in the neurodegenerative process and AD development.

*Corresponding author: Marzia Perluigi, Department of Biochemical Sciences "A. Rossi Fanelli", Sapienza University of Rome, P.le Aldo Moro, 5 00185 Rome (IT), Phone: +39 0649910885, Fax: +39 064440062, marzia.perluigi@uniroma1.it.

All authors state that they have no conflicts of interest.

8 REFERENCES

1. Duncan, A.M., et al., *Refined sublocalization of the human gene encoding the beta subunit of the S100 protein (S100B) and confirmation of a subtle t(9;21) translocation using in situ hybridization.* Cytogenet Cell Genet, 1989. **50**(4): p. 234-5.
2. Hartway, S., *A parent's guide to the genetics of Down syndrome.* Adv Neonatal Care, 2009. **9**(1): p. 27-30.
3. Kava, M.P., et al., *Down syndrome: clinical profile from India.* Arch Med Res, 2004. **35**(1): p. 31-5.
4. Society, N.D.S., *What is mosaicism?* www.ndss.org. , 2006.
5. Antonarakis, S.E., et al., *Chromosome 21 and down syndrome: from genomics to pathophysiology.* Nat Rev Genet, 2004. **5**(10): p. 725-38.
6. Perluigi, M., F. Di Domenico, and D.A. Buttterfield, *Unraveling the complexity of neurodegeneration in brains of subjects with Down syndrome: insights from proteomics.* Proteomics Clin Appl, 2014. **8**(1-2): p. 73-85.
7. Antonarakis, S.E., et al., *Differential gene expression studies to explore the molecular pathophysiology of Down syndrome.* Brain Res Brain Res Rev, 2001. **36**(2-3): p. 265-74.
8. Iannello, R.C., et al., *Oxidative stress and neural dysfunction in Down syndrome.* J Neural Transm Suppl, 1999. **57**: p. 257-67.
9. Bettcher, B.M. and J.H. Kramer, *Longitudinal inflammation, cognitive decline, and Alzheimer's disease: a mini-review.* Clin Pharmacol Ther, 2014. **96**(4): p. 464-9.
10. Victor, M. and A.H. Ropper, *Adams and Victor's principles of neurology*. 2001, New York:McGraw-Hill. 1692.
11. Gyure, K.A., et al., *Intraneuronal abeta-amyloid precedes development of amyloid plaques in Down syndrome.* Arch Pathol Lab Med, 2001. **125**(4): p. 489-92.
12. Teller, J.K., et al., *Presence of soluble amyloid beta-peptide precedes amyloid plaque formation in Down's syndrome.* Nat Med, 1996. **2**(1): p. 93-5.
13. Wilcock, D.M., *Neuroinflammation in the aging down syndrome brain; lessons from Alzheimer's disease.* Curr Gerontol Geriatr Res, 2012. **2012**: p. 170276.
14. Butterfield, D.A., et al., *Redox proteomics analysis to decipher the neurobiology of Alzheimer-like neurodegeneration: overlaps in Down's syndrome and Alzheimer's disease brain.* Biochem J, 2014. **463**(2): p. 177-89.
15. Moreira, P.I., et al., *Brain mitochondrial dysfunction as a link between Alzheimer's disease and diabetes.* J Neurol Sci, 2007. **257**(1-2): p. 206-14.
16. de la Monte, S.M., *Insulin resistance and Alzheimer's disease.* BMB Rep, 2009. **42**(8): p. 475-81.
17. Neumann, K.F., et al., *Insulin resistance and Alzheimer's disease: molecular links & clinical implications.* Curr Alzheimer Res, 2008. **5**(5): p. 438-47.
18. Griffiths-Jones, S., *The microRNA Registry.* Nucleic Acids Res, 2004. **32**(Database issue): p. D109-11.
19. Dominguez, R.O., et al., *Type 2 diabetes and/or its treatment leads to less cognitive impairment in Alzheimer's disease patients.* Diabetes Res Clin Pract, 2012. **98**(1): p. 68-74.
20. Uttara, B., et al., *Oxidative stress and neurodegenerative diseases: a review of upstream and downstream antioxidant therapeutic options.* Curr Neuropharmacol, 2009. **7**(1): p. 65-74.

21. Halliwell, B., *Reactive oxygen species in living systems: source, biochemistry, and role in human disease.* Am J Med, 1991. **91**(3C): p. 14S-22S.
22. Hansford, R.G., B.A. Hogue, and V. Mildaziene, *Dependence of H2O2 formation by rat heart mitochondria on substrate availability and donor age.* J Bioenerg Biomembr, 1997. **29**(1): p. 89-95.
23. Finkel, T. and N.J. Holbrook, *Oxidants, oxidative stress and the biology of ageing.* Nature, 2000. **408**(6809): p. 239-47.
24. Ray, P.D., B.W. Huang, and Y. Tsuji, *Reactive oxygen species (ROS) homeostasis and redox regulation in cellular signaling.* Cell Signal, 2012. **24**(5): p. 981-90.
25. Droge, W., *Free radicals in the physiological control of cell function.* Physiol Rev, 2002. **82**(1): p. 47-95.
26. Watson, J.D., *Type 2 diabetes as a redox disease.* Lancet, 2014. **383**(9919): p. 841-3.
27. Son, Y.O., et al., *Antioncogenic and Oncogenic Properties of Nrf2 in Arsenic-induced Carcinogenesis.* J Biol Chem, 2015. **290**(45): p. 27090-100.
28. Son, Y.O., et al., *Nrf2/p62 signaling in apoptosis resistance and its role in cadmium-induced carcinogenesis.* J Biol Chem, 2014. **289**(41): p. 28660-75.
29. Son, Y.O., et al., *Cadmium induces carcinogenesis in BEAS-2B cells through ROS-dependent activation of PI3K/AKT/GSK-3beta/beta-catenin signaling.* Toxicol Appl Pharmacol, 2012. **264**(2): p. 153-60.
30. Zhang, Z., et al., *Role of reactive oxygen species in arsenic-induced transformation of human lung bronchial epithelial (BEAS-2B) cells.* Biochem Biophys Res Commun, 2015. **456**(2): p. 643-8.
31. Sies, H., *Strategies of antioxidant defense.* Eur J Biochem, 1993. **215**(2): p. 213-9.
32. Berlett, B.S. and E.R. Stadtman, *Protein oxidation in aging, disease, and oxidative stress.* J Biol Chem, 1997. **272**(33): p. 20313-6.
33. Butterfield, D.A. and C.M. Lauderback, *Lipid peroxidation and protein oxidation in Alzheimer's disease brain: potential causes and consequences involving amyloid beta-peptide-associated free radical oxidative stress.* Free Radic Biol Med, 2002. **32**(11): p. 1050-60.
34. Butterfield, D.A., et al., *Redox proteomics in selected neurodegenerative disorders: from its infancy to future applications.* Antioxid Redox Signal, 2012. **17**(11): p. 1610-55.
35. Stadtman, E.R. and R.L. Levine, *Free radical-mediated oxidation of free amino acids and amino acid residues in proteins.* Amino Acids, 2003. **25**(3-4): p. 207-18.
36. Grune, T. and K.J. Davies, *The proteasomal system and HNE-modified proteins.* Mol Aspects Med, 2003. **24**(4-5): p. 195-204.
37. Yang, X., et al., *Effect of acrolein and glutathione depleting agents on thioredoxin.* Toxicology, 2004. **204**(2-3): p. 209-18.
38. Igarashi, K. and K. Kashiwagi, *Protein-conjugated acrolein as a biochemical marker of brain infarction.* Mol Nutr Food Res, 2011. **55**(9): p. 1332-41.
39. Lee, W.C., et al., *Lipid peroxidation dysregulation in ischemic stroke: plasma 4-HNE as a potential biomarker?* Biochem Biophys Res Commun, 2012. **425**(4): p. 842-7.
40. Malkus, K.A., E. Tsika, and H. Ischiropoulos, *Oxidative modifications, mitochondrial dysfunction, and impaired protein degradation in Parkinson's disease: how neurons are lost in the Bermuda triangle.* Mol Neurodegener, 2009. **4**: p. 24.
41. Grune, T., et al., *Protein oxidation and degradation during postmitotic senescence.* Free Radic Biol Med, 2005. **39**(9): p. 1208-15.
42. Metcalf, D.J., et al., *Autophagy and misfolded proteins in neurodegeneration.* Exp Neurol, 2012. **238**(1): p. 22-8.
43. Chondrogianni, N., et al., *Protein damage, repair and proteolysis.* Mol Aspects Med, 2014. **35**: p. 1-71.

44. Varshavsky, A., *The ubiquitin system.* Trends Biochem Sci, 1997. **22**(10): p. 383-7.
45. Breusing, N. and T. Grune, *Regulation of proteasome-mediated protein degradation during oxidative stress and aging.* Biol Chem, 2008. **389**(3): p. 203-9.
46. Keller, J.N., et al., *Autophagy, proteasomes, lipofuscin, and oxidative stress in the aging brain.* Int J Biochem Cell Biol, 2004. **36**(12): p. 2376-91.
47. Nixon, R.A., *The role of autophagy in neurodegenerative disease.* Nat Med, 2013. **19**(8): p. 983-97.
48. Yang, Z. and D.J. Klionsky, *Mammalian autophagy: core molecular machinery and signaling regulation.* Curr Opin Cell Biol, 2010. **22**(2): p. 124-31.
49. Grune, T., et al., *Proteolysis in cultured liver epithelial cells during oxidative stress. Role of the multicatalytic proteinase complex, proteasome.* J Biol Chem, 1995. **270**(5): p. 2344-51.
50. Di Domenico, F., et al., *Impairment of proteostasis network in Down syndrome prior to the development of Alzheimer's disease neuropathology: redox proteomics analysis of human brain.* Biochim Biophys Acta, 2013. **1832**(8): p. 1249-59.
51. Pena, L.A., C.W. Brecher, and D.R. Marshak, *beta-Amyloid regulates gene expression of glial trophic substance S100 beta in C6 glioma and primary astrocyte cultures.* Brain Res Mol Brain Res, 1995. **34**(1): p. 118-26.
52. Sanij, E., et al., *Ets-2 is induced by oxidative stress and sensitizes cells to H(2)O(2)-induced apoptosis: implications for Down's syndrome.* Biochem Biophys Res Commun, 2001. **287**(4): p. 1003-8.
53. Wolvetang, E.J., et al., *ETS2 overexpression in transgenic models and in Down syndrome predisposes to apoptosis via the p53 pathway.* Hum Mol Genet, 2003. **12**(3): p. 247-55.
54. Orr, M.E. and S. Oddo, *Autophagic/lysosomal dysfunction in Alzheimer's disease.* Alzheimers Res Ther, 2013. **5**(5): p. 53.
55. C, O.N., *PI3-kinase/Akt/mTOR signaling: impaired on/off switches in aging, cognitive decline and Alzheimer's disease.* Exp Gerontol, 2013. **48**(7): p. 647-53.
56. Richardson, A., et al., *How longevity research can lead to therapies for Alzheimer's disease: The rapamycin story.* Exp Gerontol, 2015. **68**: p. 51-8.
57. Di Domenico, F., et al., *Oxidative Stress and Proteostasis Network: Culprit and Casualty of Alzheimer's-Like Neurodegeneration.* Advances in Geriatrics, 2014. **2014**: p. 14.
58. Wojcik, S., *Crosstalk between autophagy and proteasome protein degradation systems: possible implications for cancer therapy.* Folia Histochem Cytobiol, 2013. **51**(4): p. 249-64.
59. An, W.L., et al., *Up-regulation of phosphorylated/activated p70 S6 kinase and its relationship to neurofibrillary pathology in Alzheimer's disease.* Am J Pathol, 2003. **163**(2): p. 591-607.
60. Griffin, R.J., et al., *Activation of Akt/PKB, increased phosphorylation of Akt substrates and loss and altered distribution of Akt and PTEN are features of Alzheimer's disease pathology.* J Neurochem, 2005. **93**(1): p. 105-17.
61. Pei, J.J. and J. Hugon, *mTOR-dependent signalling in Alzheimer's disease.* J Cell Mol Med, 2008. **12**(6B): p. 2525-32.
62. Tramutola, A., et al., *Alteration of mTOR signaling occurs early in the progression of Alzheimer disease (AD): analysis of brain from subjects with pre-clinical AD, amnestic mild cognitive impairment and late-stage AD.* J Neurochem, 2015. **133**(5): p. 739-49.
63. Lin, M.T. and M.F. Beal, *Mitochondrial dysfunction and oxidative stress in neurodegenerative diseases.* Nature, 2006. **443**(7113): p. 787-95.
64. Coskun, P.E., et al., *Systemic mitochondrial dysfunction and the etiology of Alzheimer's disease and down syndrome dementia.* J Alzheimers Dis, 2010. **20 Suppl 2**: p. S293-310.

65. Valenti, D., et al., *Deficit of complex I activity in human skin fibroblasts with chromosome 21 trisomy and overproduction of reactive oxygen species by mitochondria: involvement of the cAMP/PKA signalling pathway.* Biochem J, 2011. **435**(3): p. 679-88.
66. Helguera, P., et al., *Adaptive downregulation of mitochondrial function in down syndrome.* Cell Metab, 2013. **17**(1): p. 132-40.
67. Tabner, B.J., et al., *Hydrogen peroxide is generated during the very early stages of aggregation of the amyloid peptides implicated in Alzheimer disease and familial British dementia.* J Biol Chem, 2005. **280**(43): p. 35789-92.
68. Shin, J.H., et al., *Aberrant neuronal and mitochondrial proteins in hippocampus of transgenic mice overexpressing human Cu/Zn superoxide dismutase 1.* Free Radic Biol Med, 2004. **37**(5): p. 643-53.
69. Benzi, G. and A. Moretti, *Are reactive oxygen species involved in Alzheimer's disease?* Neurobiol Aging, 1995. **16**(4): p. 661-74.
70. Gulesserian, T., et al., *Antioxidant proteins in fetal brain: superoxide dismutase-1 (SOD-1) protein is not overexpressed in fetal Down syndrome.* J Neural Transm Suppl, 2001(61): p. 71-84.
71. Butterfield, D.A. and D. Boyd-Kimball, *Amyloid beta-peptide(1-42) contributes to the oxidative stress and neurodegeneration found in Alzheimer disease brain.* Brain Pathol, 2004. **14**(4): p. 426-32.
72. Butterfield, D.A., et al., *Evidence of oxidative damage in Alzheimer's disease brain: central role for amyloid beta-peptide.* Trends Mol Med, 2001. **7**(12): p. 548-54.
73. Butterfield, D.A., et al., *In vivo oxidative stress in brain of Alzheimer disease transgenic mice: Requirement for methionine 35 in amyloid beta-peptide of APP.* Free Radic Biol Med, 2010. **48**(1): p. 136-44.
74. Markesbery, W.R., *Oxidative stress hypothesis in Alzheimer's disease.* Free Radic Biol Med, 1997. **23**(1): p. 134-47.
75. Butterfield, D.A. and D. Boyd-Kimball, *The critical role of methionine 35 in Alzheimer's amyloid beta-peptide (1-42)-induced oxidative stress and neurotoxicity.* Biochim Biophys Acta, 2005. **1703**(2): p. 149-56.
76. Butterfield, D.A., et al., *Evidence that amyloid beta-peptide-induced lipid peroxidation and its sequelae in Alzheimer's disease brain contribute to neuronal death.* Neurobiol Aging, 2002. **23**(5): p. 655-64.
77. Shichiri, M., *The role of lipid peroxidation in neurological disorders.* J Clin Biochem Nutr, 2014. **54**(3): p. 151-60.
78. Cheon, M.S., et al., *Protein expression of BACE1, BACE2 and APP in Down syndrome brains.* Amino Acids, 2008. **35**(2): p. 339-43.
79. Choi, J.H., et al., *Age-dependent dysregulation of brain amyloid precursor protein in the Ts65Dn Down syndrome mouse model.* J Neurochem, 2009. **110**(6): p. 1818-27.
80. Seo, H. and O. Isacson, *Abnormal APP, cholinergic and cognitive function in Ts65Dn Down's model mice.* Exp Neurol, 2005. **193**(2): p. 469-80.
81. Prasher, V.P., et al., *Molecular mapping of Alzheimer-type dementia in Down's syndrome.* Ann Neurol, 1998. **43**(3): p. 380-3.
82. Zhou, S., et al., *CD147 is a regulatory subunit of the gamma-secretase complex in Alzheimer's disease amyloid beta-peptide production.* Proc Natl Acad Sci U S A, 2005. **102**(21): p. 7499-504.
83. Acquati, F., et al., *The gene encoding DRAP (BACE2), a glycosylated transmembrane protein of the aspartic protease family, maps to the down critical region.* FEBS Lett, 2000. **468**(1): p. 59-64.
84. Rothermundt, M., et al., *S100B in brain damage and neurodegeneration.* Microsc Res Tech, 2003. **60**(6): p. 614-32.

85. Griffin, W.S., et al., *Life-long overexpression of S100beta in Down's syndrome: implications for Alzheimer pathogenesis.* Neurobiol Aging, 1998. **19**(5): p. 401-5.
86. Hu, J., et al., *S100 beta stimulates inducible nitric oxide synthase activity and mRNA levels in rat cortical astrocytes.* J Biol Chem, 1996. **271**(5): p. 2543-7.
87. Barger, S.W. and L.J. Van Eldik, *S100 beta stimulates calcium fluxes in glial and neuronal cells.* J Biol Chem, 1992. **267**(14): p. 9689-94.
88. Griffin, W.S., et al., *Brain interleukin 1 and S-100 immunoreactivity are elevated in Down syndrome and Alzheimer disease.* Proc Natl Acad Sci U S A, 1989. **86**(19): p. 7611-5.
89. Zenke-Kawasaki, Y., et al., *Heme induces ubiquitination and degradation of the transcription factor Bach1.* Mol Cell Biol, 2007. **27**(19): p. 6962-71.
90. Ogawa, K., et al., *Heme mediates derepression of Maf recognition element through direct binding to transcription repressor Bach1.* EMBO J, 2001. **20**(11): p. 2835-43.
91. Hira, S., et al., *Bach1, a heme-dependent transcription factor, reveals presence of multiple heme binding sites with distinct coordination structure.* IUBMB Life, 2007. **59**(8-9): p. 542-51.
92. Sakoda, E., et al., *Regulation of heme oxygenase-1 by transcription factor Bach1 in the mouse brain.* Neurosci Lett, 2008. **440**(2): p. 160-5.
93. Ishikawa, M., S. Numazawa, and T. Yoshida, *Redox regulation of the transcriptional repressor Bach1.* Free Radic Biol Med, 2005. **38**(10): p. 1344-52.
94. Sun, J., et al., *Hemoprotein Bach1 regulates enhancer availability of heme oxygenase-1 gene.* EMBO J, 2002. **21**(19): p. 5216-24.
95. Maines, M.D., *The heme oxygenase system: a regulator of second messenger gases.* Annu Rev Pharmacol Toxicol, 1997. **37**: p. 517-54.
96. Mancuso, C. and E. Barone, *The heme oxygenase/biliverdin reductase pathway in drug research and development.* Curr Drug Metab, 2009. **10**(6): p. 579-94.
97. Kapitulnik, J. and M.D. Maines, *Pleiotropic functions of biliverdin reductase: cellular signaling and generation of cytoprotective and cytotoxic bilirubin.* Trends Pharmacol Sci, 2009. **30**(3): p. 129-37.
98. Gibbs, P.E., et al., *Formation of ternary complex of human biliverdin reductase-protein kinase Cdelta-ERK2 protein is essential for ERK2-mediated activation of Elk1 protein, nuclear factor-kappaB, and inducible nitric-oxidase synthase (iNOS).* J Biol Chem, 2012. **287**(2): p. 1066-79.
99. Barone, E., et al., *The Janus face of the heme oxygenase/biliverdin reductase system in Alzheimer disease: it's time for reconciliation.* Neurobiol Dis, 2014. **62**: p. 144-59.
100. Poon, H.F., et al., *Free radicals: key to brain aging and heme oxygenase as a cellular response to oxidative stress.* J Gerontol A Biol Sci Med Sci, 2004. **59**(5): p. 478-93.
101. Ota, K., et al., *Identification of senescence-associated genes and their networks under oxidative stress by the analysis of Bach1.* Antioxid Redox Signal, 2011. **14**(12): p. 2441-51.
102. Palozza, P., et al., *beta-Carotene and cigarette smoke condensate regulate heme oxygenase-1 and its repressor factor Bach1: relationship with cell growth.* Antioxid Redox Signal, 2006. **8**(5-6): p. 1069-80.
103. Perry, V.H. and S. Gordon, *Macrophages and microglia in the nervous system.* Trends Neurosci, 1988. **11**(6): p. 273-7.
104. Ling, E.A., *Some aspects of amoeboid microglia in the corpus callosum and neighbouring regions of neonatal rats.* J Anat, 1976. **121**(Pt 1): p. 29-45.
105. Colton, C. and D.M. Wilcock, *Assessing activation states in microglia.* CNS Neurol Disord Drug Targets, 2010. **9**(2): p. 174-91.
106. Gordon, S., *Alternative activation of macrophages.* Nat Rev Immunol, 2003. **3**(1): p. 23-35.

107. Xiang, Z., et al., *Microglia activation in the brain as inflammatory biomarker of Alzheimer's disease neuropathology and clinical dementia.* Dis Markers, 2006. **22**(1-2): p. 95-102.
108. Sasaki, A., et al., *Amyloid cored plaques in Tg2576 transgenic mice are characterized by giant plaques, slightly activated microglia, and the lack of paired helical filament-typed, dystrophic neurites.* Virchows Arch, 2002. **441**(4): p. 358-67.
109. Wegiel, J., et al., *Origin and turnover of microglial cells in fibrillar plaques of APPsw transgenic mice.* Acta Neuropathol, 2003. **105**(4): p. 393-402.
110. Wegiel, J., et al., *The role of microglial cells and astrocytes in fibrillar plaque evolution in transgenic APP(SW) mice.* Neurobiol Aging, 2001. **22**(1): p. 49-61.
111. Stalder, M., et al., *3D-Reconstruction of microglia and amyloid in APP23 transgenic mice: no evidence of intracellular amyloid.* Neurobiol Aging, 2001. **22**(3): p. 427-34.
112. Bornemann, K.D., et al., *Abeta-induced inflammatory processes in microglia cells of APP23 transgenic mice.* Am J Pathol, 2001. **158**(1): p. 63-73.
113. Koenigsknecht, J. and G. Landreth, *Microglial phagocytosis of fibrillar beta-amyloid through a beta1 integrin-dependent mechanism.* J Neurosci, 2004. **24**(44): p. 9838-46.
114. Combs, C.K., et al., *beta-Amyloid stimulation of microglia and monocytes results in TNFalpha-dependent expression of inducible nitric oxide synthase and neuronal apoptosis.* J Neurosci, 2001. **21**(4): p. 1179-88.
115. Combs, C.K., et al., *Identification of microglial signal transduction pathways mediating a neurotoxic response to amyloidogenic fragments of beta-amyloid and prion proteins.* J Neurosci, 1999. **19**(3): p. 928-39.
116. Akiyama, H., et al., *Inflammation and Alzheimer's disease.* Neurobiol Aging, 2000. **21**(3): p. 383-421.
117. Heneka, M.T. and M.K. O'Banion, *Inflammatory processes in Alzheimer's disease.* J Neuroimmunol, 2007. **184**(1-2): p. 69-91.
118. Rojo, L.E., et al., *Neuroinflammation: implications for the pathogenesis and molecular diagnosis of Alzheimer's disease.* Arch Med Res, 2008. **39**(1): p. 1-16.
119. Hoozemans, J.J., et al., *Neuroinflammation and regeneration in the early stages of Alzheimer's disease pathology.* Int J Dev Neurosci, 2006. **24**(2-3): p. 157-65.
120. Wyss-Coray, T., *Inflammation in Alzheimer disease: driving force, bystander or beneficial response?* Nat Med, 2006. **12**(9): p. 1005-15.
121. Versijpt, J.J., et al., *Assessment of neuroinflammation and microglial activation in Alzheimer's disease with radiolabelled PK11195 and single photon emission computed tomography. A pilot study.* Eur Neurol, 2003. **50**(1): p. 39-47.
122. Edison, P., et al., *Microglia, amyloid, and cognition in Alzheimer's disease: An [11C](R)PK11195-PET and [11C]PIB-PET study.* Neurobiol Dis, 2008. **32**(3): p. 412-9.
123. Wiley, C.A., et al., *Carbon 11-labeled Pittsburgh Compound B and carbon 11-labeled (R)-PK11195 positron emission tomographic imaging in Alzheimer disease.* Arch Neurol, 2009. **66**(1): p. 60-7.
124. Smits, H.A., et al., *Amyloid-beta-induced chemokine production in primary human macrophages and astrocytes.* J Neuroimmunol, 2002. **127**(1-2): p. 160-8.
125. El Khoury, J.B., et al., *CD36 mediates the innate host response to beta-amyloid.* J Exp Med, 2003. **197**(12): p. 1657-66.
126. Ransohoff, R.M., *The MHP36 line of murine neural stem cells expresses functional CXCR1 chemokine receptors that initiate chemotaxis in vitro.* J Neuroimmunol, 2007. **186**(1-2): p. 199; author reply 200.
127. Lyons, A., et al., *CD200 ligand receptor interaction modulates microglial activation in vivo and in vitro: a role for IL-4.* J Neurosci, 2007. **27**(31): p. 8309-13.

128. Walker, D.G., et al., *Decreased expression of CD200 and CD200 receptor in Alzheimer's disease: a potential mechanism leading to chronic inflammation.* Exp Neurol, 2009. **215**(1): p. 5-19.
129. Mott, R.T., et al., *Neuronal expression of CD22: novel mechanism for inhibiting microglial proinflammatory cytokine production.* Glia, 2004. **46**(4): p. 369-79.
130. Tan, J., et al., *Microglial activation resulting from CD40-CD40L interaction after beta-amyloid stimulation.* Science, 1999. **286**(5448): p. 2352-5.
131. Calingasan, N.Y., H.A. Erdely, and C.A. Altar, *Identification of CD40 ligand in Alzheimer's disease and in animal models of Alzheimer's disease and brain injury.* Neurobiol Aging, 2002. **23**(1): p. 31-9.
132. Togo, T., et al., *Expression of CD40 in the brain of Alzheimer's disease and other neurological diseases.* Brain Res, 2000. **885**(1): p. 117-21.
133. Tan, J., et al., *Role of CD40 ligand in amyloidosis in transgenic Alzheimer's mice.* Nat Neurosci, 2002. **5**(12): p. 1288-93.
134. Yuen, S., et al., *The coxsackie-adenovirus receptor induces an inflammatory cardiomyopathy independent of viral infection.* J Mol Cell Cardiol, 2011. **50**(5): p. 826-40.
135. Li, Y., et al., *Interleukin-1 mediates pathological effects of microglia on tau phosphorylation and on synaptophysin synthesis in cortical neurons through a p38-MAPK pathway.* J Neurosci, 2003. **23**(5): p. 1605-11.
136. Sheng, J.G., et al., *Interleukin-1 promotes expression and phosphorylation of neurofilament and tau proteins in vivo.* Exp Neurol, 2000. **163**(2): p. 388-91.
137. Kim, S.H., et al., *Mammalian type I interferon receptors consists of two subunits: IFNaR1 and IFNaR2.* Gene, 1997. **196**(1-2): p. 279-86.
138. Boselli, D., et al., *Expression of IFNgammaR2 mutated in a dileucine internalization motif reinstates IFNgamma signaling and apoptosis in human T lymphocytes.* Immunol Lett, 2010. **134**(1): p. 17-25.
139. Park, J.I., et al., *Interleukin-1beta can mediate growth arrest and differentiation via the leukemia inhibitory factor/JAK/STAT pathway in medullary thyroid carcinoma cells.* Cytokine, 2005. **29**(3): p. 125-34.
140. Rountree, R.B., et al., *RIP4 regulates epidermal differentiation and cutaneous inflammation.* J Invest Dermatol, 2010. **130**(1): p. 102-12.
141. Sen, U., et al., *Cystathionine beta-synthase and cystathionine gamma-lyase double gene transfer ameliorate homocysteine-mediated mesangial inflammation through hydrogen sulfide generation.* Am J Physiol Cell Physiol, 2011. **300**(1): p. C155-63.
142. Baranano, D.E., C.D. Ferris, and S.H. Snyder, *Atypical neural messengers.* Trends Neurosci, 2001. **24**(2): p. 99-106.
143. Taoka, S. and R. Banerjee, *Characterization of NO binding to human cystathionine beta-synthase: possible implications of the effects of CO and NO binding to the human enzyme.* J Inorg Biochem, 2001. **87**(4): p. 245-51.
144. Li, L., M. Bhatia, and P.K. Moore, *Hydrogen sulphide--a novel mediator of inflammation?* Curr Opin Pharmacol, 2006. **6**(2): p. 125-9.
145. Whiteman, M., et al., *Emerging role of hydrogen sulfide in health and disease: critical appraisal of biomarkers and pharmacological tools.* Clin Sci (Lond), 2011. **121**(11): p. 459-88.
146. Mowen, K.A., et al., *Arginine methylation of STAT1 modulates IFNalpha/beta-induced transcription.* Cell, 2001. **104**(5): p. 731-41.
147. Ganesh, L., et al., *Protein methyltransferase 2 inhibits NF-kappaB function and promotes apoptosis.* Mol Cell Biol, 2006. **26**(10): p. 3864-74.

148. Mosser, D.M. and J.P. Edwards, *Exploring the full spectrum of macrophage activation.* Nat Rev Immunol, 2008. **8**(12): p. 958-69.
149. Mantovani, A., et al., *The chemokine system in diverse forms of macrophage activation and polarization.* Trends Immunol, 2004. **25**(12): p. 677-86.
150. Wilcock, D.M., et al., *Down syndrome individuals with Alzheimer's disease have a distinct neuroinflammatory phenotype compared to sporadic Alzheimer's disease.* Neurobiol Aging, 2015. **36**(9): p. 2468-74.
151. Royston, M.C., et al., *Overexpression of s100beta in Down's syndrome: correlation with patient age and with beta-amyloid deposition.* Neuropathol Appl Neurobiol, 1999. **25**(5): p. 387-93.
152. Mann, D.M., M.C. Royston, and C.R. Ravindra, *Some morphometric observations on the brains of patients with Down's syndrome: their relationship to age and dementia.* J Neurol Sci, 1990. **99**(2-3): p. 153-64.
153. Wisniewski, K.E., et al., *Alzheimer's disease in Down's syndrome: clinicopathologic studies.* Neurology, 1985. **35**(7): p. 957-61.
154. Goldgaber, D., et al., *Interleukin 1 regulates synthesis of amyloid beta-protein precursor mRNA in human endothelial cells.* Proc Natl Acad Sci U S A, 1989. **86**(19): p. 7606-10.
155. Li, Y., et al., *S100 beta increases levels of beta-amyloid precursor protein and its encoding mRNA in rat neuronal cultures.* J Neurochem, 1998. **71**(4): p. 1421-8.
156. Sheng, J.G., et al., *In vivo and in vitro evidence supporting a role for the inflammatory cytokine interleukin-1 as a driving force in Alzheimer pathogenesis.* Neurobiol Aging, 1996. **17**(5): p. 761-6.
157. Sheng, J.G., et al., *Interleukin-1 promotion of MAPK-p38 overexpression in experimental animals and in Alzheimer's disease: potential significance for tau protein phosphorylation.* Neurochem Int, 2001. **39**(5-6): p. 341-8.
158. Barger, S.W. and A.D. Harmon, *Microglial activation by Alzheimer amyloid precursor protein and modulation by apolipoprotein E.* Nature, 1997. **388**(6645): p. 878-81.
159. Liu, L., et al., *S100B-induced microglial and neuronal IL-1 expression is mediated by cell type-specific transcription factors.* J Neurochem, 2005. **92**(3): p. 546-53.
160. Li, Y., et al., *Neuronal-glial interactions mediated by interleukin-1 enhance neuronal acetylcholinesterase activity and mRNA expression.* J Neurosci, 2000. **20**(1): p. 149-55.
161. Levin, E.D., et al., *Working memory performance and cholinergic effects in the ventral tegmental area and substantia nigra.* Brain Res, 1994. **657**(1-2): p. 165-70.
162. Whitehouse, P.J., et al., *Reductions in acetylcholine and nicotine binding in several degenerative diseases.* Arch Neurol, 1988. **45**(7): p. 722-4.
163. Whitehouse, P.J., et al., *Alzheimer's disease and senile dementia: loss of neurons in the basal forebrain.* Science, 1982. **215**(4537): p. 1237-9.
164. Callahan, L.M., W.A. Vaules, and P.D. Coleman, *Progressive reduction of synaptophysin message in single neurons in Alzheimer disease.* J Neuropathol Exp Neurol, 2002. **61**(5): p. 384-95.
165. Coleman, P.D. and P.J. Yao, *Synaptic slaughter in Alzheimer's disease.* Neurobiol Aging, 2003. **24**(8): p. 1023-7.
166. Allan, S.M., et al., *Cortical cell death induced by IL-1 is mediated via actions in the hypothalamus of the rat.* Proc Natl Acad Sci U S A, 2000. **97**(10): p. 5580-5.
167. Sheng, J.G., et al., *Progressive neuronal injury associated with amyloid plaque formation in Alzheimer disease.* J Neuropathol Exp Neurol, 1998. **57**(7): p. 714-7.
168. Collins, T., *Acute and chronic inflammation*. R. S. Cotran, V. Kumar, and T. Collins, Eds ed. Robbins Pathologic Basis of Disease. 1999, Philadelphia, Pa, USA: W.B. Saunders.

169. Anderson, M.T., et al., *Separation of oxidant-initiated and redox-regulated steps in the NF-kappa B signal transduction pathway.* Proc Natl Acad Sci U S A, 1994. **91**(24): p. 11527-31.
170. Flohe, L., et al., *Redox regulation of NF-kappa B activation.* Free Radic Biol Med, 1997. **22**(6): p. 1115-26.
171. Brasier, A.R., *The NF-kappaB regulatory network.* Cardiovasc Toxicol, 2006. **6**(2): p. 111-30.
172. Castellani, P., E. Balza, and A. Rubartelli, *Inflammation, DAMPs, tumor development, and progression: a vicious circle orchestrated by redox signaling.* Antioxid Redox Signal, 2014. **20**(7): p. 1086-97.
173. Wu, Y., et al., *Activation of TLR4 is required for the synergistic induction of dual oxidase 2 and dual oxidase A2 by IFN-gamma and lipopolysaccharide in human pancreatic cancer cell lines.* J Immunol, 2013. **190**(4): p. 1859-72.
174. Li, J., et al., *Reciprocal activation between IL-6/STAT3 and NOX4/Akt signalings promotes proliferation and survival of non-small cell lung cancer cells.* Oncotarget, 2015. **6**(2): p. 1031-48.
175. Zhou, R., et al., *A role for mitochondria in NLRP3 inflammasome activation.* Nature, 2011. **469**(7329): p. 221-5.
176. Shimada, K., et al., *Oxidized mitochondrial DNA activates the NLRP3 inflammasome during apoptosis.* Immunity, 2012. **36**(3): p. 401-14.
177. Zhou, R., et al., *Thioredoxin-interacting protein links oxidative stress to inflammasome activation.* Nat Immunol, 2010. **11**(2): p. 136-40.
178. Schroder, K. and J. Tschopp, *The inflammasomes.* Cell, 2010. **140**(6): p. 821-32.
179. Vaziri, N.D. and B. Rodriguez-Iturbe, *Mechanisms of disease: oxidative stress and inflammation in the pathogenesis of hypertension.* Nat Clin Pract Nephrol, 2006. **2**(10): p. 582-93.
180. Lagos-Quintana, M., et al., *Identification of tissue-specific microRNAs from mouse.* Curr Biol, 2002. **12**(9): p. 735-9.
181. Kim, J., et al., *Identification of many microRNAs that copurify with polyribosomes in mammalian neurons.* Proc Natl Acad Sci U S A, 2004. **101**(1): p. 360-5.
182. Sempere, L.F., et al., *Expression profiling of mammalian microRNAs uncovers a subset of brain-expressed microRNAs with possible roles in murine and human neuronal differentiation.* Genome Biol, 2004. **5**(3): p. R13.
183. Smirnova, L., et al., *Regulation of miRNA expression during neural cell specification.* Eur J Neurosci, 2005. **21**(6): p. 1469-77.
184. Ha, M. and V.N. Kim, *Regulation of microRNA biogenesis.* Nat Rev Mol Cell Biol, 2014. **15**(8): p. 509-24.
185. He, X., Z. Jing, and G. Cheng, *MicroRNAs: new regulators of Toll-like receptor signalling pathways.* Biomed Res Int, 2014. **2014**: p. 945169.
186. van Scheppingen, J., et al., *Expression of microRNAs miR21, miR146a, and miR155 in tuberous sclerosis complex cortical tubers and their regulation in human astrocytes and SEGA-derived cell cultures.* Glia, 2016. **64**(6): p. 1066-82.
187. Taganov, K.D., et al., *NF-kappaB-dependent induction of microRNA miR-146, an inhibitor targeted to signaling proteins of innate immune responses.* Proc Natl Acad Sci U S A, 2006. **103**(33): p. 12481-6.
188. Hou, J., et al., *MicroRNA-146a feedback inhibits RIG-I-dependent Type I IFN production in macrophages by targeting TRAF6, IRAK1, and IRAK2.* J Immunol, 2009. **183**(3): p. 2150-8.

189. Xie, Y.F., et al., *MicroRNA-146 inhibits pro-inflammatory cytokine secretion through IL-1 receptor-associated kinase 1 in human gingival fibroblasts.* J Inflamm (Lond), 2013. **10**(1): p. 20.
190. Li, S., et al., *MicroRNA-146a represses mycobacteria-induced inflammatory response and facilitates bacterial replication via targeting IRAK-1 and TRAF-6.* PLoS One, 2013. **8**(12): p. e81438.
191. Lin, L., et al., *Type I IFN inhibits innate IL-10 production in macrophages through histone deacetylase 11 by downregulating microRNA-145.* J Immunol, 2013. **191**(7): p. 3896-904.
192. Costinean, S., et al., *Src homology 2 domain-containing inositol-5-phosphatase and CCAAT enhancer-binding protein beta are targeted by miR-155 in B cells of Emicro-MiR-155 transgenic mice.* Blood, 2009. **114**(7): p. 1374-82.
193. An, H., et al., *Src homology 2 domain-containing inositol-5-phosphatase 1 (SHIP1) negatively regulates TLR4-mediated LPS response primarily through a phosphatase activity- and PI-3K-independent mechanism.* Blood, 2005. **105**(12): p. 4685-92.
194. O'Connell, R.M., et al., *Inositol phosphatase SHIP1 is a primary target of miR-155.* Proc Natl Acad Sci U S A, 2009. **106**(17): p. 7113-8.
195. Cremer, T.J., et al., *MiR-155 induction by F. novicida but not the virulent F. tularensis results in SHIP down-regulation and enhanced pro-inflammatory cytokine response.* PLoS One, 2009. **4**(12): p. e8508.
196. Kalesnikoff, J., et al., *SHIP negatively regulates IgE + antigen-induced IL-6 production in mast cells by inhibiting NF-kappa B activity.* J Immunol, 2002. **168**(9): p. 4737-46.
197. Boer, A.K., A.L. Drayer, and E. Vellenga, *Effects of overexpression of the SH2-containing inositol phosphatase SHIP on proliferation and apoptosis of erythroid AS-E2 cells.* Leukemia, 2001. **15**(11): p. 1750-7.
198. Robson, J.D., D. Davidson, and A. Veillette, *Inhibition of the Jun N-terminal protein kinase pathway by SHIP-1, a lipid phosphatase that interacts with the adaptor molecule Dok-3.* Mol Cell Biol, 2004. **24**(6): p. 2332-43.
199. De Felice, F.G., *Alzheimer's disease and insulin resistance: translating basic science into clinical applications.* J Clin Invest, 2013. **123**(2): p. 531-9.
200. Ott, A., et al., *Diabetes mellitus and the risk of dementia: The Rotterdam Study.* Neurology, 1999. **53**(9): p. 1937-42.
201. Crane, P.K., R. Walker, and E.B. Larson, *Glucose levels and risk of dementia.* N Engl J Med, 2013. **369**(19): p. 1863-4.
202. Willette, A.A., et al., *Association of Insulin Resistance With Cerebral Glucose Uptake in Late Middle-Aged Adults at Risk for Alzheimer Disease.* JAMA Neurol, 2015. **72**(9): p. 1013-20.
203. Banks, W.A., J.B. Jaspan, and A.J. Kastin, *Selective, physiological transport of insulin across the blood-brain barrier: novel demonstration by species-specific radioimmunoassays.* Peptides, 1997. **18**(8): p. 1257-62.
204. Baskin, D.G., et al., *Insulin in the brain.* Annu Rev Physiol, 1987. **49**: p. 335-47.
205. Ghasemi, R., et al., *Insulin in the brain: sources, localization and functions.* Mol Neurobiol, 2013. **47**(1): p. 145-71.
206. Talbot, K., et al., *Demonstrated brain insulin resistance in Alzheimer's disease patients is associated with IGF-1 resistance, IRS-1 dysregulation, and cognitive decline.* J Clin Invest, 2012. **122**(4): p. 1316-38.
207. Blazquez, E., et al., *Insulin in the brain: its pathophysiological implications for States related with central insulin resistance, type 2 diabetes and Alzheimer's disease.* Front Endocrinol (Lausanne), 2014. **5**: p. 161.

208. Freude, S., K. Schilbach, and M. Schubert, *The role of IGF-1 receptor and insulin receptor signaling for the pathogenesis of Alzheimer's disease: from model organisms to human disease.* Curr Alzheimer Res, 2009. **6**(3): p. 213-23.
209. Plum, L., M. Schubert, and J.C. Bruning, *The role of insulin receptor signaling in the brain.* Trends Endocrinol Metab, 2005. **16**(2): p. 59-65.
210. Mehta, P.D., et al., *Increased amyloid beta protein levels in children and adolescents with Down syndrome.* J Neurol Sci, 2007. **254**(1-2): p. 22-7.
211. Horwood, J.M., et al., *Signalling mechanisms mediated by the phosphoinositide 3-kinase/Akt cascade in synaptic plasticity and memory in the rat.* Eur J Neurosci, 2006. **23**(12): p. 3375-84.
212. Calabrese, V., et al., *Nitric oxide in the central nervous system: neuroprotection versus neurotoxicity.* Nat Rev Neurosci, 2007. **8**(10): p. 766-75.
213. Akter, K., et al., *Diabetes mellitus and Alzheimer's disease: shared pathology and treatment?* Br J Clin Pharmacol, 2011. **71**(3): p. 365-76.
214. Lerner-Marmarosh, N., et al., *Human biliverdin reductase: a member of the insulin receptor substrate family with serine/threonine/tyrosine kinase activity.* Proc Natl Acad Sci U S A, 2005. **102**(20): p. 7109-14.
215. Salim, M., B.A. Brown-Kipphut, and M.D. Maines, *Human biliverdin reductase is autophosphorylated, and phosphorylation is required for bilirubin formation.* J Biol Chem, 2001. **276**(14): p. 10929-34.
216. Halliwell, B., *Oxidative stress in cell culture: an under-appreciated problem?* FEBS Lett, 2003. **540**(1-3): p. 3-6.
217. Psaltis, P.J., et al., *Noninvasive monitoring of oxidative stress in transplanted mesenchymal stromal cells.* JACC Cardiovasc Imaging, 2013. **6**(7): p. 795-802.
218. Mayer, C.M. and D.D. Belsham, *Central insulin signaling is attenuated by long-term insulin exposure via insulin receptor substrate-1 serine phosphorylation, proteasomal degradation, and lysosomal insulin receptor degradation.* Endocrinology, 2010. **151**(1): p. 75-84.
219. Lerner-Marmarosh, N., et al., *Human biliverdin reductase is an ERK activator; hBVR is an ERK nuclear transporter and is required for MAPK signaling.* Proc Natl Acad Sci U S A, 2008. **105**(19): p. 6870-5.
220. Reinholdt, L.G., et al., *Molecular characterization of the translocation breakpoints in the Down syndrome mouse model Ts65Dn.* Mamm Genome, 2011. **22**(11-12): p. 685-91.
221. Bowes, C., et al., *Localization of a retroviral element within the rd gene coding for the beta subunit of cGMP phosphodiesterase.* Proc Natl Acad Sci U S A, 1993. **90**(7): p. 2955-9.
222. Oddo, S., et al., *Triple-transgenic model of Alzheimer's disease with plaques and tangles: intracellular Abeta and synaptic dysfunction.* Neuron, 2003. **39**(3): p. 409-21.
223. Braak, H., et al., *Staging of Alzheimer disease-associated neurofibrillary pathology using paraffin sections and immunocytochemistry.* Acta Neuropathol, 2006. **112**(4): p. 389-404.
224. Cenini, G., et al., *Effects of oxidative and nitrosative stress in brain on p53 proapoptotic protein in amnestic mild cognitive impairment and Alzheimer disease.* Free Radic Biol Med, 2008. **45**(1): p. 81-5.
225. Barone, E., et al., *Oxidative and nitrosative modifications of biliverdin reductase-A in the brain of subjects with Alzheimer's disease and amnestic mild cognitive impairment.* J Alzheimers Dis, 2011. **25**(4): p. 623-33.
226. Barone, E., et al., *Biliverdin reductase--a protein levels and activity in the brains of subjects with Alzheimer disease and mild cognitive impairment.* Biochim Biophys Acta, 2011. **1812**(4): p. 480-7.

227. Di Domenico, F., et al., *Protective effect of ferulic acid ethyl ester against oxidative stress mediated by UVB irradiation in human epidermal melanocytes.* Free Radic Res, 2009. **43**(4): p. 365-75.
228. Prabowo, A.S., et al., *Differential expression and clinical significance of three inflammation-related microRNAs in gangliogliomas.* J Neuroinflammation, 2015. **12**: p. 97.
229. Ravizza, T., et al., *The IL-1beta system in epilepsy-associated malformations of cortical development.* Neurobiol Dis, 2006. **24**(1): p. 128-43.
230. Iyer, A., et al., *Evaluation of the innate and adaptive immunity in type I and type II focal cortical dysplasias.* Epilepsia, 2010. **51**(9): p. 1763-73.
231. Aronica, E., et al., *Distribution, characterization and clinical significance of microglia in glioneuronal tumours from patients with chronic intractable epilepsy.* Neuropathol Appl Neurobiol, 2005. **31**(3): p. 280-91.
232. Ramakers, C., et al., *Assumption-free analysis of quantitative real-time polymerase chain reaction (PCR) data.* Neurosci Lett, 2003. **339**(1): p. 62-6.
233. Ruijter, J.M., et al., *Amplification efficiency: linking baseline and bias in the analysis of quantitative PCR data.* Nucleic Acids Res, 2009. **37**(6): p. e45.
234. Cassano, T., et al., *Olfactory memory is impaired in a triple transgenic model of Alzheimer disease.* Behav Brain Res, 2011. **224**(2): p. 408-12.
235. Romano, A., et al., *Depressive-like behavior is paired to monoaminergic alteration in a murine model of Alzheimer's disease.* Int J Neuropsychopharmacol, 2015. **18**(4).
236. Cassano, T., et al., *Glutamatergic alterations and mitochondrial impairment in a murine model of Alzheimer disease.* Neurobiol Aging, 2012. **33**(6): p. 1121 e1-12.
237. Chen, W. and C. Qin, *General hallmarks of microRNAs in brain evolution and development.* RNA Biol, 2015. **12**(7): p. 701-8.
238. Follert, P., H. Cremer, and C. Beclin, *MicroRNAs in brain development and function: a matter of flexibility and stability.* Front Mol Neurosci, 2014. **7**: p. 5.
239. Petri, R., et al., *miRNAs in brain development.* Exp Cell Res, 2014. **321**(1): p. 84-9.
240. Oddo, S., et al., *Blocking Abeta42 accumulation delays the onset and progression of tau pathology via the C terminus of heat shock protein70-interacting protein: a mechanistic link between Abeta and tau pathology.* J Neurosci, 2008. **28**(47): p. 12163-75.
241. Gibbs, P.E., T. Miralem, and M.D. Maines, *Characterization of the human biliverdin reductase gene structure and regulatory elements: promoter activity is enhanced by hypoxia and suppressed by TNF-alpha-activated NF-kappaB.* FASEB J, 2010. **24**(9): p. 3239-54.
242. Janelsins, M.C., et al., *Early correlation of microglial activation with enhanced tumor necrosis factor-alpha and monocyte chemoattractant protein-1 expression specifically within the entorhinal cortex of triple transgenic Alzheimer's disease mice.* J Neuroinflammation, 2005. **2**: p. 23.
243. Zaheer, S., et al., *Enhanced expression of glia maturation factor correlates with glial activation in the brain of triple transgenic Alzheimer's disease mice.* Neurochem Res, 2013. **38**(1): p. 218-25.
244. Copps, K.D. and M.F. White, *Regulation of insulin sensitivity by serine/threonine phosphorylation of insulin receptor substrate proteins IRS1 and IRS2.* Diabetologia, 2012. **55**(10): p. 2565-82.
245. Carlson, C.J., M.F. White, and C.M. Rondinone, *Mammalian target of rapamycin regulates IRS-1 serine 307 phosphorylation.* Biochem Biophys Res Commun, 2004. **316**(2): p. 533-9.
246. Perluigi, M., et al., *Neuropathological role of PI3K/Akt/mTOR axis in Down syndrome brain.* Biochim Biophys Acta, 2014. **1842**(7): p. 1144-53.

247. Caccamo, A., et al., *Molecular interplay between mammalian target of rapamycin (mTOR), amyloid-beta, and Tau: effects on cognitive impairments.* J Biol Chem, 2010. **285**(17): p. 13107-20.
248. Caccamo, A., et al., *Naturally secreted amyloid-beta increases mammalian target of rapamycin (mTOR) activity via a PRAS40-mediated mechanism.* J Biol Chem, 2011. **286**(11): p. 8924-32.
249. Oddo, S., *The role of mTOR signaling in Alzheimer disease.* Front Biosci (Schol Ed), 2012. **4**: p. 941-52.
250. Bove, J., M. Martinez-Vicente, and M. Vila, *Fighting neurodegeneration with rapamycin: mechanistic insights.* Nat Rev Neurosci, 2011. **12**(8): p. 437-52.
251. Tripathi, D.N., et al., *Reactive nitrogen species regulate autophagy through ATM-AMPK-TSC2-mediated suppression of mTORC1.* Proc Natl Acad Sci U S A, 2013. **110**(32): p. E2950-7.
252. Arendt, T., *Synaptic plasticity and cell cycle activation in neurons are alternative effector pathways: the 'Dr. Jekyll and Mr. Hyde concept' of Alzheimer's disease or the yin and yang of neuroplasticity.* Prog Neurobiol, 2003. **71**(2-3): p. 83-248.
253. Crino, P.B., *mTOR: A pathogenic signaling pathway in developmental brain malformations.* Trends Mol Med, 2011. **17**(12): p. 734-42.
254. Hoeffer, C.A. and E. Klann, *mTOR signaling: at the crossroads of plasticity, memory and disease.* Trends Neurosci, 2010. **33**(2): p. 67-75.
255. Laplante, M. and D.M. Sabatini, *mTOR signaling in growth control and disease.* Cell, 2012. **149**(2): p. 274-93.
256. Perluigi, M., F. Di Domenico, and D.A. Butterfield, *mTOR signaling in aging and neurodegeneration: At the crossroad between metabolism dysfunction and impairment of autophagy.* Neurobiol Dis, 2015. **84**: p. 39-49.
257. Garcia-Arencibia, M., et al., *Autophagy, a guardian against neurodegeneration.* Semin Cell Dev Biol, 2010. **21**(7): p. 691-8.
258. Ghavami, S., et al., *Autophagy and apoptosis dysfunction in neurodegenerative disorders.* Prog Neurobiol, 2014. **112**: p. 24-49.
259. Scherz-Shouval, R. and Z. Elazar, *ROS, mitochondria and the regulation of autophagy.* Trends Cell Biol, 2007. **17**(9): p. 422-7.
260. Zhang, L., et al., *Inhibition of cathepsin S induces autophagy and apoptosis in human glioblastoma cell lines through ROS-mediated PI3K/AKT/mTOR/p70S6K and JNK signaling pathways.* Toxicol Lett, 2014. **228**(3): p. 248-59.
261. Patel, S., J. Van Der Kaay, and C. Sutherland, *Insulin regulation of hepatic insulin-like growth factor-binding protein-1 (IGFBP-1) gene expression and mammalian target of rapamycin (mTOR) signalling is impaired by the presence of hydrogen peroxide.* Biochem J, 2002. **365**(Pt 2): p. 537-45.
262. Rubinsztein, D.C., *The roles of intracellular protein-degradation pathways in neurodegeneration.* Nature, 2006. **443**(7113): p. 780-6.
263. Hung, S.Y., et al., *Autophagy protects neuron from Abeta-induced cytotoxicity.* Autophagy, 2009. **5**(4): p. 502-10.
264. Di Domenico, F., et al., *Redox proteomics analysis of HNE-modified proteins in Down syndrome brain: clues for understanding the development of Alzheimer disease.* Free Radic Biol Med, 2014. **71**: p. 270-80.
265. Iyer, A.M., et al., *mTOR Hyperactivation in down syndrome hippocampus appears early during development.* J Neuropathol Exp Neurol, 2014. **73**(7): p. 671-83.
266. Ahmed, M.M., et al., *Loss of correlations among proteins in brains of the Ts65Dn mouse model of down syndrome.* J Proteome Res, 2012. **11**(2): p. 1251-63.

267. Di Domenico, F., et al., *Bach1 overexpression in Down syndrome correlates with the alteration of the HO-1/BVR-a system: insights for transition to Alzheimer's disease.* J Alzheimers Dis, 2015. **44**(4): p. 1107-20.
268. O'Neill, L.A., F.J. Sheedy, and C.E. McCoy, *MicroRNAs: the fine-tuners of Toll-like receptor signalling.* Nat Rev Immunol, 2011. **11**(3): p. 163-75.
269. Guedes, J.R., et al., *Early miR-155 upregulation contributes to neuroinflammation in Alzheimer's disease triple transgenic mouse model.* Hum Mol Genet, 2014. **23**(23): p. 6286-301.
270. Farooqui, A.A. and L.A. Horrocks, *Lipid peroxides in the free radical pathophysiology of brain diseases.* Cell Mol Neurobiol, 1998. **18**(6): p. 599-608.
271. Kanaumi, T., et al., *Non-neuronal cell responses differ between normal and Down syndrome developing brains.* Int J Dev Neurosci, 2013. **31**(8): p. 796-803.
272. Nguyen, L.S., et al., *Profiling olfactory stem cells from living patients identifies miRNAs relevant for autism pathophysiology.* Mol Autism, 2016. **7**: p. 1.
273. Keck-Wherley, J., et al., *Abnormal microRNA expression in Ts65Dn hippocampus and whole blood: contributions to Down syndrome phenotypes.* Dev Neurosci, 2011. **33**(5): p. 451-67.
274. Lopez-Gonzalez, I., et al., *Neuroinflammatory signals in Alzheimer disease and APP/PS1 transgenic mice: correlations with plaques, tangles, and oligomeric species.* J Neuropathol Exp Neurol, 2015. **74**(4): p. 319-44.
275. Iyer, A., et al., *MicroRNA-146a: a key regulator of astrocyte-mediated inflammatory response.* PLoS One, 2012. **7**(9): p. e44789.
276. Anzai, K., et al., *Oxidation-dependent changes in the stability and permeability of lipid bilayers.* Antioxid Redox Signal, 1999. **1**(3): p. 339-47.
277. Deane, R. and B.V. Zlokovic, *Role of the blood-brain barrier in the pathogenesis of Alzheimer's disease.* Curr Alzheimer Res, 2007. **4**(2): p. 191-7.
278. Jefferies, W.A., et al., *Adjusting the compass: new insights into the role of angiogenesis in Alzheimer's disease.* Alzheimers Res Ther, 2013. **5**(6): p. 64.
279. Lukiw, W.J. and P.N. Alexandrov, *Regulation of complement factor H (CFH) by multiple miRNAs in Alzheimer's disease (AD) brain.* Mol Neurobiol, 2012. **46**(1): p. 11-9.
280. Lukiw, W.J., Y. Zhao, and J.G. Cui, *An NF-kappaB-sensitive micro RNA-146a-mediated inflammatory circuit in Alzheimer disease and in stressed human brain cells.* J Biol Chem, 2008. **283**(46): p. 31315-22.
281. Janson, J., et al., *Increased risk of type 2 diabetes in Alzheimer disease.* Diabetes, 2004. **53**(2): p. 474-81.
282. Craft, S., *Alzheimer disease: Insulin resistance and AD--extending the translational path.* Nat Rev Neurol, 2012. **8**(7): p. 360-2.
283. Gibbs, P.E., et al., *Human biliverdin reductase-based peptides activate and inhibit glucose uptake through direct interaction with the kinase domain of insulin receptor.* FASEB J, 2014. **28**(6): p. 2478-91.
284. Medeiros, R., M.A. Chabrier, and F.M. LaFerla, *Elucidating the triggers, progression, and effects of Alzheimer's disease.* J Alzheimers Dis, 2013. **33 Suppl 1**: p. S195-210.
285. Butterfield, D.A. and E.R. Stadman, *Protein oxidation processes in aging brain.* Advances in Cell Aging and Gerontology, 1997. **Vol. 2**: p. 161–191.
286. Monteiro, H.P., *Signal transduction by protein tyrosine nitration: competition or cooperation with tyrosine phosphorylation-dependent signaling events?* Free Radic Biol Med, 2002. **33**(6): p. 765-73.
287. Nistico, R., et al., *Insulin receptor beta-subunit haploinsufficiency impairs hippocampal late-phase LTP and recognition memory.* Neuromolecular Med, 2012. **14**(4): p. 262-9.

288. van der Heide, L.P., et al., *Insulin modulates hippocampal activity-dependent synaptic plasticity in a N-methyl-d-aspartate receptor and phosphatidyl-inositol-3-kinase-dependent manner.* J Neurochem, 2005. **94**(4): p. 1158-66.
289. Bisht, K., et al., *Biliverdin modulates the expression of C5aR in response to endotoxin in part via mTOR signaling.* Biochem Biophys Res Commun, 2014. **449**(1): p. 94-9.
290. Lourenco, M.V., et al., *TNF-alpha mediates PKR-dependent memory impairment and brain IRS-1 inhibition induced by Alzheimer's beta-amyloid oligomers in mice and monkeys.* Cell Metab, 2013. **18**(6): p. 831-43.
291. Cui, J.G., et al., *Differential regulation of interleukin-1 receptor-associated kinase-1 (IRAK-1) and IRAK-2 by microRNA-146a and NF-kappaB in stressed human astroglial cells and in Alzheimer disease.* J Biol Chem, 2010. **285**(50): p. 38951-60.